



e-ISSN: 2149-3189

European Research Journal

Volume 10 Issue 3 May 2024

Available at <https://dergipark.org.tr/en/pub/eurj>

© 2024 by Prusa Medical Publishing



The European Research Journal

Aim and Scope

The European Research Journal (EuRJ) is an international, independent, double-blind peer reviewed, Open Access and online publishing journal, which aims to publish papers on all the related areas of basic and clinical medicine.

Editorial Board of the European Research Journal complies with the criteria of the International Council of Medical Journal Editors (ICMJE), the World Association of Medical Editors (WAME), and Committee on Publication Ethics (COPE).

The journal publishes a variety of manuscripts including original research, case reports, invited review articles, technical reports, how-to-do it, interesting images and letters to the editor. The European Research Journal has signed the declaration of the Budapest Open Access Initiative. All articles are detected for similarity or plagiarism. Publication language is English. The journal does not charge any article submission or processing charges.

EuRJ recommends that all of our authors obtain their own ORCID identifier which will be included on their article.

The journal is published bimonthly (January, March, May, July, September, and November).

Abstracting and Indexing

The journal is abstracted and indexed with the following: ULAKBİM TR Index (ULAKBİM TR DİZİN), NLM Catalog (NLM ID: 101685727), Google Scholar (h-index: 12), Index Copernicus (ICV 2022: 100), EMBASE, ProQuest Central, EBSCO Academic Search Ultimate, ROAD, SciLit, MIAR (ICDS 2021: 3.8), J-Gate, SHERPA/RoMEO, BASE, EZB, CrossRef, JournalTOCs, WorldCat, TURK MEDLINE, Turkish Citation Index, EuroPub, OpenAIRE, ResearchGate, SOBIAD, Advanced Science Index, ScienceGate, OUCI, Publons, (Clarivate Web of Science)

Publisher

The European Research Journal (EuRJ)
Prusa Medical Publishing
Konak Mh. Kudret Sk. Şenyurt İş Mrk. Blok No:6 İç kapı no: 3
Nilüfer/Bursa-Turkey
info@prusamp.com

<https://dergipark.org.tr/en/pub/eurj>
<https://www.prusamp.com>



e-ISSN: 2149-3189

The European Research Journal, hosted by Turkish JournalPark ACADEMIC, is licensed under a Creative Commons Attribution-NonCommercial-NoDerivatives 4.0 International License.



EDITORIAL BOARD

EDITOR-IN-CHIEF

Senol YAVUZ, MD,

Professor,

University of Health Sciences, Bursa Yuksek Ihtisas Training & Research Hospital,
Department of Cardiovascular Surgery,
Bursa, Turkey,

MANAGING EDITORS

Nizameddin KOCA, MD,

Associate Professor,

University of Health Sciences, Bursa Şehir Training & Research Hospital,
Department of Internal Medicine,
Bursa, Turkey

Soner CANDER, MD

Professor,

Uludag University Medical School,
Department of Endocrinology and Metabolism
Bursa, Turkey

Mesut ENGİN, MD,

Associate Professor,

University of Health Sciences, Bursa Yuksek Ihtisas Training & Research Hospital,
Department of Cardiovascular Surgery,
Bursa, Turkey

FOUNDING EDITOR

Rustem ASKIN, MD,

Professor of Psychiatry

İstanbul Ticaret University, Department of Psychology
İstanbul, Turkey

EDITORIAL ASSISTANT

Ugur BOLUKBAS

EDITORS

Omer SENORMANCI, MD

Professor,

Beykent University, Faculty of Arts-Sciences
Department of Psychology,
İstanbul, Turkey

Mahmut KALEM, MD,

Associate Professor,
Ankara University Medical School,
Department of Orthopedics and Traumatology,
Ankara, Turkey

Meliha KASAPOGLU AKSOY, MD

Associate Professor,
University of Health Sciences, Bursa Yuksek Ihtisas Training & Research Hospital,
Department of Physical Therapy and Rehabilitation,
Bursa, Turkey

Burcu DİNÇGEZ, MD

Associate Professor,
University of Health Sciences, Bursa Yuksek Ihtisas Training & Research Hospital,
Department of Gynecology and Obstetrics,
Bursa, Turkey

Arda ISIK, MD

Associate Professor,
Medeniyet University School of Medicine,
Department of General Surgery,
Istanbul, Turkey

Melih CEKINMEZ, MD

Professor,
University of Health Sciences, Adana City Training & Research Hospital,
Department of Neurosurgery,
Adana, Turkey

Kadir Kaan OZSIN, MD

Associate Professor,
University of Health Sciences, Bursa Yuksek Ihtisas Training & Research Hospital,
Department of Cardiovascular Surgery,
Bursa, Turkey

Alper KARAKUS, MD

Associate Professor,
University of Health Sciences, Bursa Yuksek Ihtisas Training & Research Hospital,
Department of Cardiology,
Bursa, Turkey

Onur KAYGUSUZ, MD.,

Associate Professor,
Uludag University School of Medicine,
Department of Urology,
Bursa, Turkey

Sayad KOCAHAN, PhD,

Professor,
University of Health Sciences, Gülhane Medical Faculty,
Department of Physiology,
Ankara, Turkey

Gokhan OCAKOGLU, Ph.D.,
Associate Professor,
Uludag University School of Medicine,
Department of Biostatistics,
Bursa, Turkey

Nurullah DOGAN, MD,
Associate Professor,
Doruk Nilüfer Hospital,
Department of Radiology,
Bursa, Turkey

INTERNATIONAL EDITORIAL BOARD MEMBERS

Ahmet KIZILAY, MD
Professor,
Inönü University School of Medicine,
Department of Otorhinolaryngology,
Malatya, Turkey

Aron Frederik POPOV, MD
Professor,
University of Frankfurt,
Department of Cardiothoracic Surgery,
Frankfurt, Germany

Cristina FLORESCU, MD
Associate Professor,
University of Craiova,
Department of Medicine and Pharmacy,
Romania

Elif EKINCI, MD
MBBS, FRACP, PhD
University of Melbourne
Department of Medicine,
Melbourne, Australia

Essam M MAHFOUZ, MD
Professor,
University of Mansoura School of Medicine
Department of Cardiology,
Mansoura, Egypt

Francesco CARELLI, MD
Professor,
University of Milan School of Medicine,
Department of Family Medicine,
Milan, Italy

Gary TSE, MD, PhD

Assistant Professor,
The Chinese University of Hong Kong,
Department of Medicine and Therapeutics,
Hong Kong, China

Kendra J. GRUBB, MD, MHA, FACC

Assistant Professor,
Emory University School of Medicine,
Department of Cardiovascular Surgery,
Atlanta, GA, USA

Muzaffer DEMIR, MD

Professor,
Trakya University School of Medicine,
Department of Hematology,
Edirne, Turkey

Nader D NADER, MD

Professor,
University of Buffalo School of Medicine
Department of Anesthesiology,
NY, USA

Sait Ait BENALI, MD

Professor,
Cadi Ayyad University School of Medicine,
Department of Neurosurgery,
Marrakech, Morocco

Sedat ALTIN, MD

Professor,
University of Health Sciences, Yedikule Training & Research Hospital,
Department of Chest Diseases,
Istanbul, Turkey

Semih HALEZEROGLU, MD, FETCS

Professor,
Acibadem University School of Medicine,
Department of Thoracic Surgery,
Istanbul, Turkey

Veysel TAHAN, MD, FACP, FACG, FESBGH

Assistant Professor,
University of Missouri,
Division of Gastroenterology and Hepatology,
Columbia, Missouri, USA

Yenal DUNDAR, MD

Consultant Psychiatrist
Central Queensland Hospital and Health Service,
QLD, Australia

Table of Contents

Original Articles

Predictive value of ACEF score for acute kidney injury after surgical aortic valve replacement 254-261
Gökhan DEMİRCİ, Ali Rıza DEMİR, Serkan KAHRAMAN, Sencer ÇAMÇI, Emre YILMAZ

Predictive value of NLRC3 levels for pulmonary hypertension in patients with chronic obstructive pulmonary disease 262-267
Meltem YILMAZ, Levent Cem MUTLU, Şeref ALPSOY, Aydın AKYÜZ, Aliye ÇELİKKOL, Özlem KAYMAZ

Relationship of breast arterial calcification and radiotherapy 268-275
Gökhan KARATAŞ, Osman KULA, Nermin TUNÇBİLEK

Evaluation of mercury in skin lightening creams commonly used in Trinidad and Tobago and their associated health risk 276-285
Terry MOHAMMED, Nadira RAMBOCAS, Sanjeev BASDEO, Yasphal KISSOON

Which pathologies of the penis can be diagnosed with computed tomography? A comprehensive approach to imaging findings 286-294
Yeliz AKTÜRK, Esra SOYER GÜLDOĞAN, Serra ÖZBAL GÜNEŞ

Association of frailty with nutritional parameters in patients with chronic kidney disease 295-302
Recep EVCEN, Mehmet Zahid KOÇAK, Rengin ELSÜRER AFŞAR

Practical method in the diagnosis of diabetic ketoacidosis: end-tidal carbon dioxide 303-310
Ahmet KAYALI, Ejder SAYLAV BORA

The relationship between fibromyalgia syndrome and inflammation parameters in hemodialysis patients 311-318
Semahat KARAHİSAR ŞİRALİ, Refika BÜBERCİ

Ultrasound-guided platelet-rich plasma vs. radiofrequency nerve ablation for refractory plantar fasciitis 319-325
Furkan ERDOĞAN, Tolgahan CENGİZ, Alparslan YURTBAŞ, İsmail BÜYÜKCERAN

Assessment of hiatus defect size in hiatal hernia patients using computed tomography 326-332
Seray Gizem GÜR ÖZCAN, Nezih ZENGİN, Burak BİLİR, Nurcan KAÇMAZ KAT, Doğukan DURAK

Case Report

Solitary myofibroma in children: a report of two cases 333-337
Çağrı COŞKUN, Kemal KÖSE MEHMETOĞLU, Mehmet AYVAZ, İbrahim VARGEL, Üstün AYDINGÖZ, Hatice NURSUN ÖZCAN, Ali Varan, Bilgehan YALÇIN

Predictive value of ACEF score for acute kidney injury after surgical aortic valve replacement

Gökhan Demirci¹, Ali Rıza Demir¹, Serkan Kahraman¹, Sencer Çamcı², Emre Yılmaz²

¹Department of Cardiology, University of Health Sciences, Istanbul Mehmet Akif Ersoy Thoracic and Cardiovascular Surgery Training and Research Hospital, Istanbul, Turkey; ²Department of Cardiology, Giresun University, Faculty of Medicine, Giresun, Turkey

ABSTRACT

Objectives: Aortic stenosis is the most common form of degenerative heart valve disease. Acute kidney injury (AKI) after aortic valve replacement (AVR) is a common complication and is related to worse outcomes. Age, creatinine, and ejection fraction (ACEF) score is a simple scoring method that includes three parameters. Our study aimed to evaluate whether ACEF score could predict the development of AKI in patients who underwent AVR.

Methods: A total of 366 consecutive patients who underwent isolated AVR for symptomatic severe aortic stenosis were evaluated retrospectively. The development of AKI was the primary endpoint of the study. The ACEF score was calculated by the formula: age (years)/left ventricular ejection fraction (%) +1 (if baseline serum creatinine was >2 mg/dL). According to the ACEF score the study population was divided into two groups.

Results: AKI was developed in 66 (18%) patients. The cut-off value of the ACEF score for the prediction of AKI was 1.07 with a sensitivity of 69.7% and a specificity of 56.7% (AUC 0.663; 95% CI: 0.589-0.736; P<0.001). AKI incidence was found to be higher in patients with high ACEF score than low ACEF score [46 (26.1%) vs. 20 (10.5%); P<0.001]. In addition, ACEF score [OR: 2.599; 95% CI: 1.399-4.828; P=0.002] and hemoglobin levels (OR: 0.837; 95% CI: 0.729-0.961; P=0.012) were found to be independent predictors of AKI.

Conclusions: Our study revealed that the ACEF score is an independent predictor of AKI. ACEF score, as a simple and objective score, can be useful in predicting AKI in patients undergoing AVR.

Keywords: Acute kidney injury, aortic stenosis, aortic valve replacement, predictors, ACEF score

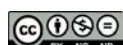
Aortic stenosis (AS) is an ordinary valvular heart disease, mainly in older adults, and is the leading reason for surgical valve replacement therapy, especially in developing countries. The recent data on the beneficial outcome of aortic valve replacement (AVR) may expand the indication for aortic valve intervention to a wider population of severe AS

[1]. Symptomatic AS is associated with significant mortality if untreated [2].

Acute kidney injury (AKI) is an increase in serum creatinine by 1.5 times and over within seven days compared to the baseline or an increase of 0.3 mg/dL and over within 48 hours following the procedure [3]. In cardiology clinical practice, contrast-induced

Corresponding author: Sencer Çamcı, MD., Associate Professor, Fax: +90 454 310 20 20, E-mail: snrcmc@gmail.com

How to cite this article: Demirci G, Demir AR, Kahraman S, Çamcı S, Yılmaz E. Predictive value of ACEF score for acute kidney injury after surgical aortic valve replacement. Eur Res J. 2024;10(3):254-261. doi: 10.18621/eurj.1334048



This is an open access article distributed under the terms of [Creative Commons Attribution-NonCommercial-NoDerivatives 4.0 International License](https://creativecommons.org/licenses/by-nc-nd/4.0/)

Received: August 4, 2023

Accepted: October 20, 2023

Published Online: December 21, 2023

Copyright © 2024 by Prusa Medical Publishing
Available at <http://dergipark.org.tr/eurj>



nephropathy, a particular type of AKI, has been a focus of interest for clinicians. In this regard, there are many risk classifications and searches for risk factors in different patient groups. For example, it has been reported that osmolarity and positive and negative acute phase reactants are risk factors for AKI in patients with ST-segment elevation myocardial infarction (STEMI) [4, 5]. However, in such studies, the amount of contrast material has been identified as a risk factor in addition to other risk scales and scores. On the other hand, determining the risk factors of AKI that occur in the postoperative period in cardiac surgery patients without using any contrast material is an endeavor that will significantly benefit the literature. AKI due to cardiac surgery is a serious complication. AKI is characterized by increased volume burden, electrolyte instability, and the risk of need for renal replacement therapy. Furthermore, AKI causes higher overall mortality, increased length of hospital stay, and costs. AKI complicates nearly 16% of total hospitalizations due to AVR and is associated with increased mortality and morbidity [6]. This increases the need to identify prognostic factors that predict AKI in patients undergoing AVR.

Age, creatinine, and ejection fraction (ACEF) score include three parameters associated with a higher risk of mortality in patients after elective coronary artery bypass graft (CABG) surgery [7]. Studies have shown that ACEF score is a determinant of AKI in subjects undergoing mitral valve repair, CABG, and percutaneous coronary intervention (PCI) [8-10]. Previously, the ACEF score has been found to be a marker of AKI in patients with AS undergoing transcatheter aortic valve replacement (TAVR), but not yet in patients treated with surgery [11]. We evaluated the prognostic value of the ACEF score in the prediction of AKI in patients with isolated severe degenerative AS undergoing surgical aortic valve replacement (SAVR).

METHODS

Study Population

This retrospective study assessed 750 patients diagnosed with severe degenerative AS who underwent successful SAVR at a tertiary cardiovascular surgery center from January 2012 to December 2019. All sub-

jects were assessed by a multidisciplinary cardiac team before the procedure. Our study was carried out according to the principles of the Declaration of Helsinki with the approval of the local ethics committee of Istanbul Mehmet Akif Ersoy Thoracic and Cardiovascular Surgery Training and Research Hospital (Date: 12.04.2022, decision no: 2022.04.26).

Exclusion criteria for the study: Emergency surgery for acute aortic regurgitation and known coronary artery disease, PCI, previous or simultaneous CABG or heart valve replacement surgery outside the aortic valve, postoperative aortic incompatibility, type A aortic dissection, malignancy or end-stage liver disease, receiving dialysis treatment, death, and demographic medical records not available during or within 72 hours of the procedure. Patients with significant coronary artery disease were excluded, because, after surgical implantation, additional coronary ischemia may have an effect of worsening renal functions. After excluding these patients, a total of 366 technically successful cases were considered as the study population.

Echocardiography

The target population of our study was patients with severe aortic stenosis. Aortic stenosis was defined according to current data: (1) Mean transvalvular gradient higher than 40 mmHg and (2) Aortic valve area less than 1 cm² [12].

Procedural Details

SAVR was carried out via traditional full sternotomy, hemisternotomy or right anterior minithoracotomy, depending on the surgeon's preference [13]. Our surgeons commonly preferred the traditional full sternotomy approach. In all median sternotomy and hemisternotomy patients, traditional central cannulation techniques were used. In case the minimally invasive approach is selected, it involves a 6 to 9 cm skin incision for the upper hemisternotomy approach was made and at the level of the fourth intercostal space the sternum was transected horizontally. At SAVR, the patient was thoroughly heparinized and the ascending aorta was evaluated by epiaortic ultrasonography for safe cannulation. Antegrade and retrograde cardioplegia were given. If there was more than mild aortic regurgitation, an aortotomy was performed for direct ostial delivery.

Data Collection

Baseline characteristics (demographic data, comorbidities, hemodynamic variables, echocardiographic parameters, and serum laboratory values), operation details and postoperative results, intensive care and inpatient follow-up records were retrospectively reviewed. Before the procedure, the estimated glomerular filtration rate (eGFR) was calculated with the Cockcroft-Gault formula [14]. We measured serum creatinine level (mg/dL) 24 hours before the process, presently after the process, and day-to-day until the discharge.

We calculated the ACEF score by the formula: ACEF = age/left ventricular ejection fraction (%) + 1 (if creatinine >2.0 mg/dL) [15]. We made the diagnosis and stage of AKI according to the standards suggested in the second consensus report disseminated by the Valve Academic Research Consortium (VARC-3) [3]. The creatinine levels before and after the procedure were compared and the diagnosis of AKI was defined as follows: (a) The absolute increase in creatinine level ≥ 0.5 mg/dL from baseline within 48 hours (may increase throughout up to seven days) and (b) Increase of creatinine levels 1.5 times when compared to the baseline.

VARC-3 score determines acute kidney injury in four different categories [3]. We determined the optimal ACEF score threshold for predicting AKI development and subsequently categorized the patients into groups based on their ACEF scores: high ACEF scores and low ACEF scores.

Study Endpoint

The ACEF score predicts Stage-1 AKI (VARC-3 criteria) in patients who have undergone SAVR. Stage-1 AKI is defined as an increase in serum creatinine by ≥ 150 – 200% (≥ 1.5 – 2.0 times) within seven days compared to the baseline or an increase of ≥ 0.3 mg/dL (≥ 26.4 $\mu\text{mol/L}$) within 48 hours following the procedure [3].

Statistical Analysis

Data analysis were performed using the Statistical Package for the Social Sciences, version 24.0 (SPSS Inc., Chicago, Illinois, USA). The distribution normality of the variables was evaluated using histograms, probability curves, and Kolmogorov-Smirnov test. Normally distributed numerical variables were ex-

pressed as mean [standard deviation (SD)]. Non-normally distributed numerical variables were expressed as median (interquartile range). Categorical variables were expressed as a percentage (%) and were compared by the chi-square or Fisher exact tests. We evaluated numerical variables using Student t-tests and the Mann-Whitney U-test. Covariates, including all baseline and procedural factors indicating significant P value in the univariable analysis, were included in a logistic regression analysis model to decide the predictive characteristics of the incidence of AKI. We employed receiver operating characteristic (ROC) curve analysis to identify the optimal ACEF cut-off value for accurate AKI prediction. Statistical significance was defined as a P value below 0.05.

RESULTS

The mean age of patients was 62 ± 11 years, 121 (33.1%) patients were female. Baseline clinical, demographic, and laboratory variables were demonstrated in Table 1. Of the patients in our study, 49.5% (n=181) had NYHA class 3-4 dyspnea, 50.8% (n=186) presented with angina, and 11.7% experienced syncope attacks. The baseline creatinine level was 0.83 (0.7-1.0) mg/dL, the postoperative 72nd hour creatinine level was 1.0 (0.8-1.4) mg/dL, and the mean ejection fraction was $57 \pm 8\%$. We detected acute kidney injury in 66 (18%) patients. We performed ROC analysis to determine the predictive value of ACEF score in predicting AKI in postoperative AVR patients. In ROC curve analysis, the curve intersected at 1.07, where the combined sensitivity and specificity values were highest (sensitivity: 69.7%; specificity: 56.7%). The area under the curve measured 0.663 (95% confidence interval (CI): 0.589-0.736, $P < 0.001$) (Fig.1). Based on the ACEF cut-off value, the study population was categorized into two groups: Group 1 consisted of 190 patients with ACEF ≤ 1.07 , and Group 2 included 176 patients with ACEF > 1.07 . Baseline clinical, demographic, and laboratory variables were also demonstrated in Table 1. The mean age was higher in Group 2 (54 ± 7 vs. 71 ± 9 years; $P < 0.001$). The incidence of angina was higher in Group 1 [108 (56.8%) vs. 78 (44.3%); $P = 0.017$]. Hemoglobin level was lower in Group 2 [13.9 (12.4-15.1) vs. 12.1 (11.2-13.8) g/dL; $P < 0.001$]. The baseline creatinine [0.8 (0.7-0.9)

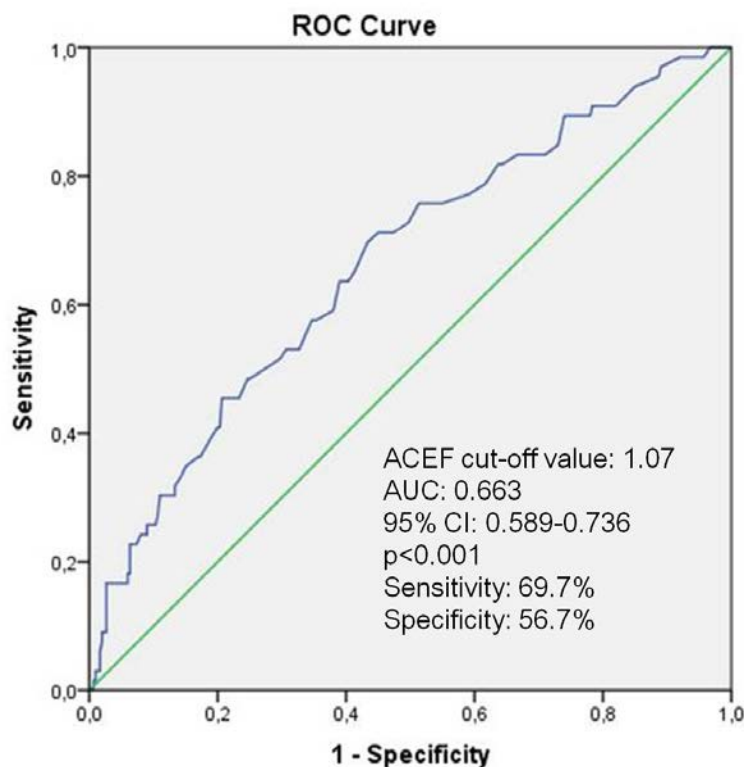


Fig. 1. Receiver operating characteristic curve showing the optimal ACEF score cut-off value to indicate acute kidney injury. ACEF=Age, creatinin, ejection fraction, AUC=Area under the curve, CI=Confidence interval, ROC=Receiver operating characteristic.

vs. 0.9 (0.8-1.1) mg/dL; $P<0.001$] and postoperative 72nd hour creatinine [0.9 (0.78-1.11) vs. 1.2 (0.93-1.54) mg/dL; $P<0.001$] were higher in Group 2. The incidence of AKI was also higher in Group 2 [20 (10.5%) vs. 46 (26.1%); $P<0.001$]. The incidences of diabetes mellitus [33 (17.4%) vs. 52 (29.5%); $P=0.006$], hypertension [68 (35.8%) vs. 108 (61.4%); $P<0.001$], chronic obstructive pulmonary disease [15 (7.9%) vs. 38 (21.6%); $P<0.001$] and peripheral artery disease [2 (1.1%) vs. 8 (4.5%); $P=0.040$] were higher in Group 2. The ejection fraction was lower in Group 2 ($61\pm 4\%$ vs. $54\pm 11\%$; $P<0.001$). Left atrium size [38 (34-41) mm vs. 41 (37-45) mm; $P<0.001$] and aortic valve maximal gradient [75 (65-87) mmHg vs. 78 (66-90) mmHg; $P=0.048$] were higher in Group 2.

We performed logistic regression, incorporating significant variables identified in the univariate analysis (Table 2). The results of the multivariate logistic regression analysis revealed that a higher ACEF score (Odds ratio (OR): 2.812; 95%CI: 1.343-4.906; $P<0.001$), higher leukocyte counts (OR: 1.089; 95% CI: 1.014-1.216; $P=0.036$) and lower hemoglobin lev-

els (OR: 0.802; 95% CI: 0.706-0.954; $P=0.002$) independently served as predictors for AKI. Variables such as diabetes, hypertension, chronic obstructive pulmonary disease, peripheral arterial disease, left atrial width, and maximal gradient of the aortic valve, which we found significant differences between ACEF groups, did not significantly affect the risk of AKI development in logistic regression analysis.

DISCUSSION

We investigated the impact of the ACEF score on predicting AKI development in patients undergoing SAVR. The incidence of AKI development after SAVR was found to be higher in patients with high ACEF scores. The ACEF score independently predicted AKI in patients undergoing SAVR.

AKI is a significant post-cardiac surgery complication, with reported incidences varying from 9% to 43%. It is linked to increased mortality rates and a heightened risk of in-hospital morbidity [16, 17]. The

Table 1. Baseline clinical, demographic, and laboratory variables

	All patients (n=366)	ACEF ≤1.07 (n=190)	ACEF >1.07 (n=176)	P value
Age (years)	62±11	54±7	71±9	<0.001
Female, n (%)	121 (33.1)	56 (29.5)	65 (36.9)	0.130
Dispne, n (%)				
NYHA Class 1-2, n (%)	185 (50.5)	99 (52.1)	86 (48.9)	0.535
NYHA Class 3-4, n (%)	181 (49.5)	91 (47.9)	90 (51.1)	
Angina, n (%)	186 (50.8)	108 (56.8)	78 (44.3)	0.017
Syncope, n (%)	43 (11.7)	26 (13.7)	17 (9.7)	0.232
Hemoglobin (g/dL)	13.2 (11.5-14.7)	13.9 (12.4-15.1)	12.1 (11.2-13.8)	<0.001
Platelet (10 ³ /uL)	229.5 (189.75-276.25)	236 (193-278)	221 (186-275)	0.266
Leukocytes (× 10 ³ /mm ³)	7.9 (6.6-9.4)	8 (6.89-9.5)	7.9 (6.5-9.35)	0.376
Bazalcreatinine (mg/dL)	0.83 (0.7-1.0)	0.8 (0.7-0.9)	0.9 (0.8-1.1)	<0.001
GFR (mL/min/1.73 m ²)	90±25	103±21	77±20	<0.001
Postoperative creatinine (mg/dL) (72 nd h)	1.0 (0.8-1.4)	0.9 (0.78-1.11)	1.2 (0.93-1.54)	<0.001
Acute kidney injury, n (%)	66 (18.0)	20 (10.5)	46 (26.1)	<0.001
Total cholesterol (mg/dL)	175.5 (149.75-211.25)	177 (147-215)	175 (154-207)	0.920
LDL-C (mg/dL)	104 (81-132)	102 (79-135)	104.5 (83-128)	0.737
HDL-C (mg/dL)	42.5 (35-51)	43 (36-50)	42 (34-52)	1.000
Triglyceride (mg/dL)	120 (91.75-174.25)	120 (93-179)	122.5 (89-162)	0.598
Diabetes mellitus, n (%)	85 (23.2)	33 (17.4)	52 (29.5)	0.006
Hypertension, n (%)	176 (48.1)	68 (35.8)	108 (61.4)	<0.001
COPD, n (%)	53 (14.5)	15 (7.9)	38 (21.6)	<0.001
Cerebrovascular disease, n (%)	0 (0)	0 (0)	0 (0)	
Peripheral artery disease, n (%)	10 (2.7)	2 (1.1)	8 (4.5)	0.040
Smoking, n (%)	92 (25.1)	55 (58.9)	37 (21.0)	0.081
Atrial fibrillation, n (%)	30 (8.2)	12 (6.3)	18 (10.2)	0.173
Ejection fraction, (%)	57±8	61±4	54±11	<0.001
LVEDD (mm)	49 (45-56)	50 (46-55)	49 (45-57)	0.833
LVESD (mm)	32 (28-38)	32 (28-37)	32 (28-41)	0.162
LA (mm)	40 (35-43)	38 (34-41)	41 (37-45)	<0.001
Maximum gradient, (mmHg)	76 (65-89)	75 (65-87)	78 (66-90)	0.048
Mean gradient, (mmHg)	50 (43-56)	48 (43-55)	51 (44-58)	0.128
Aortic valve area, (cm ²)	0.67±0.11	0.66±0.11	0.68±0.12	0.178

Data are presented as a percentage, mean±standard deviation, or median (interquartile range). ACEF=Age, creatinin, ejection fraction, COPD=chronic obstructive pulmonary disease, GFR=glomerular filtration rate, HDL-C=High-density lipoprotein cholesterol, LA=Left atrium, LDL-C=Low-density lipoprotein cholesterol, LVEDD=Left ventricular end-diastolic diameter, LVESD=Left ventricular end-systolic diameter, NYHA=New York Heart Association.

Table 2. Univariable and multivariable logistic regression analysis for independent predictors of acute kidney injury

	Univariate analysis			Multivariate analysis		
	Odds ratio	95% CI	P value	Odds ratio	95% CI	P value
Gender	1.394	0.771-2.520	0.271			
Diabetes mellitus	1.152	0.603-2.200	0.669			
ACEF	3.008	1.697-5.332	<0.001	2.812	1.343-4.906	<0.001
Hemoglobin	0.789	0.694-0.897	<0.001	0.802	0.706-0.954	0.002
Leukocytes	1.107	1.012-1.211	0.026	1.089	1.014-1.216	0.036
Hypertension	1.593	0.930-2.729	0.090			

ACEF=Age, creatinin, ejection fraction, CI=Confidence interval

occurrence of AKI increases the postoperative mortality in patients requiring dialysis, exceeding 40% or even reaching 50% in series, compared to the 0.6-2% mortality rate in patients without AKI [18]. Minor changes in serum creatinine were associated with negative outcomes [19]. Compared with CABG, it is an independent risk factor with a 2.7-fold increased risk for AKI in valve surgery [20]. The kidney has the most heightened tissue perfusion rate close to body organ weight, making it sensitive to hemodynamic injury. Cellular ischemia is an important cause of AKI in AVR. This ischemia can cause tubular epithelial damage, vascular endothelial activation, and injury. Many preoperative, intraoperative, and postoperative factors, especially perioperative renal hypoperfusion, prepare the way for this injury. Many procedural factors have been associated with AKI during AVR, such as perioperative anemia, erythrocyte transfusion, and cardiopulmonary bypass. In SAVR, cardiopulmonary bypass is thought to play an essential role in developing AKI with two mechanisms: hemodilution and hypotension. Hemodilution causes a general inflammatory state. Hypotension results from low pressures and flow rates [21].

The ACEF score is easily applicable. Firstly, Ranucci *et al.* [7] revealed the association of ACEF with mortality in elective heart surgeries. Studies have shown that ACEF score was a strong predictor for AKI in patients who underwent PCI after STEMI [22]. The ACEF score has been recognized as a straightforward tool with sufficient capability to identify patients at

risk for all stages of AKI following mitral valve repair [8]. Uygur *et al.* [11] reported a strong relationship between ACEF and AKI in severe AS patients who underwent TAVR. The ACEF score, in conjunction with other factors, demonstrated its reliability in predicting mortality among patients undergoing AVR [23].

In a study involving 2169 patients who underwent AVR, Najjar *et al.* [21] revealed that increasing age and preoperative creatinine levels increased the development of AKI, and this was supported by other studies [24]. In the study by Grayson *et al.* [20], valvular surgeries and preoperative creatinine levels were distinct risk factors independently associated with AKI development. Heart failure was stated as one of the most important perioperative risk factors for AKI. Hertzberg *et al.* [25] evaluated 36,403 patients after cardiac surgery and found that heart failure was an independent predictor of AKI. In patients undergoing AVR, proven by clinical studies, these three basal clinical variables are independent risk factors for postoperative AKI. These parameters are not only risk factors for the development of AKI but also interacting parameters. The process leading to AKI in postoperative AVR patients is not a simple process due to changing a single parameter. It is an outcome achieved by the joint interaction of mechanisms such as inflammation, hemodilution, and hypotension [21]. Therefore, it would be misleading to evaluate the development of AKI in postoperative AVR patients by measuring a single parameter. ACEF score offers us the chance to combine analysis of variables previously proven to be

risk factors for AKI development in this patient group by clinical studies. Thus, with these three important parameters, we have a better chance to make more accurate predictions for the prediction of AKI development in postoperative AVR patients. Evaluating these parameters separately may result in under-evaluation of the AKI process. Hence, incorporating various parameters enhances the precision of risk models.

ACEF score offers notable benefits regarding straightforward accessibility and rapid, uncomplicated calculation. Our study corroborates existing literature by revealing significantly lower hemoglobin levels in the AKI-developing group. Furthermore, low hemoglobin levels emerged as an independent predictor of AKI. Callejas *et al.* [26] revealed in a multicenter prospective study that peri-procedural anemia was an independent predictor for AKI. In our study, we adhered to the original version of the ACEF score. But this result is promising that the ACEF score can be modified in the future, and thus its diagnostic power can be further increased.

ACEF score was demonstrated to be useful in various patient groups, however, it has not been applied to the patients who underwent cardiac surgery. Our objective was to assess the utility of ACEF score in predicting AKI among patients who underwent a major cardiac surgery, specifically surgical aortic replacement, and it has proven to be effective. If we try to adapt these results to our clinical practice: (i) In older patients with low ejection fraction, even if their renal functions are normal; (ii) In patients older than 1.07 times the ejection fraction (e.g., a patient with an ejection fraction of 60% would be over 64 years of age), we recommend that renal protective measures be taken, as in patients with pre-SAVR renal dysfunction.

Limitations

Our retrospective study was conducted at a single center and involved a relatively modest patient cohort. Consequently, it is imperative to conduct comprehensive prospective cohort investigations to validate and substantiate our findings. Additionally, it should be noted that we were unable to calculate the STS (Society of Thoracic Surgeons) score and EuroSCORE II (European System for Cardiac Operative Risk Evaluation II) for this group due to data unavailability. Thus, we could not compare the effectiveness of predicting AKI by using three different methods. Not least of all,

this majority of the patient group consists of female patients, gender variance may have an additional effect on results. Further trials are needed to determine the long-term efficacy of ACEF score in mortality and second endpoints, including long-term renal insufficiency, in this patient group.

CONCLUSION

Our study illustrates the effectiveness of the pre-procedural ACEF score in predicting acute kidney injury in patients undergoing surgical aortic valve replacement. Patients with higher ACEF scores may require additional renal function precautions compared to patients with lower ACEF scores.

Authors' Contribution

Study Conception: GD, ARD, SK; Study Design: GD, ARD, SK; Supervision: GD, ARD, SK; Funding: N/A; Materials: N/A; Data Collection and/or Processing: GD, ARD, SK; Statistical Analysis and/or Data Interpretation: GD, ARD, SK; Literature Review: GD, ARD, SK, SÇ, EY; Manuscript Preparation: GD, ARD, SK, SÇ, EY and Critical Review: GD, ARD, SK, SÇ, EY.

Conflict of interest

The authors disclosed no conflict of interest during the preparation or publication of this manuscript.

Financing

The authors disclosed that they did not receive any grant during conduction or writing of this study.

REFERENCES

1. Kang DH, Park SJ, Lee SA, et al. Early surgery or conservative care for asymptomatic aortic stenosis. *N Engl J Med.* 2020;382(2):111-119. doi: 10.1056/NEJMoa1912846.
2. Turina J, Hess O, Sepulcri F, Krayenbuehl HP. Spontaneous course of aortic valve disease. *Eur Heart J.* 1987;8(5):471-483. doi: 10.1093/oxfordjournals.eurheartj.a062307.
3. VARC-3 WRITING COMMITTEE; Généreux P, Piazza N, Alu MC, et al. Valve Academic Research Consortium 3: updated endpoint definitions for aortic valve clinical research. *J Am Coll Cardiol.* 2021;77(21):2717-2746. doi: 10.1016/j.jacc.2021.02.038.
4. Yildiz I, Yildiz PO, Rencuzogullari I, et al. Association of serum osmolarity with contrast-induced nephropathy in patients

- with ST-segment elevation myocardial infarction. *Angiology*. 2019;70(7):627-632. doi: 10.1177/0003319719826466.
5. Karabağ Y, Çağdaş M, Rencuzogullari I, et al. The C-reactive protein to albumin ratio predicts acute kidney injury in patients with ST-segment elevation myocardial infarction undergoing primary percutaneous coronary intervention. *Heart Lung Circ*. 2019;28(11):1638-1645. doi: 10.1016/j.hlc.2018.08.009.
6. Kumar N, Garg N. Acute kidney injury after aortic valve replacement in a nationally representative cohort in the USA. *Nephrol Dial Transplant*. 2019;34(2):295-300. doi: 10.1093/ndt/gfy097.
7. Ranucci M, Castelvechio S, Menicanti L, Frigiola A, Pelissero G. Risk of assessing mortality risk in elective cardiac operations: age, creatinine, ejection fraction, and the law of parsimony. *Circulation*. 2009;119(24):3053-3061. doi: 10.1161/CIRCULATIONAHA.108.842393.
8. Chang CH, Lee CC, Chen SW, et al. Predicting acute kidney injury following mitral valve repair. *Int J Med Sci*. 2016;13(1):19-24. doi: 10.7150/ijms.13253.
9. Chen SW, Chang CH, Fan PC, et al. Comparison of contemporary preoperative risk models at predicting acute kidney injury after isolated coronary artery bypass grafting: a retrospective cohort study. *BMJ Open*. 2016;6(6):e010176. doi: 10.1136/bmjopen-2015-010176.
10. Andò G, Morabito G, de Gregorio C, Trio O, Saporito F, Oreto G. Age, glomerular filtration rate, ejection fraction, and the AGEF score predict contrast-induced nephropathy in patients with acute myocardial infarction undergoing primary percutaneous coronary intervention. *Catheter Cardiovasc Interv*. 2013;82(6):878-885. doi: 10.1002/ccd.25023.
11. Uygur B, Celik O, Demir AR, et al. A simplified acute kidney injury predictor following transcatheter aortic valve implantation: ACEF score. *Kardiol Pol*. 2021;79(6):662-668. doi: 10.33963/KP.15933.
12. Rana M. Aortic valve stenosis: diagnostic approaches and recommendations of the 2021 ESC/EACTS guidelines for the management of valvular heart disease -A review of the literature. *Cardiol Cardiovasc Med*. 2022;6(3):315-324. doi: 10.26502/fccm.92920267.
13. Hirji SA, Funamoto M, Lee J, et al. Minimally invasive versus full sternotomy aortic valve replacement in low-risk patients: Which will stand against transcatheter aortic valve replacement? *Surgery*. 2018;164(2):282-287. doi: 10.1016/j.surg.2018.02.018.
14. Cockcroft DW, Gault MH. Prediction of creatinine clearance from serum creatinine. *Nephron*. 1976;16(1):31-41. doi: 10.1159/000180580.
15. Wykrzykowska JJ, Garg S, Onuma Y, et al. Value of age, creatinine, and ejection fraction (ACEF score) in assessing risk in patients undergoing percutaneous coronary interventions in the 'All-Comers' LEADERS trial. *Circ Cardiovasc Interv*. 2011;4(1):47-56. doi: 10.1161/CIRCINTERVENTIONS.110.958389.
16. Parolari A, Pesce LL, Pacini D, et al; Monzino Research Group on Cardiac Surgery Outcomes. Risk factors for perioperative acute kidney injury after adult cardiac surgery: role of perioperative management. *Ann Thorac Surg*. 2012;93(2):584-591. doi: 10.1016/j.athoracsur.2011.09.073.
17. Brown JR, Kramer RS, Coca SG, Parikh CR. Duration of acute kidney injury impacts long-term survival after cardiac surgery. *Ann Thorac Surg*. 2010;90(4):1142-1148. doi: 10.1016/j.athoracsur.2010.04.039.
18. Englberger L, Suri RM, Li Z, et al. Clinical accuracy of RIFLE and Acute Kidney Injury Network (AKIN) criteria for acute kidney injury in patients undergoing cardiac surgery. *Crit Care*. 2011;15(1):R16. doi: 10.1186/cc9960.
19. Hobson CE, Yavas S, Segal MS, et al. Acute kidney injury is associated with increased long-term mortality after cardiothoracic surgery. *Circulation*. 2009;119(18):2444-2453. doi: 10.1161/CIRCULATIONAHA.108.800011.
20. Grayson AD, Khater M, Jackson M, Fox MA. Valvular heart operation is an independent risk factor for acute renal failure. *Ann Thorac Surg*. 2003;75(6):1829-1835. doi: 10.1016/s0003-4975(03)00166-8.
21. Najjar M, Salna M, George I. Acute kidney injury after aortic valve replacement: incidence, risk factors and outcomes. *Expert Rev Cardiovasc Ther*. 2015;13(3):301-316. doi: 10.1586/14779072.2015.1002467.
22. Araujo GN, Pivatto Junior F, Fuhr B, et al. Simplifying contrast-induced acute kidney injury prediction after primary percutaneous coronary intervention: the age, creatinine and ejection fraction score. *Cardiovasc Interv Ther*. 2018;33(3):224-231. doi: 10.1007/s12928-017-0472-y.
23. Laurent M, Fournet M, Feit B, et al. Simple bedside clinical evaluation versus established scores in the estimation of operative risk in valve replacement for severe aortic stenosis. *Arch Cardiovasc Dis*. 2013;106(12):651-660. doi: 10.1016/j.acvd.2013.09.001.
24. Thakar CV. Perioperative acute kidney injury. *Adv Chronic Kidney Dis*. 2013;20(1):67-75. doi: 10.1053/j.ackd.2012.10.003.
25. Hertzberg D, Sartipy U, Lund LH, Rydén L, Pickering JW, Holzmann MJ. Heart failure and the risk of acute kidney injury in relation to ejection fraction in patients undergoing coronary artery bypass grafting. *Int J Cardiol*. 2019;274:66-70. doi: 10.1016/j.ijcard.2018.09.092.
26. Callejas R, Panadero A, Vives M, Duque P, Echarri G, Monedero P; Renal Dysfunction in Cardiac Surgery Spanish Group (GEDRCC2). Preoperative predictive model for acute kidney injury after elective cardiac surgery: a prospective multicenter cohort study. *Minerva Anesthesiol*. 2019;85(1):34-44. doi: 10.23736/S0375-9393.18.12257-7.

Predictive value of NLRC3 levels for pulmonary hypertension in patients with chronic obstructive pulmonary disease

Meltem Yılmaz¹, Levent Cem Mutlu¹, Şeref Alpsoy², Aydın Akyüz², Aliye Çelikkol³, Özlem Kaymaz³

¹Department of Chest Diseases, Namık Kemal University, Faculty of Medicine, Tekirdağ, Turkey; ²Department of Cardiology, Namık Kemal University, Faculty of Medicine, Tekirdağ, Turkey; ³Department of Medical Biochemistry, Namık Kemal University, Faculty of Medicine, Tekirdağ, Turkey

ABSTRACT

Objectives: Chronic obstructive pulmonary disease (COPD) is a medical condition defined by persistent air-flow limitation and respiratory symptoms caused by airway and/or alveolar abnormalities. Pulmonary hypertension (PH) is one of the cardiovascular comorbidities associated with COPD. We investigated the correlation of NLRC3 levels in patients with COPD with prognostic and surrogate parameters of PH on echocardiography and examined whether it could be used to predict PH in this patient population.

Methods: A total of 80 patients diagnosed with COPD and 40 healthy volunteers as the control group were included in the study. The COPD group was further divided into two subgroups according to the systolic pulmonary artery pressure (sPAP) as follows: sPAP<35 mmHg and sPAP≥35 mmHg. The enzyme-linked immunosorbent assay (ELISA) method was used to determine the levels of NLRC3 in peripheral blood.

Results: Patients with sPAP≥35 mmHg had a lower mean NLRC3 level than those with sPAP<35 mmHg (P=0.006). The NLRC3 levels showed a significant negative correlation with sPAP, tricuspid regurgitation velocity, right atrium, and pulmonary artery diameter. For NLRC3, the cut-off value was found to be 271,486 ng/L, with a sensitivity of 74%, and specificity of 63% in distinguishing patients with sPAP≥35 mmHg from all patients with sPAP<35 mmHg.

Conclusion: Our study results suggest that NLRC3 levels measured from peripheral blood are predictive of PH in patients with COPD. Although the exact function of NLRC3 in the lungs, COPD, and PH have not been completely understood, we believe these findings will serve as a model for future studies.

Keywords: NLRC3, chronic obstructive pulmonary disease, pulmonary hypertension, echocardiography

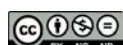
Chronic obstructive pulmonary disease (COPD) is one of the leading causes of morbidity and mortality worldwide [1]. Cardiovascular entities are the most frequent comorbidities in patients with COPD. Pulmonary hypertension (PH) is a signif-

icant cause of disease prognosis and is associated with an increased risk of exacerbation and decreased survival [2].

Potential mechanisms leading to PH in COPD; hypoxia-hypercapnia, inflammation, endothelial shear

Corresponding author: Meltem Yılmaz, MD.,
Phone: +90 282 250 51 77, E-mail: drmeltemyilmaz59@gmail.com

How to cite this article: Yılmaz M, Mutlu LC, Alpsoy Ş, Akyüz A, Çelikkol A, Kaymaz Ö. Predictive value of NLRC3 levels for pulmonary hypertension in patients with chronic obstructive pulmonary disease. Eur Res J. 2024;10(3):262-267. doi: 10.18621/eurj.1357708



This is an open access article distributed under the terms of [Creative Commons Attribution-NonCommercial-NoDerivatives 4.0 International License](https://creativecommons.org/licenses/by-nc-nd/4.0/)

Received: September 11, 2023
Accepted: December 21, 2023
Published Online: December 28, 2023

Copyright © 2024 by Prusa Medical Publishing
Available at <http://dergipark.org.tr/eurj>



stress, and endothelial dysfunction cause pulmonary vascular remodeling [2,3].

Nucleotide-oligomerization domain (NOD)-like receptor subfamily C3 (NLRC3) is a recently discovered member of the Nucleotide-binding oligomerization domain-like receptors (NLR) family that negatively regulates inflammatory responses [4, 5]. NLRs are a family of intracellular proteins that play important roles in inflammation and immunity [6]. Some researchers have recently shown that NLRC3 has a role in cell antiproliferation and promoting proapoptotic signals by inhibiting cell proliferation and inflammation [7].

The study aimed to determine the correlation of NLRC3 levels with the prognostic and supportive parameters of PH in echocardiography in COPD patients and to determine its clinical utility in the prediction of PH in these patients.

METHODS

Study Design and Population

This single-center, cross-sectional was conducted at the Department of Chest Diseases of a tertiary care center between June 2020 and November 2020. A total of 80 patients with stable COPD over 40 years of age who were spirometrically diagnosed with COPD according to the 2020 Global Initiative for Chronic Obstructive Lung Disease (GOLD) guidelines and met the inclusion criteria were included. The control group consisted of 40 healthy volunteers. Inclusion criteria for the patient group were age ≥ 40 years, a diagnosis of COPD, post-bronchodilator FEV1/FVC $< 70\%$, and giving consent for participation in the study. Patients having a recent COPD exacerbation or pneumonia within the previous four weeks, having coronary artery disease, obstructive sleep apnea diagnosis by polysomnography, bronchiectasis, asthma, malignancies, diabetes, and known chronic liver and/or kidney disease were excluded from the study. The COPD group was divided into two groups according to the systolic pulmonary artery pressure (sPAP) as follows: 41 patients with sPAP < 35 mmHg and 39 patients with sPAP ≥ 35 mmHg. For the healthy control group, 40 individuals were selected and divided into two groups smokers and non-smokers, including 20 individuals in each group.

Before this cross-sectional study, all participants were informed about the nature of the study and written informed consent was obtained. The study protocol was approved by the the Tekirdağ Namık Kemal University, Non-Interventional Clinical Research Ethics Committee (No: 2019.164.09.24, date: 24/09/2019). The study was conducted on the principles of the Declaration of Helsinki. Informed consent was obtained from all individual participants included in the study

Blood samples

Blood samples from peripheral veins were centrifuged at 4 °C for 20 min and stored at -80 °C until analysis. On the analysis day, stored samples were brought to room temperature, and NLRC3 serum levels were measured by ELISA using commercially available kits. (Human NLR Family, CARD Domain Containing 3 ELISA KIT, Bioassay Technology Laboratory Shanghai, China # E6709Hu).

Echocardiography

Echocardiographic measurements were performed by the same cardiologist according to ACC/AHA/ASE 2003 Guideline Update for the Clinical Application of Echocardiography (<https://doi.org/10.1161/01.CIR.0000073597.57414.A9>).

Statistical Analysis

Statistical analysis was performed using the SPSS for Mac version 22.0 software (IBM Corp., Armonk, NY, USA). The normality of numerical variables was analyzed using the Shapiro–Wilk or Kolmogorov–Smirnov test, where appropriate. Descriptive data were presented in mean \pm standard deviation (SD), and median (min–max) for continuous numerical variables, and in number and frequency for categorical variables. To compare the continuous variables between the groups, the independent samples t-test or one-way analysis of variance (ANOVA) was used for normally distributed variables, whereas the Mann–Whitney U analysis or Kruskal–Wallis test was used for non-normally distributed variables. The homogeneity of variance was checked using the Levene test. The Welch test was used to analyze parameters with a non-homogeneous distribution. A P-value < 0.05 was considered statistically significant. Tamhane’s T2 test was used as the post-hoc test to determine which groups resulted in a significant difference. A P-value

Table 1. Demographic characteristics of patients

Variables	COPD group		Control group	
	sPAP <35 mmHg (n=41)	sPAP ≥35 mmHg (n=39)	Smokers (n=20)	Non-smokers (n=20)
Gender				
Female/Male	8/35	8/31	8/12	9/11
Age (years)	61.34±8.61 (44-80)	65.72±7.20 (55-82)	59.25±8.39 (44-74)	59.45±7.68 (48-72)
Smoking (pack/year)	48.40±24.60 (0-120)	49.06 ±21.05 (0-100)	27.05 ±10.93 (10-45)	0
BMI (kg/m²)	26.69±3.84 (20.67-37.46)	25.68±4.62 (15.60-35.90)	28.38±3.89 (22.03-37.46)	28.26±5.13 (20.43-41.01)

Data are shown as mean±standard deviation (minimum-maximum). COPD=Chronic obstructive pulmonary disease, sPAP=Systolic pulmonary artery pressure, BMI=Body mass index

<0.008 was considered statistically significant for the post-hoc analysis. The Spearman correlation analysis was used to compare two continuous numerical variables, whereas the Pearson correlation analysis was used to compare categorical variables. The receiver operating characteristic (ROC) analysis was performed to identify the predictors of PH with an area under the curve (AUC) and 95% confidence interval (CI).

RESULTS

A total of 80 COPD patients and 40 healthy individuals were included in this study. There was no statistically significant difference between the groups in terms of age, sex, and body mass index (BMI). The demographic characteristics of the patients are shown in Table 1.

The NLRC3 level was found to be significantly different between the groups ($P<0.001$). Although

NLRC3 level was lower in the group with COPD with sPAB≥35 mmHg, no statistically significant difference was found between COPD without sPAB<35 mmHg in post-hoc analyses ($P=0.628$). When the whole COPD group was compared with the control group, the NLRC3 level was found to be significantly lower in the COPD group ($P=0.002$). When the sPAB≥35 mmHg group was compared with the group that included all patients with sPAB<35 mmHg, NLRC3 levels were found to be significantly lower in the group with sPAB≥35 mmHg ($P=0.006$). NLRC3 results are shown in Table 2. In correlation analysis, a negative correlation was observed between NLRC3 levels and sPAB, tricuspid regurgitation velocity (TRV), right atrium (RA) diameter, and pulmonary artery (PA) diameter (Table 3).

The ROC analysis revealed a cut-off value of 271,486 ng/L, with 74% sensitivity and 63% specificity in distinguishing patients with sPAP ≥35 mmHg from all patients with sPAP <35 mmHg (Table 4).

Table 2. NLRC3 levels

	COPD group		Control group	
	sPAP <35 mmHg	sPAP ≥35 mmHg	Smoker	Non-smoker
NLRC3 (ng/L)	387.52±292.10 (163.67-1256.69)	304.09±220.16 (86.226-1047.36)	317.23±204.47 (117.04-949.05)	800.74±572.23 (264.78-1804.99)

Data are shown as mean±standard deviation (minimum-maximum). COPD=Chronic obstructive pulmonary disease, sPAP=Systolic pulmonary artery pressure

Table 3. The correlation between NLRC3 and echocardiographic parameters in the overall patient group

	NLRC3	
	<i>r</i>	P value
TRV	-0,253	0.005
sPAP	-0,299	0.001
PA diameter	-0,270	0.003
RA	-0,276	0.002

sPAP=Systolic Pulmonary Artery Pressure, TRV=Tricuspid regurgitation velocity, PA=Pulmonary artery, RA=Right atrium.

r =correlation coefficient, P<0.05

DISCUSSION

COPD is the leading cause of morbidity and mortality worldwide. In the GOLD 2023 report, it is estimated that the increased prevalence of smoking in LMICs coupled with aging populations in high-income countries will result in over 5.4 million annual deaths from COPD and related conditions by 2060 [1]. Cardiovascular comorbidities are the most common comorbidity in COPD, among which PH is a serious condition that determines the prognosis of the disease and is associated with an increased risk of exacerbations and reduced survival [2]. Although the echocardiographic examination is not a definitive diagnostic method for PH, it is an essential, easily accessible, non-invasive diagnostic method in the follow-up of confirmed patients by screening patients in the PH risk group, and providing support and diagnosing clinically [2, 8]. Our results showed that the mean NLRC3 levels were significantly different between the groups. There was a statistically significant negative correlation between

NLRC3 levels and sPAP, TRV, RA diameter, and PA diameter.

Nucleotide-binding oligomerization domain-like receptors (NLRs) belong to an intracellular protein family that has important roles in inflammation and immunity [4, 5]. NLRC3 is a newly discovered member of the NLR family and has been described as a negative regulator of the inflammatory response [6]. It is involved in the inhibition of cellular proliferation and the promotion of pro-apoptotic signals [7]. NLRC3 is expressed in macrophages and lymphocytes. Its expression in lung tissue remains controversial [9, 10].

In a 2018 study by Zha *et al.* [7] involving 40 patients (diagnosed as having PH with RHC) and 20 healthy controls, PH patients were found to have significantly lower NLRC3, which also negatively correlated with mPAP and PVR. However, ECHO parameters did not correlate with NLRC3 levels, and no negative correlations with WHOFC were also found. An NLRC3 cut-off of 2.897 ng/L was found to be 88% sensitive and 85% specific for predicting the presence of PHT. These authors concluded that NLRC3 concentrations could be used as a diagnostic and prognostic tool for PHT and that their observations warranted further study [7].

Our findings are consistent with literature data, indicating significantly lower NLRC3 levels in patients with elevated pulmonary artery pressure. Additionally, negative correlations of NLRC3 with TRV, sPAP, RA diameter, and PA diameter were found.

Right atrial dilation is common in PH patients as a result of right ventricular failure, increased right ventricular diastolic pressure, functional tricuspid failure, and increased right atrial dimensions representing a poor prognostic sign [11]. According to our results, TRV and RA diameter negatively correlate with

Table 4. ROC analysis for NLRC3

Area Under Curve				
Test result for NLRC3 variable				
Area	Standard error ^a	Asymptotic Sig. ^b	95% Confidence interval for the odds ratio	
			Lower limit	Upper limit
,655	,052	,006	,554	,756

a. Under non-parametric assumptions.

b. Null hypothesis: actual area = 0.5

NLRC3, and we believe that this might be useful in screening and monitoring these patients.

One of the most important mechanisms for the development of PH in COPD patients involves chronic inflammation and vascular remodeling. Activation of phosphoinositide 3-kinase (PI3K) plays a critical role in the vascular remodeling of the pulmonary vasculature in PH [6, 12]. NLRC3 has been shown to inhibit cellular proliferation and inflammation, through the inhibition of the PI3K signals in colorectal cancer [6]. Based on these observations, Zha *et al.* [12] published their study in 2019 that showed reduced levels of NLRC3 in pulmonary arteries as well as in pulmonary arterial smooth muscle cells stimulated with platelet-derived growth factor -BB (PDGF-BB) in animal models of PH. Administration of NLRC3 protein for therapeutic purposes resulted in decreased right ventricular systolic pressure, reduced pulmonary vascular remodeling, and alleviation of proliferation, migration, and inflammation [12]. Our results are consistent with these results and showed reduced NLRC3 levels in patients with elevated pulmonary arterial pressure as compared to other study groups. Since our samples were limited to peripheral blood, we may assume that NLRC3 may be related to the development of PH in COPD patients, although it is obvious that further studies are required to better understand the role of NLRC3 in PH.

Most of the previous publications regarding NLRC3 focused on malignant conditions and immunity. To the best of our knowledge, no previous studies examined the role and effect of NLRC3 in COPD patients or the development of PH in COPD. Therefore, we believe that our study may represent the first of its kind.

The disease burden associated with COPD is continuously increasing. PH in COPD patients is an established risk factor for worse prognosis and increased mortality, underscoring the importance of detecting and screening PH. Our data suggest that NLRC3 levels may be predictive of PH in COPD patients. PH occurs via multiple mechanisms in COPD. Furthermore, the exact function(s) of NLRC3 in COPD and PH are yet to be elucidated. Therefore, we believe that our findings may provide some guidance for future studies.

Limitations

This study had certain limitations. First, as right

heart catheterization could not be performed in our patients, the elevation of mean pulmonary artery pressure could not be definitively proven. Second, our study had a single-center design, which precludes the generalizability of the results. Finally, the use of biomarkers regularly in our study would incur a certain expense. Therefore, additional studies are warranted to establish which groups should be screened. In our study, those with sPAP ≥ 35 mmHg were older on average and had a lower BMI, although no statistically significant difference was present. In addition, DLCO and FEV1 values were lower in this group of patients. For screening, we recommend using our biomarker primarily in these patients.

CONCLUSION

Our results indicate a significant reduction in NLRC3 levels measured in peripheral blood samples from COPD patients presenting with PH. NLRC3 also was found to have a significant negative correlation with sPAP, TRV, RA, and PA diameter, which are ECHO parameters supportive of a diagnosis of PH and which also have prognostic implications. We believe that this biomarker may be predictive of PH in this setting. The role of NLRC3 in lungs, COPD patients, and PH is still unknown, indicating the need for further studies.

Authors' Contribution

Study Conception: MY, LCM; Study Design: MY, LCM; Supervision: LCM; Funding: MY, LCM; Materials: MY, LCM, SA, AA, AÇ, ÖK; Data Collection and/or Processing: MY, LCM, SA, AA, AÇ, ÖK; Statistical Analysis and/or Data Interpretation: MY, LCM; Literature Review: MY; Manuscript Preparation: MY and Critical Review: LCM.

Conflict of interest

The authors disclosed no conflict of interest during the preparation or publication of this manuscript.

Financing

This study was funded by the Coordination Unit of Scientific Research Projects, Tekirdağ Namık Kemal University (project number: NKUBAP.02.TU.20.249).

REFERENCES

1. Global Strategy for the Diagnosis, Management and Prevention of COPD, Global Initiative for Chronic Obstructive Lung Disease (GOLD) 2023. Available from: <https://goldcopd.org/2023-gold-report-2/> Accessed on September 1, 2023.
2. Jyothula S, Safdar Z. Update on pulmonary hypertension complicating chronic obstructive pulmonary disease. *Int J Chron Obstruct Pulmon Dis.* 2009;4:351-63. doi: 10.2147/copd.s5102.
3. Seeger W, Adir Y, Barberà JA, et al. Pulmonary hypertension in chronic lung diseases. *J Am Coll Cardiol.* 2013;62(25 Suppl):D109-116. doi: 10.1016/j.jacc.2013.10.036.
4. Davis BK, Wen H, Ting JP. The inflammasome NLRs in immunity, inflammation, and associated diseases. *Annu Rev Immunol.* 2011;29:707-735. doi: 10.1146/annurev-immunol-031210-101405.
5. Chen G, Shaw MH, Kim YG, Nuñez G. NOD-like receptors: role in innate immunity and inflammatory disease. *Annu Rev Pathol.* 2009;4:365-398. doi: 10.1146/annurev.pathol.4.110807.092239.
6. Karki R, Man SM, Malireddi RKS, et al. NLRC3 is an inhibitory sensor of PI3K-mTOR pathways in cancer. *Nature.* 2016;540(7634):583-587. doi: 10.1038/nature20597.
7. Zha LH, Zhou J, Li TZ, et al. NLRC3: a novel noninvasive biomarker for pulmonary hypertension diagnosis. *Aging Dis.* 2018;9(5):843-851. doi: 10.14336/AD.2017.1102.
8. Chaouat A, Naeije R, Weitzenblum E. Pulmonary hypertension in COPD. *Eur Respir J.* 2008;32(5):1371-1385. doi: 10.1183/09031936.00015608.
9. Chaput C, Sander LE, Suttorp N, Opitz B. NOD-like receptors in lung diseases. *Front Immunol.* 2013;4:393. doi: 10.3389/fimmu.2013.00393.
10. Schneider M, Zimmermann AG, Roberts RA, et al. The innate immune sensor NLRC3 attenuates Toll-like receptor signaling via modification of the signaling adaptor TRAF6 and transcription factor NF- κ B. *Nat Immunol.* 2012;13(9):823-831. doi: 10.1038/ni.2378.
11. Ghio S, Klersy C, Magrini G, et al. Prognostic relevance of the echocardiographic assessment of right ventricular function in patients with idiopathic pulmonary arterial hypertension. *Int J Cardiol.* 2010;140(3):272-278. doi: 10.1016/j.ijcard.2008.11.051.
12. Zha LH, Zhou J, Li TZ, et al. NLRC3 inhibits MCT-induced pulmonary hypertension in rats via attenuating PI3K activation. *J Cell Physiol.* 2019;234(9):15963-15976. doi: 10.1002/jcp.28255.

Relationship of breast arterial calcification and radiotherapy

Gökhan Karataş¹, Osman Kula², Nermin Tunçbilek²

¹Department of Radiology, VM Medical Park Bursa Hospital, Bursa, Turkey; ²Department of Radiology, Trakya University, Faculty of Medicine, Edirne, Turkey

ABSTRACT

Objectives: The purpose of this research is to compare the pre and post-radiotherapy mammograms of patients who had breast-conserving surgery (BCS) and radiotherapy to see how radiotherapy affects breast arterial calcifications (BAC).

Methods: The study retrospectively compared the mammography examinations at least 24 months after radiotherapy and pre-radiotherapy mammography examinations of 123 female patients diagnosed with breast cancer and treated with BCS and radiotherapy between December 2001 and July 2011.

Results: Breast arterial calcifications (BAC) increased statistically significantly in 25 patients who underwent radiotherapy after BCS.

Conclusion: Our results indicate that BAC increases significantly after RT, especially in breasts treated with radiotherapy, with age being also a risk factor for BAC development.

Keywords: Breast arterial calcification, radiotherapy, mammography

Breast cancer is the most frequent cancer in women worldwide, except from non-melanoma skin cancer [1]. Breast cancer accounts for approximately 30% of all malignancies diagnosed among the adult women [2].

Breast-conserving surgery (BCS) followed by radiation therapy (RT) is the preferred treatment for early-stage breast cancer [3-6]. Administration of RT following BCS can be greatly reduce the recurrences and the breast cancer deaths [3-6]. Yet, there is worry that radiation therapy may have an effect on the cardiovascular architecture and other comorbidities [7, 8].

Breast arterial calcifications (BAC) are medial calcifications that are a manifestation of arteriosclerosis [9, 10]. Calcification in the medial layer occurs independently of atherosclerosis or inflammation, happens

in both small and big arteries, and is considered harmful as it lowers arterial compliance [11]. BAC has also been linked to hypertension, diabetes, and cardiovascular diseases in some studies [12-14]. However, only one study was found in the literature examining the relationship between BAC and RT [15].

In this study, we examined the relationship between RT and BAC with the hypothesis that RT would increase BAC by predicting that BAC is a form medial arteriosclerosis.

METHODS

This study retrospectively evaluated 123 female patients who had BCS due to breast cancer and then re-

Corresponding author: Gökhan Karataş, MD.,
Phone: +90 224 270 60 00, E-mail: gokhankaratas1984@gmail.com

Received: October 28, 2023
Accepted: November 28, 2023
Published Online: December 29, 2023

How to cite this article: Karataş G, Kula O, Tunçbilek N. Relationship of breast arterial calcification and radiotherapy. Eur Res J. 2024;10(3):268-275. doi: 10.18621/eurj.1382545

Copyright © 2024 by Prusa Medical Publishing
Available at <http://dergipark.org.tr/eurj>



This is an open access article distributed under the terms of [Creative Commons Attribution-NonCommercial-NoDerivatives 4.0 International License](https://creativecommons.org/licenses/by-nc-nd/4.0/)



ceived RT between December 2001 and July 2011 at Trakya University Medical Faculty Hospital. This study was approved Trakya University Faculty of Medicine Non-Interventional Clinical Research Ethics Committee under protocol number TÜTF-GOKAEK 2012/179 dated 22/02/2012.

All patients underwent BCS and RT, and regular control mammography was done at Trakya University Faculty of Medicine's Department of Radiology and evaluated by consensus of a resident radiologist and a 10 year experienced Radiologist in Breast Radiology. The research included only individuals with routine control mammography who underwent BCS and RT. In the inclusion criteria, a period of at least 2 years after RT was looked for in cases where RT was performed following BCS.

Cases with a length of less than two years and cases with inaccessible personal background material were excluded from the research. A personal history form asking chronic illnesses such as age, smoking, diabetes, hypertension, cardiac diseases, malignancy, and stroke was regularly filled out in all cases during

the pre-surgical time.

The mammography images of the cases who applied between December 2001 and July 2011 are returned to the workstation from MIMS (Mammography Image Management Solutions), the digital archive of the full-field digital mammography 'Selenia Digital Mammography System' (2008 Lorad, Hologic, USA) device in the Radiology Department. It was evaluated by calling or examining old conventional mammography films.

In all cases evaluated with full-field digital mammography, images were obtained from both breasts in standard CC and MLO positions. Additional radiographs for diagnostic purposes (spot compression, magnification, axillary, mediolateral, rounded inner and outer quadrant images) were taken in cases deemed necessary. In the digital mammography archive system, mammography images are compressed by 1/3 and archived and images can be recalled without loss of information. Digital mammography images were evaluated on a Barco MGD 521 M, 2x2.5 K medical monitor. This monitor is a 5 Megapixel medical monitor designed to display digital mammography images.

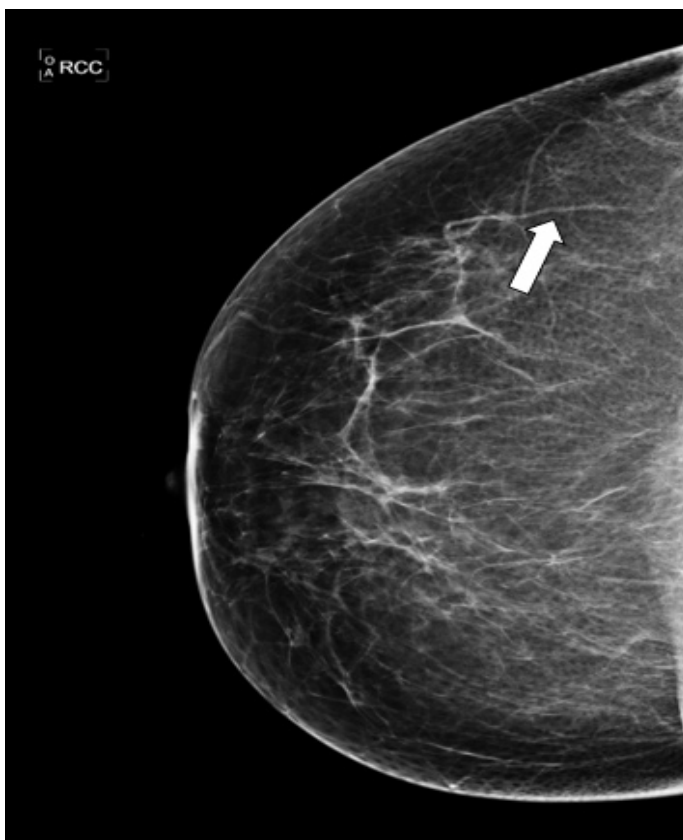


Fig. 1. Grade 1 breast arterial calcification(arrow).



Fig. 2. Grade 2 breast arterial calcification (arrow).



Fig. 3. Breast arterial calcification (arrow).

In the study, BACs detected by mammography were graded from zero to three by consensus according to the literature [16].

Grade 0 (none): No surrounded calcium.

Grade 1 (mild): Artery or arteries are slightly surrounded by calcium (Fig. 1).

Grade 2 (moderate): Artery or arteries are markedly surrounded by calcium (Fig. 2).

Grade 3 (severe): Artery or arteries are surrounded by a prominent and thick column of calcium (Fig. 3). With this grading system, pre and post-RT mammograms of all cases were evaluated and recorded in terms of BAC by consensus of a resident radiologist and a 10 year experienced Radiologist in Breast Radiology.

Statistical Analysis

The analyses were carried out using the IBM Statistics V19 application. Descriptive Statistical Metrics for qualitative variables include frequency and per-

centage, whereas quantitative variables include mean, standard deviation, minimum, maximum, and median. Chi-square analysis was used to investigate the relationships between qualitative variables. Pearson Chi-square in cross tables when the predicted incidence of variable does not exceed 20%, and Final Test results in cross tables where it exceeds 20%.

RESULTS

The mean age of the patients participating in the study ranged from 30 to 76, with a mean age of 48 (Table 1). All 123 patients in the research were diagnosed with primary breast cancer and got BCS+RT treatment.

When the accompanying systemic diseases were investigated, there was hypertension (HT) in 14 cases (11.4%), multiple chronic diseases in 11 (8.9%) cases, chronic liver disease in 1 (0.8%) case, and chronic kidney disease in 1 (0.8%) case. One (0.8%) patient (0.8%) had hypothyroidism and 1 (0.8%) patient had hyperthyroidism. No systemic pathology was observed in the remaining 94 (76.4%) cases (Table 1). Twenty (16.3%) patients were smokers.

Prior to RT, BAC was detected in 9 (7.3%) out of 123 cases, while 114 (92.7%) cases showed no evi-

Table 1. Characteristics of the subjects included in the study

Characteristics	Data
Age (years)	48±8.872 (30-76)
Time elapsed after radiotherapy (years)	7±2.4 (3-12)
Comorbidities, n (%)	
None	94 (76.4)
Hypertension	14 (11.4)
Multiple chronic diseases	11 (8.9)
Chronic liver disease	1 (0.8)
Chronic kidney disease	1 (0.8)
Hyperthyroidism	1 (0.8)
Hypothyroidism	1 (0.8)

Data are shown as mean±standard deviation or minimum-maximum or n (%)

Table 2. Number of people with mammographic breast arterial calcification before radiotherapy

n=123	Pre-RT BAC (+)
Breasts Underwent RT, n (%)	9 (7.3)
Contralateral Breasts, n (%)	9 (7.)

RT=Radiotherapy, BAC=Breast Arterial Calcification

dence of BAC (Table 3). Similarly, in the contralateral breast, BAC was found in 9 (7.3% cases) and not detected in 114 (92.7%) cases prior to RT (Table 2).

The cases who underwent RT were compared in terms of pre- and post-RT BAC. There was an increase in BAC in 25 (20.3%) patients, and an increase in BAC was found in both breasts in 7 (5.7%) of these patients. The increase in BAC on the side that underwent RT was found to be statistically significant (P<0.001) (Table 3).

Pre- and post-RT BAC increase in both breasts was detected in 7 (5.6%) cases, with a mean age of 55 years. It was statistically significant that the increase in BAC in the cases was compatible with age (P<0.001) (Table 4).

There was no cigarette smoking in the cases with increased BAC after post-RT. In our study, when pre-RT BAC and post-RT BAC were compared, no statis-

tically significant relationship was found between smoking and increased BAC.

The duration of the RT treatments to the post-RT mammograms we have evaluated of the cases ranged from a minimum of 3 years to a maximum of 13 years. There was no statistically significant relationship between the time elapsed after RT and BAC (P>0.05).

Case 1: In the control MG of a 50-year-old patient who underwent RT after BCS, did not have a history of comorbid disease, and was a non-smoker, shows increase in BAC was found on the side with BC and underwent RT (Fig. 4).

Case 2: No increase in BAC was detected in the control MG after 3 years of a 64-year-old patient who underwent RT after BCS, had a history of known HT for 5 years, and was a non-smoker (Fig. 5).

DISCUSSION

In this study, we evaluated the relationship between RT and Breast Arterial Calcification (BAC) by using mammography. The results showed that BAC increased significantly after RT only in the breasts underwent RT.

There is only one research [15] studied the impact of RT on BAC that we could find in the English liter-

Table 3. Increased mammary arterial calcification in pre- and post-radiotherapy mammograms of both breasts

	Pre-RT BAC case number	Post-RT BAC case number	Increase in BAC case number	(%)
Breasts Underwent RT	9	26	25	20.3
Contralateral Breasts	9	16	10	8.1

RT=Radiotherapy, BAC=Breast Arterial Calcification

Table 4. The relationship of increased arterial calcification of the breast between breasts receiving and not receiving radiotherapy

	No increase in BAC case number	Increase in BAC case number	Mean age of the Increase in BAC
Breasts Underwent RT	98	25	47
Contralateral Breasts	113	10	50
Bilateral	116	7	55

RT=Radiotherapy, BAC=Breast Arterial Calcification

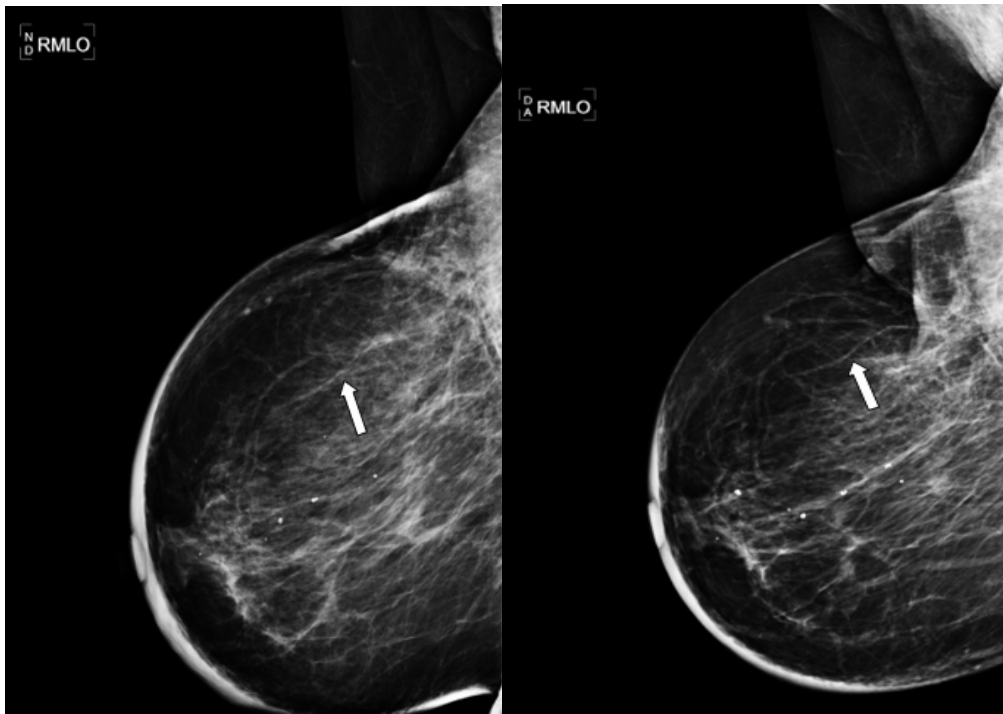


Fig. 4. Arterial calcification of the breast at 1 and 4 years after radiotherapy (arrows).

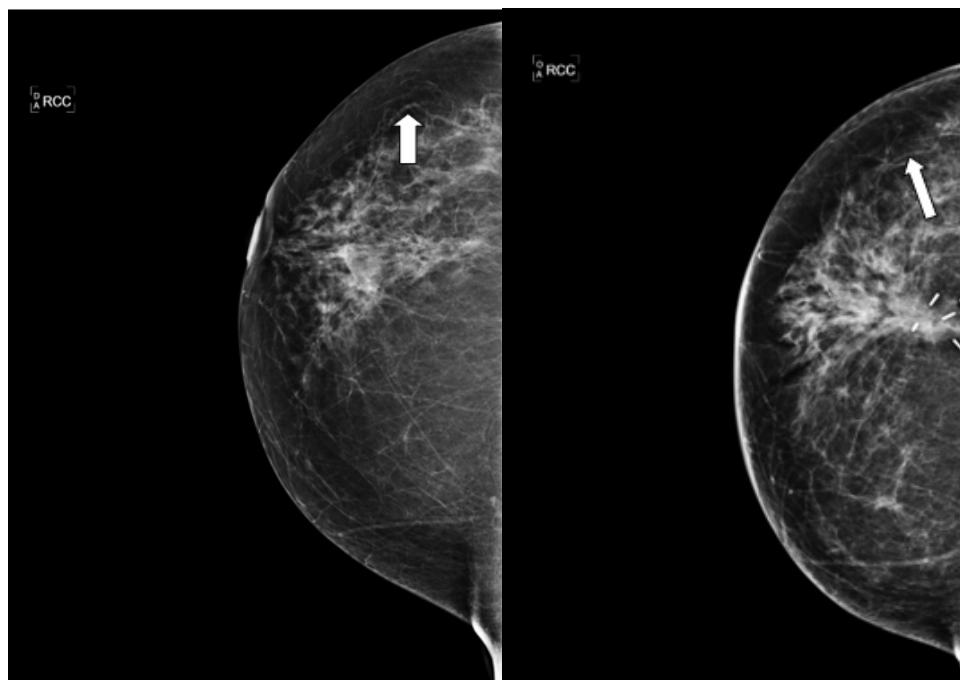


Fig. 5. No change was detected in breast arterial calcification after radiotherapy (arrows).

ature. Yet, they discovered differences in their research. They reported no statistically significant relationship between BAC observed on baseline mammography and BAC found on follow-up (post-RT) mammography and later cardiac events. They found that subdividing individuals with a left-sided tumor based on BAC did not predict cardiac events either [15].

We attribute the existence of different results to the diversity of study populations and the complexity of the relationship between the diseases that we think may affect cardiovascular events, let alone the fact that radiotherapy in a patient with breast cancer causes an intense pathophysiological change. Therefore, it is crucial to conduct further research to better understand the relationship between RT and BAC [17].

Radiation damage to artery walls, followed by accelerated arteriosclerosis development in the irradiated arteries, is a well-documented phenomena in both experimental animals [18-20] and humans [9, 16, 21, 22].

A meta-analysis [16] found that while radiation therapy reduced local recurrence in individuals with early breast cancer, there was a statistically significant rise in blood vessel-related mortality 10 years later [16]. This study found that RT leads to long-term vascular illness [16]. Another study reported that women with a history of cardiac illness who had radiation therapy for left-sided breast cancer had higher incidence of Percutaneous Cardiac Interventions (PCI) and a worse chance of survival if treated with PCI [9]. In patients getting RT for breast cancer, Roos *et al.* [21] discovered a direct link between the calcium value of the coronary artery prior to treatment with acute coronary events.

However, we should also mention that there are studies reporting different results in the literature on this subject. A study conducted in 2018 showed no variation in the incidence of cardiac side effects observed in standard and hypofraction RT systems [22].

Another meta-analysis suggested BAC as an expression of arteriosclerosis and reported that it appears to be related with an elevated risk of cardiovascular disease events while only being associated with part of the recognized cardiovascular risk factors [9]. Osman *et al.* [23] found a statistically significant association between BAC and Coronary Artery Disease (CAD). They suggest that BAC is a potential noninvasive imaging marker that may improve CAD risk

prediction in women. A different meta-analysis showed that BAC is highly associated with both CAD and stroke [24].

Our study also found a statistically significant difference in the mean age of the cases with increased BAC in both breasts compared to the cases without BAC increase or only on the side that underwent RT. This result suggests that age may be a risk factor for the development of BAC after RT. Topal *et al.* investigated the relationship between BAC detected in mammography and Cardiovascular diseases (CVD); they found a relationship between BAC and age and duration of menopause [16]. Hendriks *et al.* [9] showed a clear and constant link between increasing age and the prevalence of BAC.

Smoking was also evaluated in our study, and no statistically significant result was found between smoking and BAC increase. Shah *et al.* [25] reported reduced prevalence of BAC among women who smoke. Hendriks *et al.* [9] are also in line with the results in their meta-analysis.

Limitations

While our findings provide insight on the relation between RT and BAC, it is necessary to appreciate the limitations of our study. The following might have impacted the validity of our findings. Firstly, because the study is retrospective in nature, it may have limitations in terms of data accuracy and completeness. Secondly, the study's sample size is relatively small, which can reduce the statistical power and precision of the results. Finally, the interobserver variability of the grading method used to evaluate BAC was not assessed in the study, which may have affected the reliability of the results.

CONCLUSION

As a conclusion, our research provides insight on the long-term effects of radiation on BAC. Our results indicate that BAC increases considerably after RT, especially in RT-affected breasts, with age being also a risk factor for BAC development.

Keypoints

(1) Administration of Radiotherapy (RT) following Breast Conserving Surgery (BCS) can be greatly

reduce the recurrences and the breast cancer deaths [3-6]. Yet, there is worry that radiation therapy may have an effect on the cardiovascular architecture and other comorbidities [7, 8].

(2) Breast arterial calcifications (BAC) are medial calcifications that are a manifestation of arteriosclerosis [9, 10].

(3) In our study the results showed that BAC increased significantly after RT only in the breasts underwent RT.

Authors' Contribution

Study Conception: NT, GK; Study Design: NT, GK; Supervision: NT; Funding: GK; Materials: GK; Data Collection and/or Processing: GK; Statistical Analysis and/or Data Interpretation: OK, NT; Literature Review: OK, GK; Manuscript Preparation: GK and Critical Review: GK, OK, NT.

Conflict of interest

The authors disclosed no conflict of interest during the preparation or publication of this manuscript.

Financing

The authors disclosed that they did not receive any grant during conduction or writing of this study.

REFERENCES

- Bray F, Ferlay J, Soerjomataram I, Siegel RL, Torre LA, Jemal A. Global cancer statistics 2018: GLOBOCAN estimates of incidence and mortality worldwide for 36 cancers in 185 countries. *CA Cancer J Clin.* 2018;68(6):394-424. doi: 10.3322/caac.21492.
- Siegel RL, Miller KD, Jemal A. Cancer statistics, 2019. *CA Cancer J Clin.* 2019;69(1):7-34. doi: 10.3322/caac.21551.
- Breast Cancer. National Comprehensive Cancer Network: National Clinical Practice Guidelines in Oncology. Version 3. 2018. https://www.nccn.org/professionals/physician_gls/pdf/breast.pdf
- Fisher B, Jeong JH, Anderson S, Bryant J, Fisher ER, Wolmark N. Twenty-five-year follow-up of a randomized trial comparing radical mastectomy, total mastectomy, and total mastectomy followed by irradiation. *N Engl J Med.* 2002;347(8):567-575. doi: 10.1056/NEJMoa020128.
- Early Breast Cancer Trialists' Collaborative Group (EBCTCG); Darby S, McGale P, Correa C, et al. Effect of radiotherapy after breast-conserving surgery on 10-year recurrence and 15-year breast cancer death: meta-analysis of individual patient data for 10,801 women in 17 randomised trials. *Lancet.* 2011;378(9804):1707-1716. doi: 10.1016/S0140-6736(11)61629-2.
- EBCTCG (Early Breast Cancer Trialists' Collaborative Group); McGale P, Taylor C, Correa C, et al. Effect of radiotherapy after mastectomy and axillary surgery on 10-year recurrence and 20-year breast cancer mortality: meta-analysis of individual patient data for 8135 women in 22 randomised trials. *Lancet.* 2014;383(9935):2127-2135. doi: 10.1016/S0140-6736(14)60488-8.
- Grantzau T, Overgaard J. Risk of second non-breast cancer among patients treated with and without postoperative radiotherapy for primary breast cancer: a systematic review and meta-analysis of population-based studies including 522,739 patients. *Radiother Oncol.* 2016;121(3):402-413. doi: 10.1016/j.radonc.2016.08.017.
- Boero IJ, Paravati AJ, Triplett DP, et al. Modern radiation therapy and cardiac outcomes in breast cancer. *Int J Radiat Oncol Biol Phys.* 2016;94(4):700-708. doi: 10.1016/j.ijrobp.2015.12.018.
- Hendriks EJ, de Jong PA, van der Graaf Y, Mali WP, van der Schouw YT, Beulens JW. Breast arterial calcifications: a systematic review and meta-analysis of their determinants and their association with cardiovascular events. *Atherosclerosis.* 2015;239(1):11-20. doi: 10.1016/j.atherosclerosis.2014.12.035.
- Duhn V, D'Orsi ET, Johnson S, D'Orsi CJ, Adams AL, O'Neill WC. Breast arterial calcification: a marker of medial vascular calcification in chronic kidney disease. *Clin J Am Soc Nephrol.* 2011;6(2):377-382. doi: 10.2215/CJN.07190810.
- Blacher J, Guerin AP, Pannier B, Marchais SJ, London GM. Arterial calcifications, arterial stiffness, and cardiovascular risk in end-stage renal disease. *Hypertension.* 2001;38(4):938-942. doi: 10.1161/hy1001.096358.
- Rotter MA, Schnatz PF, Currier AA Jr, O'Sullivan DM. Breast arterial calcifications (BACs) found on screening mammography and their association with cardiovascular disease. *Menopause.* 2008;15(2):276-281. doi: 10.1097/gme.0b013e3181405d0a.
- Topal U, Kaderli A, Topal NB, et al. Relationship between the arterial calcification detected in mammography and coronary artery disease. *Eur J Radiol.* 2007;63(3):391-395. doi: 10.1016/j.ejrad.2007.01.035.
- Chadashvili T, Litmanovich D, Hall F, Slanetz PJ. Do breast arterial calcifications on mammography predict elevated risk of coronary artery disease? *Eur J Radiol.* 2016;85(6):1121-1124. doi: 10.1016/j.ejrad.2016.03.006.
- Soran O, Vargo JA, Polat AV, Soran A, Sumkin J, Beriwal S. No association between left-breast radiation therapy or breast arterial calcification and long-term cardiac events in patients with breast cancer. *J Womens Health (Larchmt).* 2014;23(12):1005-1011. doi: 10.1089/jwh.2014.4748.
- Maas AH, van der Schouw YT, Mali WP, van der Graaf Y. Prevalence and determinants of breast arterial calcium in women at high risk of cardiovascular disease. *Am J Cardiol.* 2004;94(5):655-659. doi: 10.1016/j.amjcard.2004.05.036.
- Cihan YB. Can radiotherapy for breast cancer increase breast arterial calcification? *Natl Med J India.* 2019;32(3):190. doi: 10.4103/0970-258X.278680.
- GOLD H. Production of arteriosclerosis in the rat. Effect of x-ray and a high-fat diet. *Arch Pathol.* 1961;71:268-273.
- Aarnoudse MW, Lamberts HB. Arterial wall damage by X-rays and fast neutrons. *Int J Radiat Biol Relat Stud Phys Chem Med.* 1977;31(1):87-94. doi: 10.1080/09553007714550081.
- Marcial-Rojas RA, Castro JR. Irradiation injury to elastic arteries in the course of treatment for neoplastic disease. *Ann Otol Rhinol*

- Laryngol. 1962;71:945-958. doi: 10.1177/000348946207100408.
21. Roos CTG, van den Bogaard VAB, Greuter MJW, et al. Is the coronary artery calcium score associated with acute coronary events in breast cancer patients treated with radiotherapy? *Radiother Oncol.* 2018;126(1):170-176. doi: 10.1016/j.radonc.2017.10.009.
22. James M, Swadi S, Yi M, Johansson L, Robinson B, Dixit A. Ischaemic heart disease following conventional and hypofractionated radiation treatment in a contemporary breast cancer series. *J Med Imaging Radiat Oncol.* 2018;62(3):425-431. doi: 10.1111/1754-9485.12712.
- 23 Osman M, Regner S, Osman K, et al. Association between breast arterial calcification on mammography and coronary artery disease: a systematic review and meta-analysis. *J Womens Health (Larchmt).* 2022;31(12):1719-1726. doi: 10.1089/jwh.2020.8733.
24. Jiang X, Clark M, Singh RK, Juhn A, Schnatz PF. Association of breast arterial calcification with stroke and angiographically proven coronary artery disease: a meta-analysis. *Menopause.* 2015;22(2):136-143. doi: 10.1097/GME.0000000000000300.
25. Shah N, Chainani V, Delafontaine P, Abdo A, Lafferty J, Abi Rafeh N. Mammographically detectable breast arterial calcification and atherosclerosis. *Cardiol Rev.* 2014;22(2):69-78. doi: 10.1097/CRD.0b013e318295e029.

Evaluation of mercury in skin lightening creams commonly used in Trinidad and Tobago and their associated health risk

Terry Mohammed¹, Nadira Rambocas², Sanjeev Basdeo¹, Yasphal Kissoon³

¹Department of Chemistry, University of the West Indies, Faculty of Science and Technology, St. Augustine, Trinidad and Tobago; ²Aniya Aesthetic Limited, Valsayn, Trinidad and Tobago; ³Department of Sociology, University of the West Indies, Faculty of Social Sciences, St. Augustine, Trinidad and Tobago

ABSTRACT

Objectives: This study investigated the presence of mercury in commonly used over the counter skin-lightening creams available in Trinidad and Tobago. The objective of this study was to evaluate if skin-lightening creams commonly used in Trinidad and Tobago contained Mercury, and establish the health risks presented by these products.

Methods: Nineteen skin-lightening creams were analysed using Cold Vapor Atomic Absorption Spectrophotometry (CV-AAS). Margin of Safety (MoS) and Hazard Quotient (HQ) calculations were used to assess risk to users.

Results: Of the nineteen creams assessed, sixteen contained high concentrations of mercury (0.294-14414.5 µg/g), only three creams had no mercury detected. 9 of the 19 samples contained levels of mercury that exceed the Minamata convention's accepted limit of 1 µg/g, with 3 samples exceeding 3800.000 µg/g. Risk assessments using MoS and HQ showed that 3 of the samples were unsafe for use and are considered hazardous. The study also revealed that many creams do contain mercury even if it did not constitute part of the product formulation.

Conclusion: The data infers that some manufacturers do add mercury to their formulations while others are the victims of contaminated raw materials. MoS and HQ show that 21% of the samples were unsafe and 16% can be considered hazardous for human use. It is possible that with such levels of mercury in these products and the popularity of these products within the Caribbean Community and its diaspora, that there exists a significant amount of members with higher than acceptable mercury levels, with undiagnosed clinical symptoms.

Keywords: Mercury, mercury toxicity, skin lightening, skin whitening, skin brightening, bleaching, consumer safety, risk assessment, spectrophotometry

The population of Trinidad and Tobago consists mostly of African and East Indian descendants, and skin lightening practices such as the use of skin lightening or bleaching creams have been commonly used by individuals with darker skin

tones from the African [1] and East Indian [2] populations. In these populations and among many others, a lighter complexion is deemed more beautiful, signifies a higher social status [3] and enhanced economic mobility [4]. Studies show that skin bleaching is on the

Corresponding author: Dr. Terry I. Mohammad, Ph.D., MBA.,
Phone: +1 868 302 1762, E-mail: terry.mohammed@sta.uwi.edu

How to cite this article: Mohammed T, Rambocas N, Basdeo S, Kissoon Y. Evaluation of mercury in skin lightening creams commonly used in Trinidad and Tobago and their associated health risk. Eur Res J. 2024;10(3):276-285. doi: 10.18621/eurj.1314329

Received: June 23, 2023
Accepted: December 21, 2023
Published Online: January 5, 2024

Copyright © 2024 by Prusa Medical Publishing
Available at <https://dergipark.org.tr/en/pub/eurj>



This is an open access article distributed under the terms of [Creative Commons Attribution-NonCommercial-NoDerivatives 4.0 International License](https://creativecommons.org/licenses/by-nc-nd/4.0/)

rise and is more prevalent among females [5] and research have also found that skin bleaching is more prevalent among women with higher academic achievement [4] who are more prone to seek professional employment. This is further supported by studies in hiring practices where lightly colored individuals have a statistically higher chance of being hired than darker colored persons [6]. There is evidence that the existence of pigmentocracy, particularly in Jamaica and Trinidad and Tobago, is a driver for skin bleaching in the region [7].

The use of skin bleaching creams in the Caribbean is not restricted to women only but also to men who are seeking a lighter skin complexion. In 2011, a famous regional singer launched his own line of skin whitening products to add to the already popular men's line of skin whitening creams, and his wife launched a similar line in 2021 [8]. Lighter skin not only enhances the perception of greater attraction but also enhances the appearance of tattoos on skin as the darker colored tattoos contrast better with light skin than dark skin.

Mercury exists in inorganic, elemental, and organic forms. Ammoniated mercury ointments were commonly used for the treatment of psoriasis, but cases of nephrotic syndrome from use of these ointments have been reported since 1962 [9]. The adverse effects of alkyl mercury on the central nervous system have been reported since 1949 [10]. The adverse effects of mercury on the skin and eyes of Iranian dentists have been reported since 1949 [11]. Ammoniated mercury was first studied as a skin lightening agent when it was found in 1952 that the ions reduced melanin production and resulted in a 15% reduction in skin tone [12]. More recently, methylmercury is currently used in some skin-lightening products [13]. Mercury inhibits production of the skin pigment melanin in epidermal melanocytes by inactivating sulfhydryl mercaptan enzymes, which leads to the subsequent inactivation of tyrosinase, which is critical in melanin production [14]. The forms of mercury commonly used in skin-lightening products include; ammoniated mercury, mercury iodide, mercurous chloride, mercurous oxide, or mercuric chloride [15].

Mercury absorption can occur through inhalation, dermal absorption or orally, as advised in some products [16]. The main factors influencing dermal absorption are the amount and the frequency of application

and the skin layer hydration [13]. Other factors affecting the rate of mercury absorption are external temperature and skin thickness.

Long-term exposure to mercury caused by repeated applications can lead to damaging impacts to skin [17], nervous system [18] and kidneys [19]. Dermal effects following mercury-related skin-lightening products include scarring, skin discoloration, and rashes [17]. Additionally, mercury may cause skin-related diseases such as contact dermatitis, pink disease (acro-dynia), and mercury exanthema [18].

Neurological effects relating to mercury in skin-lightening products are headaches, tremors, ataxia, irritability, numbness, paranoid delusions, depression, and insomnia. Renal effects include nephrotic syndrome – a non-specific kidney disorder characterized by oedema, proteinuria, albumin, and globulins [19]. Al-Saleh [20] argues that mercury toxicity affects unborn children when their mothers use mercury-related creams on their bodies. Ricketts *et al.* [13] confirmed that pregnant women using creams with mercury can transfer mercury to the child; a case in Belgium indicated that high levels of mercury in a pregnant woman's urine and blood were also traced to her infant. Furthermore, in November 2022, as reported in CNN Edition, a mother lost her peripheral vision from clear exposure to mercury in beauty creams and the toxic levels in her home placed her entire family at risk [21].

Although there have not been any reported cases of mercury poisoning due to skin creams in Trinidad and Tobago, this does not mean that they do not exist. Literature has discussed at length the adverse health effects of skin-lightening creams. One study found that repeated applications of skin-lightening products with high mercury content were associated with kidney damage [20]. A recent systematic review using 832 individuals from Kenya, the United States (US), Jamaica, and Hong Kong found that nine individuals from Kenya experienced tremors, lassitude, vertigo, and neurasthenia [22]. In Jamaica, 139 individuals reported itchiness, irritability, and other effects such as headaches, depression, and in the US and Hong Kong, the most frequently reported outcomes include fatigue, nervousness/irritability, severe headaches, depression and anxiety, weakness, insomnia, memory loss, tremors, and body/joint pain [22].

Regulations

The effects of Mercury on the human body are well known, and it has been well established that the use of Mercury and Mercury Compounds in skin lightening creams and products constitutes a hazard to users of these products [23]. As such, many nations have instituted regulations governing the use of mercury in cosmetic products either as a component or contaminant. The regulatory limits set by various nations varied from 0 µg/g to 3µg/g [24] in the few countries that implemented such regulations; however, signatories to the Minamata Convention have adopted the limit of 1µg/g of inorganic mercury. The convention does not cover eye cosmetics that may use thimerosal (an organic form of Mercury) as a preservative.

The United States Food and Drug Administration (US FDA) sets a limit of 65 µg/g of total mercury in eye cosmetics where no alternatives are present [25].

Trinidad and Tobago is not a signatory to the Minamata Convention and currently has no regulatory limits for mercury in products. However, the islands of the Caribbean who are signatories of the Minamata Convention have adopted the 1 µg/g limit, but there appears to be little enforcement.

METHODS

Sample Collection

Samples of skin lightening creams were purchased over the counter at various pharmacies and cosmetic stores throughout Trinidad and Tobago in April 2022 and analysed during the period May-June 2022. One sample of each of the available skin lightening creams was purchased. Nineteen samples were collected and represent at least one sample of all of the available brands on the market at the time. Only over-the-counter commercially available products were used in this study.

Equipment and Reagent

Ultrapure water having a resistivity of <18 mΩ.cm was used to prepare all reagents, standards and samples. All chemicals used were of the American Chemical Society (ACS) grade or better.

1. Nitric Acid, ACS Grade 70% (Sigma-Aldrich, USA)

2. Hydrogen Peroxide, ACS Grade 30% (Sigma-Aldrich, USA)
3. Triton-X 100, ACS Grade (Sigma-Aldrich, USA)
4. 50 mL Boiling Tubes (Pyrex, USA)
5. Whatman No.541 Hardened Ashless Filter Paper (Sigma-Aldrich, USA)
6. Class A 50 mL and 25 mL Volumetric Flasks (Pyrex, USA)
7. 1000 µg/mL Stock Solution Hg (Accustandard, USA)
8. Tin (II) chloride, ACS Grade (Sigma-Aldrich, USA)
9. VWR Dry Heating Block (VWR)
10. Varian SpectrAA-800 Atomic Absorption Spectrophotometer with Deuterium Background Correction (Agilent)
11. Varian VGA77 Hydride Generator (Agilent)
12. The quartz Mercury flow cell (Agilent)
13. P100 Micropipette (Gilson Pipetman)

Glassware Preparation

All glassware were washed with anionic detergent and rinsed with tap water followed by deionized water. They were then soaked for a minimum of 24 hours in a diluted nitric acid bath, after which they were rinsed with deionized water. The glassware was then dried in an oven at 60 °C overnight and allowed to cool to room temperature before being used.

Sample Preparation

A 0.5 ± 0.1 g of each skin lightening cream sample was weighed in triplicate into clean, dried labelled boiling tubes. 5 mL of a mixture of 70% Nitric and 30% Hydrogen peroxide were added along with 1mL of a 5% TritonX-100 solution to each of the boiling tubes, mixed, and allowed to pre-digest at room temperature for 24 h. The boiling tubes were then placed in a heating block set to 95 °C and allowed to digest for 3 h as per the method of Maharaj *et al.* [26]. The digested samples were cooled to room temperature and filtered through a Whatman No. 541 hardened ashless filter paper into a 50 mL class 'A' volumetric flask. The contents were made to volume and homogenized by inverting several times. These samples were analysed for Mercury by Cold Vapor Atomic Absorption Spectrophotometry (CV-AAS).

Sample Analysis

Samples were analysed using CV-AAS method as described by Mohammed *et al.* [27]. The VGA77 Hydride Generation Accessory was coupled with Varian SpectraAA800 AAS. The reductant used was Tin (II) Chloride (25%) made up in 20% HCl. The flow rate of the reduction was kept at 1.0 mL/min, the sample was 6.71 mL/min, argon was 2.0 L/min and a delay time of 70 seconds was used in this analysis.

Calibration was performed using working mercury standards of 5 µg/L, 10 µg/L, 20 µg/L, 30 µg/L, 40 µg/L, and 50 µg/L prepared by serial dilution from a 10 µg/mL NIST Traceable Mercury Standard Solution. Quality was assured by the use of spiked samples. Samples were spiked by adding 50 µL of a 10 µg/mL of the stock standard to a 50 mL volumetric flask using a P100 micropipette, and made up to volume with the sample solution. This gave a 10 µg/mL addition of Mercury, and this was analysed in triplicate. The recoveries determined were between 96-102% [28].

Risk Assessment

The assessment of health risks of mercury-containing skin lightening creams was evaluated using the noncancerous risk approach as defined by the Scientific Committee on Consumer Safety (SCCS) safety evaluation model for dermal risk [29], and the US Environmental Protection Agency (USEPA) risk assessment guidelines for dermal risk [30].

Margin of Safety (MoS)

The margin of Safety (MoS) is used to evaluate the risk characterization and is calculated with equation (1) for dermal exposure. A MoS above 100 is considered safe, while values below 100 are considered unsafe [29].

$$MOS = \frac{NOAEL \left(\frac{mg}{kg.day}\right)}{SED_{dermal} \left(\frac{mg}{kg}\right)} \quad (1)$$

The exposure where no adverse effect is observable is referred to as No Observed Adverse Effect Level (NOAEL) and is calculated using equation (2). This is used to evaluate the relationship between exposure and toxic response [29].

$$NOAEL = RfD_{dermal} \times UF \times MF \quad (2)$$

RfD_{dermal} (mg/kg.day) is the dermal reference dose for a specific metal, UF is an uncertainty factor, and

MF are a modulating factor [29]. The default values for UF and MF are 100 and 1, respectively [29, 31]. RfD_{dermal} for calculating risk assessment via dermal uptake has not been established by regulatory bodies [32].

RfD_{dermal} is calculated from the established RfD_{oral} using the fraction of metal Absorbed in the Gastrointestinal Tract (ABSGI) [33]. The RfD_{dermal} for Inorganic Mercury is established at 0.0003mg/kg.day [30], and the ABSGI for Inorganic Mercury is 1.0. [30] RfD_{dermal} was calculated using equation (3).

$$RfD_{dermal} = RfD_{oral} \times ABSGI \quad (3)$$

$$RfD_{dermal\ Hg} = 0.0003 \times 1.0 = 0.0003 \text{ mg/kg.day}$$

The U.S. EPA 2021 outlined non-cancer hazard concern levels for the NOAEL as follows [34];

- NOAEL > 1000 mg/kg.day minor clinical signs of toxicity
- NOAEL < 1000 mg/kg.day, moderate clinical chemistry and organ weight
- NOAEL ≤ 10 mg/kg.day is high evidence of adverse health effects in humans.

SED_{dermal} is the systemic exposure dose for dermal exposure (mg/kg.day) and is calculated using equation (4).

$$SED_{dermal} = \frac{DA_{event} \times SSA \times f}{BW} \quad (4)$$

SSA is the skin surface area in cm² and is calculated as 0.165 [35] fraction of the total body surface area of 18,000 cm² as defined by the USEPA [36] and constitutes the face, neck and arms. The SSA can be calculated to be 2,970 cm². DA_{event} is the absorbed dose per event (mg/cm²), The Scientific Committee on Consumer Safety (SCCS) recognizes that in many conventional calculations of MoS, oral bioavailability of an element is assumed to be 100% if oral absorption data are not available. The standard fingertip unit for a female is 0.4 g [37], and application to hand, arm and face + neck is 1, 3 and 2.5 fingertip units respectively [37], 6.5 fingertip units or 2.6g of cream can be used to cover 2,970 cm². DA_{event} can be calculated to be 0.875 mg/cm². “f” is the frequency of application of the final product (day⁻¹) [29]. Application frequency of 2 day⁻¹ was used [13] and average body weight of 60 kg for adult [30].

Hazard Quotient (HQ)

Hazard quotient (HQ) is a common tool for estimating

health risk in cosmetics[38-40], and is the ratio of systemic exposure dose (SED) of a substance as compared to the dermal reference dose (RfD) of the heavy metal [41]. HQ values more than 1 indicate that potential non-carcinogenic health effects are present. While HQ<1 are considered safe for human health. The Hazard Index was not determined in this study since only one hazard was evaluated.

HQ is calculated as shown in equations (5).

$$HQ = \frac{SED_{dermal}}{RfD_{dermal}} \quad (5)$$

Statistical Analysis

Statistical analysis of mercury concentrations in skin-lightening creams was determined by Pearson correlation analysis, with a P<0.05 value being considered significant

RESULTS

Mercury Content of Skin Lightening Creams

The 19 samples of the skin-lightening creams were analysed for their total Mercury content by CV-AAS (Table 1). These creams originated from Jamaica, Pakistan, India, China, U.K, Singapore, Philippines, the EU, the United States and Trinidad and Tobago. None of which were registered by the Food and Drug Administration of Trinidad and Tobago. Only one sample identified “Ammoniated Mercury” as a component. Three samples contained no detectable mercury (Nu Brite Plus Cream, Fade Off Serum and KAVI Advance Melanin Repair Serum), whereas 16 samples contained measurable levels of mercury (0.294-14414.5 µg/g of Hg).

Significant levels of mercury were found in

Table 1. The mercury content in µg g⁻¹ of various over the counter skin lightening creams

The name of product	Origin	Mercury (µg/g)	%RSD
Nu brite plus cream	U.S.A	<DL	NA
Himalaya radiant glow fairness cream	India	0.413	2.384
Zero marks	India	0.321	3.354
Fair and white gel	EU France	0.303	0.568
African formula skin tone cream	EU Spain	0.300	1.236
Ever fairness day cream	Sri Lanka	0.294	0.876
Crusader ultra skin lightening carrot cream	EU Spain	0.301	1.245
Sandal beauty cream	Pakistan	3855.478	2.609
Fade off serum	Trinidad	<DL	NA
KAVI advanced melanin repair serum	Singapore	<DL	NA
Movate cream	EU Spain	2.223	2.815
Fair and white cream	EU France	1.894	1.018
Deluxe silken	Jamaica	14414.496	3.644
Skin white	Philippines	1.914	2.180
Trin-brite	India	1.275	4.421
7 days magic brightening cream	U.S.A	4005.548	0.799
Ravima’s beauty discoloration defense	Trinidad	3.264	4.258
Kojic acid collagen whitening facial serum	China	1.226	3.163
Topiclear	EU France	0.375	0.056

Detection limit= (3.3×SD)/m, DL= 0.2825ug/g, N/A= not available, %RSD= relative standard deviation

Deluxe Silken (14.414 µg/g), 7 Days Magic Brightening Cream (4005.548 µg/g), and Sandal Beauty Cream (3855.478 µg/g).

Health Risk Assessment

The Margin of Safety (MoS) and Hazard Quotient (HQ) are calculated in Table 2.

DISCUSSION

There is currently no standard for the recommended

concentration of mercury in skin care products by the Food and Drug Administration (FDA) of Trinidad and Tobago as this country is not yet a signatory of the Minamata Convention.

Significant levels of mercury can have severe health effects and permanent irreparable damage to organs, sight, and hearing. The rate of dermal absorption of mercury compounds increases with the concentration of mercury and prior hydration of the skin [42]. At such high levels, the rate of dermal absorption can be rapid. The degree of dermal absorption can also vary with the skin integrity and lipid solubility of cos-

Table 2. Calculation of Margin of Safety and Hazard Quotient for skin lightening creams

The name of product	Mercury (µg/g)	RfD (mg/kg.day)	NOAEL (mg/kg.day)	SED (mg/kg.day)	MoS	HQ
Deluxe silken	14414.496	0.0003	0.030	1.250E+00	0.024	4166.667
7 days magic brightening cream	4005.548	0.0003	0.030	3.470E-01	0.086	1156.667
Sandal beauty cream	3855.478	0.0003	0.030	3.340E-01	0.090	1113.333
Ravima’s beauty discoloration defense	3.264	0.0003	0.030	2.830E-04	106.007	0.943
Movate cream	2.223	0.0003	0.030	1.930E-04	155.440	0.643
Skin white	1.914	0.0003	0.030	1.660E-04	180.723	0.553
Fair and white cream	1.894	0.0003	0.030	1.640E-04	182.927	0.547
Trin-brite	1.275	0.0003	0.030	1.100E-04	272.727	0.367
Kojic acid collagen whitening facial serum	1.226	0.0003	0.030	1.060E-04	283.019	0.353
Himalaya radiant glow fairness cream	0.413	0.0003	0.030	3.580E-05	837.989	0.119
Topiclear	0.375	0.0003	0.030	3.250E-05	923.077	0.108
Zero marks	0.321	0.0003	0.030	2.780E-05	1079.137	0.093
Fair and white gel cream	0.303	0.0003	0.030	2.620E-05	1145.038	0.087
Crusader ultra skin lightening carrot cream	0.301	0.0003	0.030	2.600E-05	1153.846	0.087
African formula skin tone cream	0.300	0.0003	0.030	2.600E-05	1153.846	0.087
Ever fairness day cream	0.294	0.0003	0.030	2.540E-05	1181.102	0.085
Nu brite plus cream	0.000	0.0003	0.030	0.000	NA	0.000
Fade off (?Fade out night cream)	0.000	0.0003	0.030	0.000	NA	0.000
KAVI advanced melanin repair serum	0.000	0.0003	0.030	0.000	NA	0.000

RfD= Reference Dose, NOAEL= No Observed Adverse Effect Level, SED= Systematic Exposure Dose, MoS= Margin of Safety, HQ= Hazard Quotient, N/A= not available

metic products. Other avenues for entry of mercury from such creams may be from ingestion of the product after topical application around the mouth and hand-to-mouth contact, including intimate partner contact. The use of mercury-containing cosmetic products such as these can also contaminate the home and its occupants, resulting in secondary mercury poisoning [43].

The levels obtained from these three products suggest that mercury compounds are added as part of the formulation either as an active ingredient or as a preservative, yet only one sample (Deluxe Silken) shows Ammoniated Mercury on its label. The labeling of cosmetics globally is very relaxed and varies from country to country. Most countries do not require detailed listing of ingredients and except for colour additives, the United States FDA does not require cosmetic products and ingredients for premarket approval [44].

Six other samples contained mercury levels exceeding the $1\mu\text{g/g}$ limit adopted by most countries. These values varied from $1.223\mu\text{g/g}$ to $2.223\mu\text{g/g}$ and may be attributed to contamination from machinery or from contaminated raw material such as vegetable based oils[45] or naturally sourced emulsifiers.

In all cases, mercury absorption through the skin, frequency of use and the bioaccumulation of the metal can result in all the creams containing even traces of mercury to be potentially hazardous to human health. Chronic exposure to mercury can lead to tremors, insomnia, memory loss, neuromuscular effects, headaches, and cognitive and motor dysfunction. Mild subclinical symptoms of central nervous system and cardiovascular toxicity can be seen at exposure levels as low as $0.070\mu\text{g/kg/day}$ [46]. This dismisses the notion of safe level for Mercury.

The results of this study correspond well with previous studies. Mohammed *et al.* [16] in 2017 found similar levels of mercury in skin lightening creams sold in Trinidad and Tobago with values ranging from a low of $0.473\mu\text{g/g}$ to a high of $14.507.741\mu\text{g/g}$ for a sample of Deluxe Silken cream. Rickets *et al.* [13] in 2020 found in Jamaica Mercury ranging from $0.050\mu\text{g/g}$ to $17345.000\mu\text{g/g}$. Hamann *et al.* [14] in 2014 found in the US Mercury ranging from $1729.000\mu\text{g/g}$ to $45,622.000\mu\text{g/g}$. Peregrino *et al.* [47] found in 2011 mercury levels ranging from $878.000\mu\text{g/g}$ to $36,000.000\mu\text{g/g}$ and Prevodnik *et al.* [48] in 2018

found mercury levels in skin lightening creams ranging from $93.000\mu\text{g/g}$ to $16,353.000\mu\text{g/g}$ from 338 samples taken from 22 countries. Majeed *et al.* [49] in 2021 found levels ranging from $3.600\mu\text{g/g}$ to $240.000\mu\text{g/g}$, Sin and Tsang [50] in 2003 found levels ranging from $660.000\mu\text{g/g}$ to $57,000.000\mu\text{g/g}$, Pramanik *et al.* [39] in 2021 found levels ranging from $0.004\mu\text{g/g}$ to $31,700.000\mu\text{g/g}$ and Dwijayanti and Susanti [51] in 2018 found levels ranging from $47.180\mu\text{g/g}$ to $4,554.000\mu\text{g/g}$ of mercury in creams.

The World Health Organization (WHO) identifies Bangladesh, China, Dominican Republic, Hong Kong, Jamaica, Lebanon, Malaysia, Mexico, Pakistan, Philippines, Republic of Korea, Thailand, and the United States of America as the main producers of mercury-containing skin lightening products [23]. However, this study shows that 31% of skin-lightening products tested in this study were produced in the EU and contain some levels of mercury. Mohammed *et al.* [16] found that 60% of the skin lightening products available in the Trinidad and Tobago Market in 2017 were manufactured in the EU, and Rickets *et al.* found 19% of the skin lightening products available in Jamaica were produced in the EU.

The Margin of Safety (MoS) levels determined in this study show that Deluxe Silken, 7 Days Magic Brightening Cream, and Sandal Beauty Cream, exceeded the USEPA guidelines for MoS having values that fell below 100. These samples are considered unsafe for usage and hazardous to human health. The extremely low MoS obtained for Deluxe Silken, 7 Days Magic and Sandal Beauty Cream are of particular concern as these can lead to severe medical conditions even from short term usage and could be considered proximal hazards as mercury from these products can affect persons in close proximity to the user.

Ravima's Beauty Discoloration Defense can also be considered unsafe for use. This sample had a MoS of 106.007 and fell above the USEPA guidelines of 100 MoS but may be within the margin of error of this study and could easily fall below 100 MoS.

The results of MoS correlate very strongly with the Hazard Quotient (HQ) calculation with the same samples being determined to be hazardous. Deluxe Silken, 7 Days Magic Brightening Cream and Sandal Beauty Cream did not only exceed the HQ limit of 1 but did so by a margin of several thousands, further highlighting the severe health hazard these three prod-

ucts pose to the users and their immediate surroundings. Ravima's Beauty Discoloration Defense also showed similar behavior where its HQ value was marginal at 0.943 and should be considered unsafe for use by users.

In this study, four of the samples analyzed can be considered hazardous; this represents 21% of the skin lightening products available on the Trinidad and Tobago market. Furthermore, three of the samples or 16% can be considered extreme hazards. As these are popular brands easily available and commonly used in Trinidad and Tobago, the health risks of exposure to mercury both acute and chronic are extremely high. This risk can easily be extended to close members of the household, including children and intimate partners. It should be noted that this risk assessment assumes that the products are used exclusively on the face, neck, and arms. It did not consider the use of these skin-lightening products on intimate areas where the skin is thinner and blood flow is greater. Bleaching of intimate areas has been growing in popularity among both gay and heterosexual populations [52] and introduces an even greater risk since these areas show increased absorption.

CONCLUSION

In this study, 84% of samples contained mercury and 47% exceeded the Minamata limit of 1µg/g. From the health risk, three samples are unsafe and one marginal. This study indicates that for some products, manufacturers deliberately add Mercury compounds without appropriately representing the components on the labels and shows the need for more appropriate labeling regulation and enforcement in the cosmetic industry. This study also revealed the potential risks posed using manufacturing processes and raw material selection. Since Trinidad and Tobago is not a signatory to the Minamata convention, manufacturers and distributors are not mandated to enforce the 1ppm limit set by the convention for cosmetic products; however, the obvious health risks to the population pose by these products must be considered. The popularity of skin whitening products in Trinidad and Tobago places the population at significant risk of chronic mercury poisoning with implications to the cost of healthcare, reduced productivity, and quality of life. This study only

considered over the counter readily available commercial skin lightening creams and did not consider "under the counter" products which can pose significant hazards to its users.

Authors' Contribution

Study Conception: TM; Study Design: TM; Supervision: MT; Funding: The University of the West Indies; Materials: NR; Data Collection and/or Processing: SB; Statistical Analysis and/or Data Interpretation: TM; Literature Review: NR, TM; Manuscript Preparation: TM, NR and Critical Review: YK.

Conflict of interest

The authors disclosed no conflict of interest during the preparation or publication of this manuscript.

Financing

The authors disclosed that they receive a grant from the University of the West Indies, St. Augustine, Trinidad and Tobago.

Aknowledgement

The authors acknowledge the Department of Chemistry at The University of The West Indies for facilitating all analyses.

REFERENCES

1. Adetoogun JI, Aderinto N, Ashimi AA, Akano DF, Ogundipe TO, Fikayomi PB. Practice and motivations for skin bleaching among Africans. *Int J Surg.* 2023;109(2):218-219. doi: 10.1097/JS9.000000000000141.
2. Daftary K, Krishnam NS, Kundu RV. Uncovering the roots of skin bleaching: colorism and its detrimental effects. *J Cosmet Dermatol.* 2023;22(1):337-338. doi: 10.1111/jocd.15049.
3. Dhillon-Jamerson KK. Key concepts in advertising: colorism. *Advertising & Society Quarterly.* 2022;23(1).
4. Peltzer K, Pengpid S, James C. The globalization of whitening: prevalence of skin lighteners (or bleachers) use and its social correlates among university students in 26 countries. *Int J Dermatol.* 2016;55(2):165-172. doi: 10.1111/ijd.12860.
5. Wone I, Ngom NB, Leye MN, Fall F, Timera B, Ly F. Prevalence of skin bleaching cosmetics use in Senegal: trends and action prospects. *Cent Afr J Pub Health.* 2022;8(5):198-202. doi: 10.11648/j.cajph.20220805.12.
6. Wade TJ, Romano MJ, Blue L. The effect of African American skin color on hiring preferences. *J Appl Soc Psychol.* 2004;34(12):2550-2558. doi: 10.1111/j.1559-1816.2004.tb01991.x.
7. Kelly MD. Racial inequality in the Anglophone Caribbean: comparing the cases of Jamaica and Trinidad and Tobago. *J Ethn Mig*

- Stud. 2023;49(5):1125-1153. doi: 10.1080/1369183X.2022.2044767
8. Baugh C. Vybz Kartel's Wife Tanesha 'Shorty' Johnson Launches 'Skin Bleaching' Products. *Dancehallmag*; 2021.
9. Becker CG, Becker EL, Maher JF, Schreiner GE. Nephrotic syndrome after contact with mercury. A report of five cases, three after the use of ammoniated mercury ointment. *Arch Intern Med*. 1962;110:1781-86. doi: 10.1001/archinte.1962.03620200038008.
10. Lundgren KD, Swensson A. Occupational poisoning by alkyl mercury compounds. *J Ind Hyg Toxicol*. 1949;31(4):190-200.
11. Gaul LE, Underwood GB. Epidermal and dermal sensitization from mercury; its effect on vision and nail growth. *J Indiana State Med Assoc*. 1949;42(12):1258.
12. Lerner AB. Effect of ions on melanin formation. *J Invest Dermatol*. 1952;18(1):47-52. doi: 10.1038/jid.1952.6.
13. Ricketts P, Knight C, Gordon A, Boischio A, Voutchkov M. Mercury exposure associated with use of skin lightening products in Jamaica. *J Health Pollut*. 2020;10(26):200601. doi: 10.5696/2156-9614-10.26.200601.
14. Hamann CR, Boonchai W, Wen L, et al. Spectrometric analysis of mercury content in 549 skin-lightening products: is mercury toxicity a hidden global health hazard? *J Am Acad Dermatol*. 2014;70(2):281-287.e3. doi: 10.1016/j.jaad.2013.09.050.
15. Park JD, Zheng W. Human exposure and health effects of inorganic and elemental mercury. *J Prev Med Public Health*. 2012;45(6):344-352. doi: 10.3961/jpmph.2012.45.6.344.
16. Mohammed T, Mohammed E, Bascombe S. The evaluation of total mercury and arsenic in skin bleaching creams commonly used in Trinidad and Tobago and their potential risk to the people of the Caribbean. *J Public Health Res*. 2017;6(3):1097. doi: 10.4081/jphr.2017.1097.
17. McNutt M. Mercury and health. *American Association for the Advancement of Science*; 2013: p. 1430.
18. Maqbool F, Niaz K, Hassan FI, Khan F, Abdollahi M. Immunotoxicity of mercury: Pathological and toxicological effects. *J Environ Sci Health C Environ Carcinog Ecotoxicol Rev*. 2017;35(1):29-46. doi: 10.1080/10590501.2016.1278299.
19. Risher JF, De Rosa CT. Inorganic: the other mercury. *J Environ Health*. 2007;70(4):9-16.
20. Al-Saleh I. Potential health consequences of applying mercury-containing skin-lightening creams during pregnancy and lactation periods. *Int J Hyg Environ Health*. 2016;219(4-5):468-474. doi: 10.1016/j.ijheh.2016.03.002.
21. Senthilingam M. Mother loses peripheral vision from apparent exposure to mercury in beauty creams. Toxic levels in her home put family at risk, say experts <https://edition.cnn.com/>: CNN; 2022 [Available from: www.cnn.com/2022/11/29/health/skin-whitening-beauty-creams-mercury-vision-loss-mother-families-as-equals-intl-cmd/index.html].
22. Bastiansz A, Ewald J, Rodríguez Saldaña V, Santa-Rios A, Basu N. A systematic review of mercury exposures from skin-lightening products. *Environ Health Perspect*. 2022;130(11):116002. doi: 10.1289/EHP10808.
23. WHO. Preventing disease through healthy environments: Mercury in skin lightening products. *World Health Organization*; 2019.
24. Safety CP. Guidance on Heavy Metal Impurities in Cosmetics. modified 2016-02-29. Available from: <http://www.hesc.gc.ca/cps-spc/pubs/indust>.
25. USFDA. Prohibited and Restricted Ingredients in Cosmetics: UDSFDA; 2010. Available from: <https://www.fda.gov/cosmetics/cosmetics-laws-regulations/prohibited-restricted-ingredients-cosmetics>.
26. Maharaj D, Mohammed T, Mohammed A, Addison L. Enhanced digestion of complex cosmetic matrices for analysis of As, Hg, Cd, Cr, Ni, and Pb using triton X-100. *MethodsX*. 2021;8:101241. doi: 10.1016/j.mex.2021.101241.
27. Mohammed E, Mohammed T, Mohammed A. Optimization of instrument conditions for the analysis for mercury, arsenic, antimony and selenium by atomic absorption spectroscopy. *MethodsX*. 2018;5:824-833. doi: 10.1016/j.mex.2018.07.016.
28. Abbas HH, Sakakibara M, Sera K, Andayanie E. Mercury exposure and health problems of the students using skin-lightening cosmetic products in Makassar, South Sulawesi, Indonesia. *Cosmetics*. 2020;7(3):58. doi: 10.3390/cosmetics7030058.
29. The Scientific Committee on Consumer Safety. The SCCS's Notes of Guidance for the testing of Cosmetic Substance and their Safety Evaluation 10th Revision Europe2018 [updated 24th-25th October, 2018. 1-152]. Available from: https://ec.europa.eu/health/sites/default/files/scientific_committees/consumer_safety/docs/sccs_o_224.pdf.
30. United States Environmental Protection Agency. Risk Assessment Guidance for Superfund Volume 1: Human Health Evaluation Manual (Part E, Supplemental Guidance for Dermal Risk Assessment) 2004. Available from: <https://www.epa.gov/>.
31. Arshad H, Mehmood MZ, Shah MH, Abbasi AM. Evaluation of heavy metals in cosmetic products and their health risk assessment. *Saudi Pharm J*. 2020;28(7):779-790. doi: 10.1016/j.jsps.2020.05.006.
32. Meng Y, Li Y, Zheng N, et al. Potential health risks of metals in skin care products used by Chinese consumers aged 19-29 years. *Ecotoxicol Environ Saf*. 2021;216:112184. doi: 10.1016/j.ecoenv.2021.112184.
33. Ho YB, Abdullah NH, Hamsan H, Tan ESS. Mercury contamination in facial skin lightening creams and its health risks to user. *Regul Toxicol Pharmacol*. 2017;88:72-76. doi: 10.1016/j.yrtph.2017.05.018.
34. United States Environmental Protection Agency (U.S. EPA). Sustainable Futures/P2 Framework Manual 2012 Section 13: Quantitative Risk Assessment Calculations United States 2021 [updated 2021]. Available from: <https://www.epa.gov/sustainable-futures/sustainable-futures-p2-framework-manual>.
35. Liu Y, Stowe MH, Bello D, et al. Skin exposure to aliphatic polyisocyanates in the auto body repair and refinishing industry: III. A personal exposure algorithm. *Ann Occup Hyg*. 2009;53(1):33-40. doi: 10.1093/annhyg/men070.
36. Emergency USEPAOo, Response R. Risk Assessment Guidance for Superfund: pt. A. Human health evaluation manual: Office of Emergency and Remedial Response, US Environmental Protection Agency; 1989.
37. Long CC, Finlay AY. The finger-tip unit--a new practical measure. *Clin Exp Dermatol*. 1991;16(6):444-447. doi: 10.1111/j.1365-2230.1991.tb01232.x.
38. Podgórska A, Puścion-Jakubik A, Grodzka A, Naliwajko SK, Markiewicz-Żukowska R, Socha K. Natural and conventional cosmetics - mercury exposure assessment. *Molecules*. 2021;26(13):4088. doi: 10.3390/molecules26134088.

39. Pramanik S, Kumar M, Qureshi A. Mercury in skin-care products in India and consumer exposure risks. *Regul Toxicol Pharmacol.* 2021;121:104870. doi: 10.1016/j.yrtph.2021.104870.
40. Gnonsoro UP, Ake Assi YED, Sangare NS, Kouakou YU, Trokourey A. Health risk assessment of heavy metals (Pb, Cd, Hg) in hydroalcoholic gels of Abidjan, Côte d'Ivoire. *Biol Trace Elem Res.* 2022;200(5):2510-2518. doi: 10.1007/s12011-021-02822-y.
41. Agency for Toxic Substances and Disease. Calculating Hazard Quotients and Cancer Risk Estimates 2023. Available from: https://www.atsdr.cdc.gov/pha-guidance/conducting_scientific_evaluations/epcs_and_exposure_calculations/hazardquotients_cancer-risk.html#.
42. Chan TY. Inorganic mercury poisoning associated with skin-lightening cosmetic products. *Clin Toxicol (Phila).* 2011;49(10):886-891. doi: 10.3109/15563650.2011.626425.
43. Ori MR, Larsen JB, Shirazi FM. Mercury poisoning in a toddler from home contamination due to skin-lightening cream. *J Pediatr.* 2018;196:314-317.e1. doi: 10.1016/j.jpeds.2017.12.023.
44. Rai S, Gupta A, Punetha V. Regulations of Cosmetics Across the Globe. *Appl Clin Res Clin Trials Regul Aff.* 2015;2(3):137-144. doi: 10.2174/2213476X03666151125220117.
45. Brodziak-Dopierała B, Fischer A, Chrzanowska M, Ahnert B. Mercury exposure from the consumption of dietary supplements containing vegetable, cod liver, and shark liver oils. *Int J Environ Res Public Health.* 2023;20(3):2129. doi: 10.3390/ijerph20032129.
46. Fernandes Azevedo B, Barros Furieri L, Peçanha FM, et al. Toxic effects of mercury on the cardiovascular and central nervous systems. *J Biomed Biotechnol.* 2012;2012:949048. doi: 10.1155/2012/949048.
47. Peregrino CP, Moreno MV, Miranda SV, Rubio AD, Leal LO. Mercury levels in locally manufactured Mexican skin-lightening creams. *Int J Environ Res Public Health.* 2011 Jun;8(6):2516-2523. doi: 10.3390/ijerph8062516.
48. Prevodnik A, Willcox A, Lymberidi-Settimo E, Bender M, Lane O. Mercury-added skin-lightening creams: available, inexpensive and toxic. European Environmental Bureau, Zero Mercury Working Group. Brussels, Belgium, 2018.
49. Majeed T, Shah SH, Anjum I. Estimation of mercury and hydroquinone content in skin whitening creams and the potential risks to the health of women in Lahore, Pakistan. *J Pak Assoc Dermatol.* 2021;31(1):33-41.
50. Sin KW, Tsang HF. Large-scale mercury exposure due to a cream cosmetic: community-wide case series. *Hong Kong Med J.* 2003 Oct;9(5):329-334.
51. Dwijayanti E, Susanti S. Analysis of mercury (Hg) in whitening cream distributed in Palu City by atomic absorption spectroscopy. *J Appl Chem Sci.* 2018;5(1):430-433. doi: 10.35508/jacs.v5i1.1751.
52. Calderwood B. Anal bleaching is all the rage. *The Gay & Lesbian Review Worldwide.* 2008;15(4):17-18.

Which pathologies of the penis can be diagnosed with computed tomography? A comprehensive approach to imaging findings

Yeliz Aktürk^{1,2}, Esra Soyer Güldoğan^{2,3}, Serra Özbal Güneş^{1,2}

¹Department of Radiology, Ministry of Health Etlik City Hospital, Keçiören, Ankara, Turkey, ²Department of Radiology, Health Sciences University, Ankara Dışkapı Yıldırım Beyazıt Training and Research Hospital, Dışkapı, Ankara, Turkey, ³Department of Radiology, Turkish Hospital Qatar, Doha, Qatar

ABSTRACT

Objectives: Since there are various benign and malignant diseases of the penis, different imaging methods can be used for diagnosis. Abdominal computed tomography (CT) is not a frequently used imaging method in diagnosing penile pathologies. In an abdominal CT scan performed with the standard technique, the slices are obtained by scanning from the diaphragm's dome to the symphysis pubis's lower edge. Although the whole penis is not always captured, almost all abdomen scans include a portion of the penis. Penile pathologies can be detected with careful evaluation by CT.

Methods: In this study, we aim to investigate incidental penile pathologies detected in abdominal CT performed for other reasons and whether abdominal CT contributes to showing penile pathologies. Therefore, abdominal CTs of 3,698 male patients were re-evaluated for penile pathologies.

Results: The mean age was 52.2 years. Of the CT scans, 38% were obtained due to trauma, 16% were taken for oncological causes, 16% for abdominal pain and acute abdominal pathologies, 10% for urological reasons, 20% for other causes. Penile pathology was detected in 33 (0.83%) of 3968 patients. The patients were divided into four groups according to the pathologies observed in the penis: Traumatic, inflammatory, tumoral, and other findings.

Conclusion: Although CT is not routinely used to diagnose penile pathologies, it may be necessary if the whole penis is included in the examination.

Keywords: Penile imaging, penile pathologies, incidental findings, male health, penile trauma

Various benign and malignant diseases of the penis can be evaluated with different imaging methods. Ultrasonography (US), color Doppler US, computed tomography (CT), magnetic resonance imaging (MRI), and retrograde urethrography are imaging methods that can be employed to confirm the

clinical diagnosis, evaluate the disease extent, and help to select the appropriate treatment [1]. US is the first step imaging method in evaluating many penile pathologies [2]. The advantages of the US are that it is low cost and easily accessible, does not contain ionizing radiation, and is a method that can take real-time

Corresponding author: Esra Soyer Güldoğan, MD.,
Phone: +974 5539 7959, E-mail: esra_soyer@hotmail.com

How to cite this article: Aktürk Y, Soyer Güldoğan E, Özbal Güneş S. Which pathologies of the penis can be diagnosed with computed tomography? A comprehensive approach to imaging findings. Eur Res J. 2024;10(3):286-294. doi: 10.18621/eurj.1386294

Received: November 5, 2023
Accepted: January 2, 2024
Published Online: January 22

Copyright © 2024 by Prusa Medical Publishing
Available at <https://dergipark.org.tr/en/pub/eurj>



This is an open access article distributed under the terms of [Creative Commons Attribution-NonCommercial-NoDerivatives 4.0 International License](https://creativecommons.org/licenses/by-nc-nd/4.0/)

images. However, it also has disadvantages due to its relatively small field of view, being an operator-dependent examination, and providing limited information on soft tissue pathologies [3, 4]. Because of its high soft tissue resolution, MRI is an excellent diagnostic method when clinical and / or US findings are doubtful or inconclusive. It is a preferred imaging method in surgical planning, cancer staging, and evaluation of penis [2, 3, 5]. Traumatic injuries of the penis are initially visualized by US and MRI. CT is not a frequently used examination in routine penile imaging. However, penile pathologies that can be detected by CT are also quite high [6]. The penile bulb is an easily recognizable anatomical structure on axial CT images. It is surrounded by a paired crura laterally, corpus cavernosum anteriorly, and levator ani posteriorly [7]. In a routine abdominal CT scan, images are obtained by scanning from the diaphragm's dome to the symphysis pubis's lower edge [8]. So that the glans penis is usually included in the image. We aimed to investigate the presence of incidental pathologies in the penis at the abdominal CT scan performed for dif-

ferent reasons. In addition, we aimed to review the imaging findings of penile pathologies that can be seen on CT examination.

METHODS

Study Design

After obtaining the approval of the required ethics committee, the abdominal CT of male patients aged 18 and over, present in the Picture Archiving Communication System (PACS) between March 2020 and June 2020, a total of 4,116 abdomen CTs were retrospectively re-evaluated. CT scans were taken for different reasons. Regardless of the reason for the scan, images were evaluated blindly to the preliminary information, and the presence of penile pathology was noted. If the patients had more than one CT scan, only the images of the first examination were evaluated and that could not be assessed optimally due to motion artifacts were excluded. One hundred twelve patients who had more than one examination and 12 patients



Fig. 1. Axial images. (a) Metallic foreign bodies due to gunshot injury, (b) Hematoma in the anterior of the glans penis, and (c) Air densities near the dorsum penis and contour irregularity due to penile fracture.

who could not be evaluated due to intense motion artifacts were excluded from the study. Also, 24 patients whose CT images did not include the penis at all were excluded from the study. Finally 3,968 patients were included in the study.

Imaging Technique

All abdominal CTs were obtained with the same screening protocol on the same device. The screening was done by scanning the diaphragmatic cupolas to the iliac crest level using a 128-slice CT (Optima CT 660, General Electric Healthcare Systems, Milwaukee, USA). The slice thickness was 5 mm in axial images. All CT scans were obtained during a single breath, covering the area from the level of the diaphragm to the symphysis pubis. If contrast material was administered, it was done according to the following protocol: with non-ionic contrast agents (1.5-2 mL/kg) at the portal venous phase (65-70 s). All CT images were reconstructed using an algorithm suited to soft-tissue analysis with the medical image processing software (AW Volume Share 5).

CT Evaluation

CT evaluation was performed by two radiologists, one 10 years and the other 15 years experienced in tomography. Penile pathologies were divided into four groups: Traumatic, inflammatory, and tumoral. The distribution of patients with penile pathology according to age groups was evaluated. In addition, the frequency of association of penile pathologies with abdominal pathologies was investigated.

Statistical Analysis

Continuous data expressed as the mean \pm standard deviation or median (interquartile range [IQR]) were analyzed using a t or Mann-Whitney U test. Statistical analysis was conducted with statistical software (SPSS, version 21.0; SPSS Inc, Chicago, IL, USA).

RESULTS

Between March 2020 and June 2020, 3968 male patients aged 18 and over underwent abdominal CT. The ages of the patients ranged from 18 to 84 years. The mean age was 52.2 years. Of the CT scans, 38% were obtained due to trauma, 16% were taken for oncolog-

ical causes (suspicion of malignancy, newly diagnosed malignancy, and follow-up), 16% for abdominal pain and acute abdominal pathologies, 10% for urological reasons (renal cyst, benign prostate hypertrophy, hematuria), 20% for other causes.

Penile pathology was detected in 33 (0.83%) of 3968 patients. The patients who had penil pathologies were divided into four groups according to the pathologies observed in the penis: Traumatic, inflammatory, tumoral, and other findings.

There were four (0.1%) patients with penile

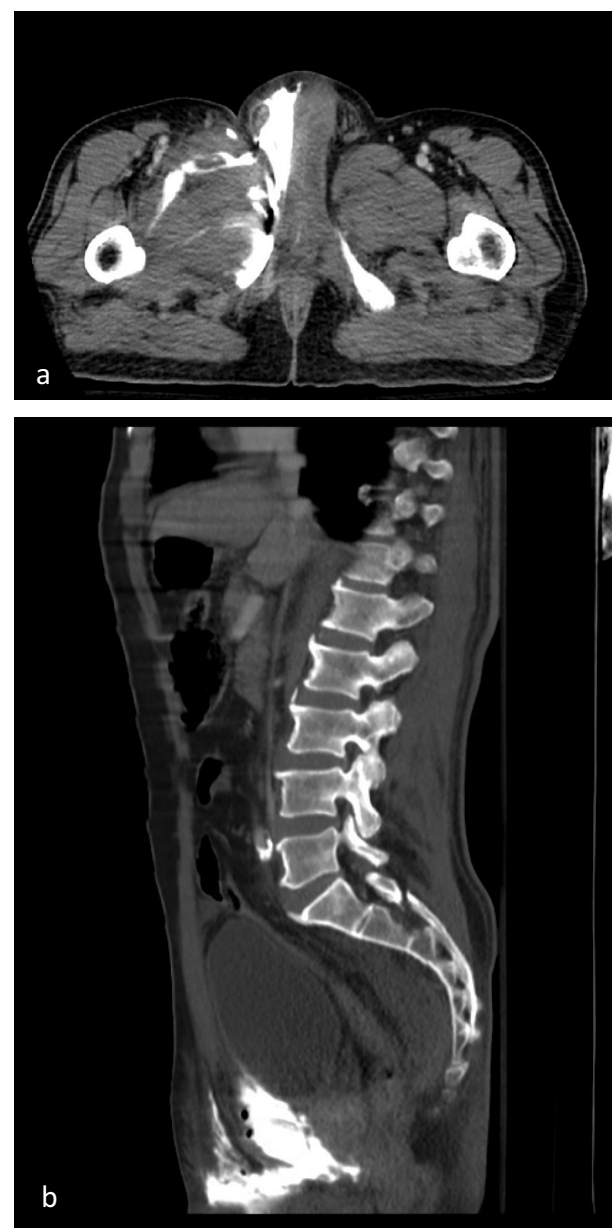


Fig. 2. Axial (a) and sagittal (b) image. Contrast material accumulated in the perineum and near the penis due to type III urethral injury.

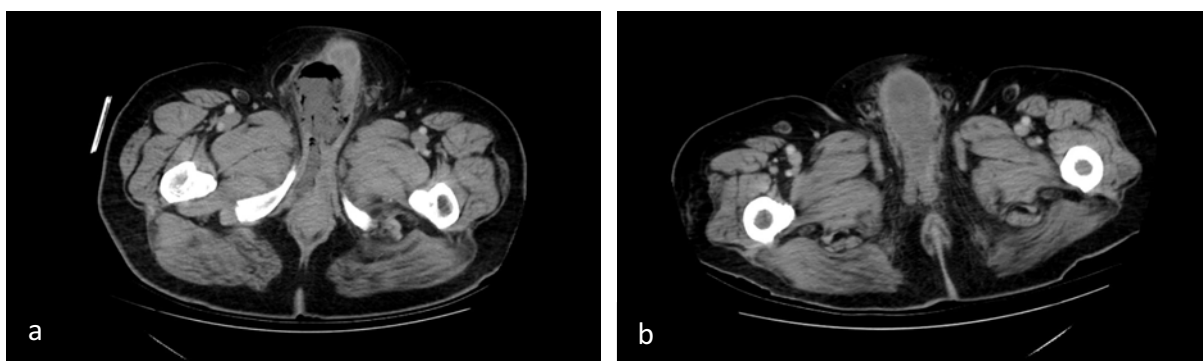


Fig. 3. Axial images. (a) Air densities consistent with necrotizing infection in the glans penis and scrotum and (b) Edematous and heterogeneous appearance consistent with balanitis on the glans penis.

trauma findings in the trauma patients group. Three patients had signs of penetrating penile trauma, aged 33 to 41 years. CT scanings of these three patients revealed air densities near the dorsum penis, metallic foreign bodies due to gunshot injury, and hematoma in the anterior of the glans penis (Figs. 1a and 1b) and one of them had penile fracture (Fig. 1c). In a 45-year-old trauma case, there was no traumatic injury of the penis, but contrast material accumulated in the perineum and near the penis due to type III urethral injury (Fig. 2).

There were four (0.1%) patients in the inflammatory pathologies group. Their age ranged from 54 to 68 years. In three cases, there were inflammatory heterogeneities in the skin and subcutaneous tissue, abscess formation in the perineal area and adjacent to the dorsum penis. Two of four cases had air densities consistent with necrotizing infection in the glans penis and

scrotum (Fig. 3a). One patient had an edematous and heterogeneous appearance consistent with balanitis on the glans penis (Fig. 3b).

Two (0.05%) patients were classified in the tumoral pathologies group. Penile squamous carcinoma was detected in a 75-year-old patient who had mild



Fig. 4. Axial image shows a metastatic mass lesion with contrast enhancement at the penile crura.

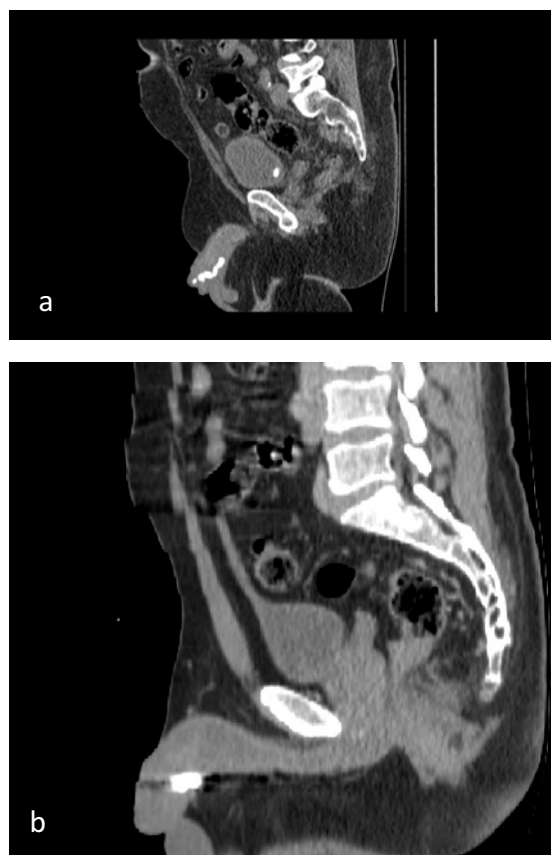


Fig. 5. Sagittal images. (a) Multiple urinary stones in the penile urethra and the bladder and (b) A metallic density due to a foreign body in the glans penis.

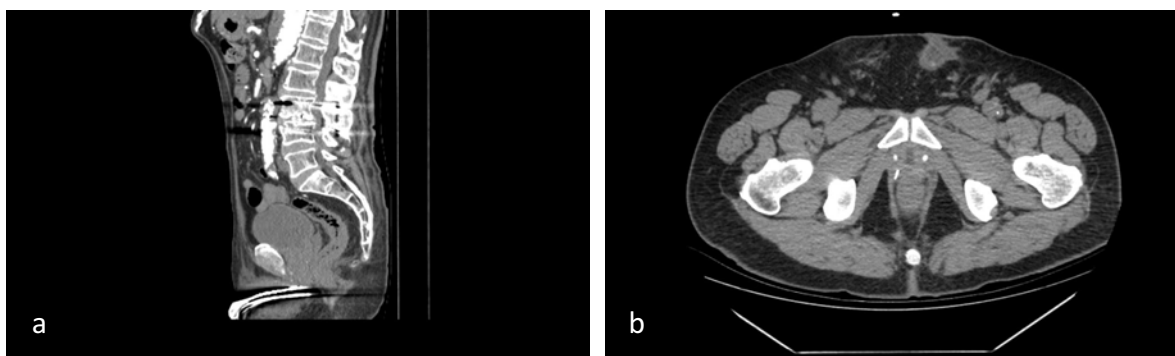


Fig. 6. Sagittal (a) and axial (b) image. (a) Penile prosthesis and (b) Abscess showed cutaneous extension and inflammatory changes around it.

skin thickening and contrast enhancement at the corpus cavernosum. There was an enlarged inguinal lymph node on the right side, suggesting metastasis. In a 68-year-old case, in the abdominal CT scan that was performed due to bladder carcinoma during follow-up, there was a metastatic mass lesion with contrast enhancement at the penil crura (Fig. 4).

In the other findings group, there were 23 (0.57%) patients. Three (0.075%) cases aged 36 and 65 had urinary stones in the penile urethra. In the other findings group, three cases between ages of 36 and 65 had urinary stone in the penile urethra and one of them has hydronephrosis (Fig. 5a). A 50-year-old patient had a metallic density due to a foreign body in the glans penis (0.025%) (Fig. 5b). Four (0.1%) patients between the ages of 49 and 77 had penile prostheses. In one (0.025%) of these cases, there was an abscess adjacent to the catheter of the prosthesis. In one of these

cases, there was an abscess adjacent to the catheter of the prosthesis with periferal contrast enhancement. The abscess showed cutaneous extension and there were inflammatory changes around it (Figs. 6a and 6b). Linear calcifications were observed in the tunica albuginea in 15 (0.37%) cases aged 52 to 80 (Fig. 7).

Findings observed in the traumatic, inflammatory, tumoral pathologies and other findings groups are summarized in Table 1 and Table 2.

DISCUSSION

Different imaging techniques are used in penile imaging according to pathologies [9]. Ultrasound is the first-line imaging modality in penile imaging that can show anatomy and blood flow, detect abnormalities such as penile masses or plaques, and evaluate conditions such as priapism or erectile dysfunction. It is a fast, noninvasive imaging method that is easily accessible in many places, if not all over the world. Doppler ultrasound can be used to evaluate erectile dysfunction by measuring penile blood flow during different stages of an erection. Doppler ultrasound is particularly useful in diagnosing vascular conditions, such as arterial insufficiency or venous leakage. MRI is useful for evaluating complex penile conditions and provides excellent soft tissue resolution but may require the use of contrast agents for better visualization. CT imaging is typically reserved for investigating penile trauma, assessing the extent of penile fractures, or evaluating suspected penile cancer.

Focal or diffuse penile induration is a common problem in urological practice. It often occurs due to



Fig. 7. SLinear calcifications in the tunica albuginea.

Table 1. Penile pathologies detected on CT

Penile pathologies	Number of cases	Age (years) (min-max)	CT findings
Traumatic	4 (0.1%)	33-41	Air densities, metallic foreign bodies, hematoma, contour irregularity in the penis
Inflammatory	4 (0.1%)	54-68	Heterogeneities in the skin and subcutaneous tissue, abscess in the perineal area, air densities in the glans penis and scrotum, edematous and heterogeneous appearance on the glans penis
Tumoral	2 (0.05%)	68-75	Skin thickening and contrast enhancement at the corpus cavernosum, enlarged inguinal lymph node, mass lesion with contrast enhancement
Other findings	23 (0.57%)	36-80	Findings regarding foreign bodies, penile prosthesis and calcifications

CT=computed tomography

Peyronie's disease. However, other benign and malignant pathologies are also included in the differential diagnosis. In addition to a physical examination, imaging modalities are often required to confirm the diagnosis and assess the extent of the disease. US and MRI are the most commonly used methods. In addition, retrograde urethrography and CT can be used in selected cases [9]. Peyronie's disease is a condition in which fibrous tissue plaques form in the tunica albuginea, leading to penile deformity and shortening [10]. The diagnosis is made by questioning the patient's medical history, autophotography, and palpation of the plaques. Imaging is needed to evaluate the extension of the plaques, the involvement of the penile septum, and the relationship of plaques with penile vascular structures [11]. Although calcified plaques can be di-

agnosed better with US in Peyronie's disease, MRI is more valuable than US in detecting non-palpable plaques and evaluating their size [1]. Albugineal calcifications are sometimes difficult to evaluate [12]. CT can be used to evaluate non-calcified plaques [13]. CT is not employed in the investigation of Peyronie's disease. If CT is performed for other reasons, plaques may be seen incidentally. Our incidental penile calcific plaque detection rate was 0.37%. Case ages ranged from 52 to 80.

Imaging is essential in the initial evaluation, treatment planning, and patient follow-up in penile carcinoma [14]. Because of its high soft tissue contrast and spatial resolution, MRI is used more than in the US in both defining primary penile malignancies and showing lymph node involvement (1). MRI is used in T

Table 2. Distribution of pathologies in the other findings group

Penile pathologies	Number of cases	Age (years) (min-max)	CT findings
Urinary stone	3 (0.075%)	36-65	Urinary stone in the penile urethra, hydronephrosis
Foreign body	1 (0.025%)	50	Metallic density in the glans penis
Penile prostheses	4 (0.1%)	49-77	Abscess near the catheter of the prosthesis, a cutaneous extension of inflammatory changes
Penile calcifications	15 (0.37%)	52-80	Linear calcifications in the tunica albuginea
Total	23 (0.57%)		

CT=computed tomography

staging of the primary tumor and screening for local recurrence. CT and positron emission tomography (PET) / CT are useful in scanning regional nodal and distant metastases [14]. CT is usually not indicated in newly diagnosed penile cancers without palpable inguinal lymph nodes [15]. Penile squamous carcinoma was detected in one of our cases. This patient had mild skin thickening and contrast enhancement at the corpus cavernosum. An enlarged inguinal lymph node on the right side suggests metastasis. In one patient, an abdominal CT scan was performed due to bladder carcinoma during follow-up, and there was a metastatic mass lesion showing contrast enhancement in the penile crura.

Penile prostheses are MRI-compatible, so MRI is increasingly used to evaluate postoperative changes [1]. However, CT is cheaper and more usable for some patients, especially in emergencies, post-surgical hematoma, and suspected infection [16]. In the infection of penile prostheses, thickening of the skin, soft tissue swelling, and fat stranding are seen on CT. In cases with abscess, a rim-like enhancing fluid collection with or without gas is detected. Irregularity and ulceration of the skin may accompany [16, 17]. In our case with a penile prosthesis, there was an abscess with peripheral contrast enhancement with cutaneous extension in the left inguinal region adjacent to the catheter and inflammatory changes around it.

Genital emergencies are rare in men; therefore, the role of imaging is essential. First, it is necessary to know the specific imaging findings of the injuries [6]. Contrast-enhanced abdominal and pelvis CT is the gold standard for abdominal trauma imaging [18, 19]. However, the US initially visualizes traumatic injuries to the penis and scrotum. It should be evaluated whether the tunicae albuginea surrounds the penile corpora and testis seminiferous tubules. Herniation of the contents and discontinuity of the tunica albuginea make the diagnosis of rupture [6]. The bulbocavernosus muscle is a small muscle associated with the corpus spongiosum. It is the ventral muscle of the penis and surrounds the bulbus. In cases of pelvic fracture accompanied by urethral injury, it has been reported that this usually symmetrical midline structure has asymmetry in its outer edges, contour, or size [18]. Because the urethra is longer in men, urethral trauma is more common in men than in women. Posterior urethral injury occurs in the membranous and prostatic urethra.

A straddle-type injury usually causes bulbar urethral injuries, while penile urethral damage is associated with penile fracture [20, 21]. Even if the damage is not in the penile urethra, pathological findings around the penis can be seen on abdominal CT. One of our post-traumatic patients had a type III urethra injury. There was contrast media accumulation in the perineum and near the penis due to injury to the urogenital diaphragm and the membranous urethra extending to the proximal bulbous urethra.

Different types of foreign bodies have been reported in the urethra. Although the presentation of foreign bodies in the lower urinary system varies, dysuria and hematuria are the most common symptoms. The severity of the clinical situation depends on the nature of the foreign body and, more importantly, the time of the medical intervention. Therefore, early recognition and removal of foreign bodies are crucial [22]. US pelvic roentgenogram or CT can be used to evaluate the shape and position of a foreign body [23]. In our cases, the foreign bodies observed in the penis and its neighborhood were metallic foreign bodies due to gunshots.

Inflammation of the glans penis is defined as balanitis, and inflammation of the prepuce as posthitis. Balanitis is a descriptive term that includes various conditions, and sometimes a biopsy may be required to rule out premalignant diseases [24]. Penile cellulitis and balanitis can be treated with antibiotics, while penile abscess and infection of the corpus cavernosum can be life-threatening [10]. US is important in excluding corpus cavernosum involvement and abscess in patients with inflammation [25]. In severe inflammatory conditions, urgent CT or MRI is required for the extension of the infection to the perineum, abdominal wall, and fasciae [26]. As with abscesses elsewhere in the body, fluid accumulation is seen on CT in penile abscesses. The fluid collection sometimes includes air densities. In addition, the surrounding adipose tissue has edema and environmental contrast enhancement. Imaging allows the identification of the location of the abscess and its relationship to nearby anatomical structures and guides drainage [10]. Fournier's gangrene is a genitourinary necrotizing fasciitis that can be fatal if not quickly diagnosed and surgically debrided. It is typically a male-predominant disease [27]. Although usually diagnosed clinically, CT may be required to assess the extent of the disease or to plan surgical treat-

ment. The presence of fascial gas and inflammation findings on CT should suggest the diagnosis [28]. Two of our patients had rectal fluctuation and fever, and there were signs of necrotizing infection on CT.

Limitations

The limitations of our study are that the object of the tomography scan is not aimed at detecting penile pathology and as with all retrospective studies, there may be deficiencies in patient data. Although CT can diagnose many penile pathologies, it does not seem possible to replace ultrasound in diagnosis due to the radiation dose. However, due to its high diagnostic sensitivity, it should be kept in mind that BT is a diagnostic test for penile pathology in cases where ultrasound cannot be reached and in patients who will undergo pelvic tomography for any other reason.

CONCLUSION

Although CT is not routinely used in the diagnosis of penile pathologies, careful evaluation of the penis included in the examination may be important in the diagnosis. In particular, the penis should be included pelvic tomography scans especially in emergency, and it should not be forgotten that CT can reveal the diagnosis of many pathologies despite known of the low soft tissue resolution in penile imaging.

Authors' Contribution

Study Conception: YA; Study Design: YA, ESG; Supervision: SÖG; Funding: YA; Materials: ESG, YA; Data Collection and/or Processing: ESG, YA; Statistical Analysis and/or Data Interpretation: ESG, YA; Literature Review: ESG; Manuscript Preparation: ESG and Critical Review: SÖG, YA, ESG.

Conflict of interest

The authors disclosed no conflict of interest during the preparation or publication of this manuscript.

Financing

The authors disclosed that they did not receive any grant during conduction or writing of this study.

The institution where study was developed

Department of Radiology, Health Sciences Uni-

versity Ankara Dışkapı Yıldırım Beyazıt Training and Research Hospital, Dışkapı, 06130, Ankara, Turkey.

REFERENCES

- Shenoy-Bhangle A, Perez-Johnston R, Singh A. Penile imaging. *Radiol Clin North Am.* 2012;50(6):1167-1181. doi: 10.1016/j.rcl.2012.08.009.
- Kirkham A. MRI of the penis. *Br J Radiol.* 2012;85 Spec No 1(Spec Iss 1):S86-93. doi: 10.1259/bjr/63301362.
- Parker RA 3rd, Menias CO, Quazi R, et al. MR Imaging of the Penis and Scrotum. *Radiographics.* 2015;35(4):1033-1050. doi: 10.1148/rg.2015140161.
- Pretorius ES, Siegelman ES, Ramchandani P, Banner MP. MR imaging of the penis. *Radiographics.* 2001;21 Spec No:S283-S298. doi: 10.1148/radiographics.21.suppl_1.g01oc24s283.
- Tu LH, Spektor M, Ferrante M, Mathur M. MRI of the Penis: Indications, Anatomy, and Pathology. *Curr Probl Diagn Radiol.* 2020;49(1):54-63. doi: 10.1067/j.cpradiol.2018.12.004.
- Avery LL, Scheinfeld MH. Imaging of penile and scrotal emergencies. *Radiographics.* 2013;33(3):721-740. doi: 10.1148/rg.333125158.
- Wallner KE, Merrick GS, Benson ML, Butler WM, Maki J, Tollenaar BG. Penile bulb imaging. *Int J Radiat Oncol Biol Phys.* 2002;53(4):928-933. doi: 10.1016/s0360-3016(02)02805-5.
- Hodler J, Kubik-Huch RA, von Schulthess GK, editors. *Diseases of the Abdomen and Pelvis 2018-2021: Diagnostic Imaging - IDKD Book* [Internet]. Cham (CH): Springer; 2018.
- Bertolotto M, Pavlica P, Serafini G, Quaia E, Zappetti R. Painful penile induration: imaging findings and management. *Radiographics.* 2009;29(2):477-493. doi: 10.1148/rg.292085117.
- El-Sakka AI, Hassoba HM, Pillarisetty RJ, Dahiya R, Lue TF. Peyronie's disease is associated with an increase in transforming growth factor-beta protein expression. *J Urol.* 1997;158(4):1391-1394.
- Bertolotto M, Coss M, Neumaier C. US evaluation of patients with Peyronie's disease. In: Bertolotto M, ed. *Color Doppler US of the penis.* Berlin, Germany: Springer-Verlag, 2008; pp. 61-69.
- Vosshenrich R, Schroeder-Printzen I, Weidner W, Fischer U, Funke M, Ringert RH. Value of magnetic resonance imaging in patients with penile induration (Peyronie's disease). *J Urol.* 1995;153(4):1122-1225.
- Al-Thakafi S, Al-Hathal N. Peyronie's disease: a literature review on epidemiology, genetics, pathophysiology, diagnosis and work-up. *Transl Androl Urol.* 2016;5(3):280-9. doi: 10.21037/tau.2016.04.05.
- Suh CH, Baheti AD, Tirumani SH, et al. Multimodality imaging of penile cancer: what radiologists need to know. *Abdom Imaging.* 2015;40(2):424-435. doi: 10.1007/s00261-014-0218-6.
- Clark PE, Spiess PE, Agarwal N, et al; National Comprehensive Cancer Network. Penile cancer: Clinical Practice Guidelines in Oncology. *J Natl Compr Canc Netw.* 2013;11(5):594-615. doi: 10.6004/jnccn.2013.0075.
- Chou HL, Mohsen NA, Garber BB, Feldstein DC. CT imaging of inflatable penile prosthesis complications: a pictorial essay. *Abdom Radiol (NY).* 2019;44(2):739-748. doi: 10.1007/s00261-

018-1764-0.

17. Darouiche RO. Device-associated infections: a macroproblem that starts with microadherence. *Clin Infect Dis*. 2001;33(9):1567-1572. doi: 10.1086/323130.
18. Ali M, Safriel Y, Sclafani SJ, Schulze R. CT signs of urethral injury. *Radiographics*. 2003;23(4):951-963. doi: 10.1148/rg.234025097.
19. Dane B, Baxter AB, Bernstein MP. Imaging Genitourinary Trauma. *Radiol Clin North Am*. 2017;55(2):321-335. doi: 10.1016/j.rcl.2016.10.007.
20. Brandes S. Initial management of anterior and posterior urethral injuries. *Urol Clin North Am*. 2006;33(1):87-95, vii. doi: 10.1016/j.ucl.2005.10.001.
21. Rosenstein DI, Alsikafi NF. Diagnosis and classification of urethral injuries. *Urol Clin North Am*. 2006;33(1):73-85, vi-vii. doi: 10.1016/j.ucl.2005.11.004.
22. Mak CWH, Cho CL, Chan WKW, Chu RWH, Law IC. Per urethral insertion of foreign body for erotism: case reports. *Hong Kong Med J*. 2019;25(4):320-322. doi: 10.12809/hkmj177044.
23. Gunasekaran K, Murthi S. Unusual metallic penile foreign body. *BMJ Case Rep*. 2017;2017:bcr2017219377. doi: 10.1136/bcr-2017-219377.
24. Edwards SK, Bunker CB, Ziller F, van der Meijden WI. 2013 European guideline for the management of balanoposthitis. *Int J STD AIDS*. 2014;25(9):615-626. doi: 10.1177/0956462414533099.
25. Pearle MS, Wendel EF. Necrotizing cavernositis secondary to periodontal abscess. *J Urol*. 1993;149(5):1137-1138. doi: 10.1016/s0022-5347(17)36321-8.
26. Kickuth R, Adams S, Kirchner J, Pastor J, Simon S, Liermann D. Magnetic resonance imaging in the diagnosis of Fournier's gangrene. *Eur Radiol*. 2001;11(5):787-790. doi: 10.1007/s003300000599.
27. Singh A, Ahmed K, Aydin A, Khan MS, Dasgupta P. Fournier's gangrene. A clinical review. *Arch Ital Urol Androl*. 2016;88(3):157-164. doi: 10.4081/aiua.2016.3.157.
28. Ballard DH, Raptis CA, Guerra J, et al. Preoperative CT Findings and Interobserver Reliability of Fournier Gangrene. *AJR Am J Roentgenol*. 2018;211(5):1051-1057. doi: 10.2214/AJR.18.19683.

Association of frailty with nutritional parameters in patients with chronic kidney disease

Recep Evcen¹, Mehmet Zahid Koçak², Rengin Elsürer Afşar³

¹Department of Internal Medicine, Division of Clinical Immunology and Allergy, Necmettin Erbakan University, Meram Faculty of Medicine, Konya, Türkiye; ²Department of Medical Oncology, Konya City Hospital, Konya, Türkiye; ³Department of Internal Medicine, Division of Nephrology, Süleyman Demirel University, Faculty of Medicine, Isparta, Türkiye

ABSTRACT

Objectives: Frailty is a significant clinical syndrome characterized by greater susceptibility to stressors due to the dysfunction of multiple organ systems, which increases in prevalence with age. This study was performed to investigate relations between frailty and nutritional parameters in patients with chronic kidney disease (CKD).

Methods: This cross-sectional study involved 100 CKD patients aged 50 years or older. Frailty was assessed using the Edmonton Frailty Scale (EFS) and Fried's Frailty Scale (FFS). The patients nutritional status was assessed using the Mini Nutritional Assessment (MNA) and the routine laboratory tests.

Results: The study included 100 patients, consisting of 41 females and 59 males. The mean age of the participants was 65.3±9.3 years. The median glomerular filtration rate (GFR) of the patients was 23 mL/min/1.73 m² (min: 3-max: 65). According to the MNA, 15 patients had normal nutritional status, 63 were at risk of malnutrition, and 22 were malnourished. According to the EFS score, four patients were categorized as not frail, 11 as vulnerable, 25 with mild frailty, 21 with moderate frailty, and 39 with severe frailty. According to the FFS score, six patients were non-frail, 30 were classified as pre-frail, and 64 were considered frail.

Conclusions: Frailty and malnutrition in patients with CKD were independently related to all other factors examined in this study. Screening for malnutrition at the early stages in patients with CKD and the appropriate treatment may prevent the development of frailty.

Keywords: Chronic kidney disease, frailty, malnutrition

Frailty is a significant clinical syndrome in elderly populations characterized by an increased vulnerability to stressors due to dysfunction in multiple organ systems. Its prevalence increases with age due to diminishing physiological reserves and sub-clinical organ dysfunction [1]. Additionally, individuals with chronic diseases appear to be predisposed to frailty [2].

Nutritional status is a compound concept involving food intake, body composition, and functional capacity. Nutritional assessment to identify malnutrition is based on anthropometric measurements and laboratory tests [3]. Renal dysfunction represents a substantial risk factor for mortality in elderly patients. A lower-than-expected glomerular filtration rate (GFR) for a person's age is linked to an increased risk of death

Corresponding author: Recep Evcen, MD,
Phone: +90 332 223 70 00, E-mail: r_evcen@hotmail.com

How to cite this article: Evcen R, Koçak MZ, Elsürer Afşar R. Association of frailty with nutritional parameters in patients with chronic kidney disease. Eur Res J. 2024;10(3):295-302. doi: 10.18621/eurj.1376545



This is an open access article distributed under the terms of [Creative Commons Attribution-NonCommercial-NoDerivatives 4.0 International License](https://creativecommons.org/licenses/by-nc-nd/4.0/)

Received: October 16, 2023
Accepted: January 25, 2024
Published Online: March 17, 2024

Copyright © 2024 by Prusa Medical Publishing
Available at <https://dergipark.org.tr/en/pub/eurj>



[4, 5]. The risk of developing sarcopenia rises as renal function declines in individuals with CKD. The major causes of sarcopenia are considered to be type II muscle atrophy resulting from changes in protein metabolism and a decline in mitochondrial function [6]. Muscle mass loss in CKD patients is associated with reduced grip strength and slow walking speed, leading to poor muscle mass [7].

Although there have been many studies on frailty in CKD, there have been few studies regarding the relationship between frailty and nutritional status in CKD. Therefore, this study was conducted to examine the association between frailty and nutritional parameters in patients with CKD.

METHODS

Study Design

A total of 100 patients diagnosed with CKD, who had no active infection or malignancy, and were over 50 years of age, presenting to Selçuk University School of Medicine Nephrology Outpatient Clinic, Konya, Turkey, between October 2015 and July 2016 were included in the cross-sectional study. The study protocol was approved by the local ethics committee (approval number: 2015/208, Date: 23.06.2015). All of the patients had no history of chronic alcohol consumption. We recorded patients' demographic characteristics, duration of illness, medications taken, and whether they lived alone, with family, or with a partner.

The diagnosis of CKD was established following the diagnostic criteria outlined: Improving Global Outcomes (KDIGO) guidelines. CKD stage was determined according to the KDIGO guidelines [8].

Evaluation of Nutritional Status

The Mini-Nutritional Assessment (MNA) was employed to assess the nutritional status [9]. Patients were divided into three groups according to their MNA scores: ≤ 17 points, malnutrition; 17–23.5 points, risk of malnutrition; ≥ 24 points, normal nutritional status. Muscle power was assessed by testing hand grip strength using a hand dynamometer (JIMCO rehab®). Measurements were obtained on both sides with the elbow flexed at 90°, the upper arm aligned with the patient's side, and recorded as the average of

three measurements. Average measurements below the expected values according to the patient's BMI indicated low muscle strength. Anthropometric measurements (height, weight, BMI, mid-arm circumference [MAC], hip circumference, calf circumference, and subcutaneous fat thickness measurements) were obtained during outpatient visits.

Evaluation of Frailty

Frailty was evaluated using both the Edmonton Frailty Scale (EFS) and Fried's Frailty Scale (FFS) [10, 11]. The EFS contains nine components, each scored from 0 to 17. Patients were categorized based on their EFS score as follows: 0-4, not frail (subgroup E1); 6-7, vulnerable (subgroup E2); 8-9, mild frailty (subgroup E3); 10-11, moderate frailty (subgroup E4); 12-17, severe frailty (subgroup E5). The FFS contains five components: unintentional weight loss, self-reported exhaustion, weakness, slow walking speed, and low physical activity. Patients fulfilling none of these criteria were classified as not frail (subgroup F1), those fulfilling 1-2 criteria as pre-frail (subgroup F2), and those fulfilling ≥ 3 criteria as frail (subgroup F3). Routine laboratory parameters were recorded.

Statistical Analysis

Variables (age, sex, weight, and BMI) are presented as the mean \pm standard deviation (SD), range (min–max), or median and percentage (%) as appropriate. The χ^2 test was employed to compare categorical data across different groups. The Kruskal–Wallis test was utilized for the analysis of laboratory parameters, and the Mann–Whitney U test was employed for subgroup analysis due to the non-normal distribution of patients in accordance with the frailty scale groups. Multivariable linear regression analysis (independent variables: age, sex, diabetes mellitus, hemoglobin, albumin, MNA, and GFR) was used to determine factors independently associated with EFS and FFS scores.

RESULTS

The study included 100 patients aged 50 years or older with CKD. This group consisted of 41 females and 59 males, averaging 65.3 \pm 9.3 years. The demographic information and anthropometric measurements of the

patients are presented in Table 1. The median GFR of the patients was 23 mL/min/1.73 m² (min: 3-max: 65), and the median follow-up duration for CKD was 44 months (min: 3-max: 300 months). The patients had a mean BMI of 29.4±6.3 kg/m². Seventy-one patients (71%) were not on dialysis, 21 (21%) were on hemodialysis, and 8 (8%) were on peritoneal dialysis. The median follow-up duration for patients undergoing hemodialysis was 36 months (min: 12-max: 180), while for peritoneal dialysis patients, the median follow-up period was 30.5 months (min: 12-max: 48). The distribution patients according to CKD stage was as follows; stage 2 (n = 4), stage 3 (n = 39), stage 4 (n = 19), and stage 5 (n = 38) CKD.

Table 1. Demographic characteristics and anthropometric measurements of patients with chronic kidney disease

Demographic characteristics of patients	n=100
Age (year)	65.3±9.3
Height (cm)	162.6±7.8
Weight (kg)	76.9±15.9
Body mass index (kg/m ²)	29.4±6.3
Anthropometric measurements	
Middle arm circumference (cm)	24.3±3.8
Calf circumference (cm)	32.5±4.6
Hip circumference (cm)	103.5±11.9
Waist circumference (cm)	95.7±12.6
Biceps skin fold thickness (mm)	1.35 (0.7-9.3)
Triceps skin fold thickness (mm)	2 (1-14.2)
Muscle strength (kg)	20 (7-45)
Walking Speed (sec)	11 (6-18)
Comorbidities, n (%)	
Cerebrovascular events	16 (16)
Hypertension	88 (88)
Coronary artery disease	50 (50)
Hyperlipidemia	36 (36)
Chronic obstructive pulmonary disease	28 (28)
Chronic heart failure	27 (27)
Diabetes mellitus	49 (49)

According to EFS score, 4 patients were not frail, 11 were vulnerable, 25 had mild frailty, 21 had moderate frailty, and 39 had severe frailty. According to FFS score, 6 were not frail, 30 were pre-frail, and 64 were frail. According to the MNA scores, 15 patients had normal nutritional status, 63 were at risk of malnutrition, and 22 were malnourished. The comparison of laboratory test results and anthropometric measurements of the patients with different levels of frailty based on EFS results is shown in Table 2. In the whole study population, serum albumin (P=0.003), total cholesterol (P=0.019), LDL (P = 0.025), iron (P=0.008), biceps skinfold thickness (P=0.008), and triceps skinfold thickness (P<0.0001) were significantly different (Table 2).

Laboratory parameters and anthropometric measurements were compared between patients classified according to FFS score (Table 3). In the whole study group, serum creatinine (P = 0.032), serum albumin (P=0.034), vitamin D (P=0.018), GFR (P=0.012), MAC (P=0.009), biceps skinfold thickness (P=0.006), and triceps skinfold thickness (P=0.011) were significantly different (Table 3).

When patients with CKD were grouped based on EFS, the MNA scores significantly differed in the whole study population (P trend = 0.005). As a result of this evaluation, 15 (15%) of the patients were in normal nutritional status, 63 (63%) were at risk of malnutrition, and 22 (22%) were malnourished. In subgroup analysis, MNA scores showed significant differences between the not frail and moderately frail patients (P=0.035), not frail and severely frail patients (P=0.009), vulnerable and severely frail patients (P=0.010), and mildly frail and severely frail patients (P=0.016) (Fig. 1).

Similarly, when patients with CKD were grouped based on FFS, the MNA scores were significantly in in the whole study population (P trend =0.0001). In subgroup analysis, MNA scores showed significant variance between not frail and frailty (P<0.001) and pre-frailty and frailty (P<0.001) (Fig. 2).

In a multivariable linear regression analysis, several factors were identified as independently associated with the EFS and FFS scores. For the EFS score, these factors included age (beta = 0.342, 95% CI = 0.021 - 0.066, P<0.0001), MNA (beta = 0.334, 95% CI: 0.309 - 1.000, P<0.0001), and serum albumin level

Table 2. Laboratory results and anthropometric measurements of patients with chronic kidney disease based on Edmonton Frailty Scale subgroups

Parameters	E1	E2	E3	E4	E5	P value
Age (year)	63.0±5.2	62.6±7.5	60.4±8.2	65.6±9.3	69.2±9.4	0.008
Gender (M/F) (n)	3/1	8/3	16/9	12/9	20/19	0.639
Urea (mg/dL)	75.1±51.3	73.2±54.8	91.6±36.4	94.8±45.6	92.3±33.0	0.139
Creatinine (mg/dL)	1.4 (1.4-6.7)	1.4 (1.2-11.8)	3.1 (1.2-10.8)	3 (1.2-11.7)	2.7 (1.1-13.6)	0.136
Albumin (g/dL)	4.2±0.2	4.2±0.4	3.6±0.6	3.9±0.5	3.7±0.4	0.003
Total cholesterol (mg/dL)	156±42.1	222±50.6	190±54.2	168±26.7	187.4±36.2	0.019
LDL cholesterol (mg/dL)	92.5±35.6	144.9±38	114±50.3	103±25.4	117.5±30.2	0.025
HDL cholesterol (mg/dL)	29.0±3.1	36.3±8.6	40.8±13.5	34.2±9.2	39.8±13.0	0.147
Iron (uq/dL)	66.5 (51-300)	73 (21-120)	51 (21-124)	73 (35-212)	51 (13-143)	0.008
Ferritin (ng/mL)	152.2 (11-490)	90 (8.5-427)	208 (23-2000)	248 (11-1444)	237 (13-2000)	0.269
Vitamin D (ng/mL)	15.4±9.7	19.3±9.6	18.1±10.1	15.2±10.4	13.3±7.7	0.240
GFR (mL/dk/1.73 m ²)	47.5 (7-51)	38 (3-52)	13 (5-64)	17 (5-48)	19 (4-65)	0.091
Middle arm circumference (cm)	27±2.4	26.4±3.6	24.1±3.4	24.1±3.7	23.6±4	0.114
Calf circumference (cm)	34.7±3.7	34.4±3.2	32.4±5.5	32.2±4.1	32±4.6	0.350
Hip circumference (cm)	109±11.1	106±5.6	99±11.9	104±12.7	104±12.5	0.075
Waist circumference (cm)	97±12.1	103±6.5	91±13.2	96±12.3	95±13.2	0.084
Biceps skin fold thickness (mm)	2.5 (1.9-2.8)	2.1 (1.2-2.5)	1.4 (0.7-8)	1.2 (0.8-2.4)	1.2 (0.8-9.3)	0.008
Triceps skin fold thickness (mm)	3.8 (2.2-5.4)	2,3 (1.4-3.6)	2 (1-9)	1.8 (1.1-3.1)	2 (1.1-14.2)	0.047
Muscle strength (kg)	37 (25-45)	30 (13-38)	22 (10-40)	20 (12-35)	18 (7-30)	<0.0001

Data are shown as mean±standard deviation or median (minimum-maximum or number. Patients were categorized based on their EFS score as follows: 0-4, not frail (subgroup E1); 6-7, vulnerable (subgroup E2); 8-9, mild frailty (subgroup E3); 10-11, moderate frailty (subgroup E4); 12-17, severe frailty (subgroup E5). LDL=Low-Density Lipoprotein, HDL=High-Density Lipoprotein, GFR=Glomerular Filtration Rate

(beta: -0.208, 95% CI: -0.885 - -0.022) (P=0.042). For the FFS score, the factors included age (beta: 0.232, 95% CI: 0.004 - 0.026, P=0.007), MNA (beta: 0.371, 95% CI: 0.202 - 0.538, P=0.016), and GFR (beta: -0.244, 95% CI: -0.016 - -0.002, P=0.008).

DISCUSSION

The term "frail" typically encompasses unexplained weight loss, muscle weakness, reduced walking speed, and diminished physical activity. Medical, socioeconomic, and psychiatric problems in CKD contribute to the development of frailty. Frailty is a multisystemic condition that causes reduced physiological capacity. In patients not undergoing renal replacement therapy,

a decrease in GFR of less than 50 mL/min/1.73 m² has been shown to reduce oral intake in patients with poor renal function, leading to poor nutritional status, and malnutrition [1, 3, 12].

The frailty seen in end-stage renal disease (ESRD) patients is independent of age, and most patients show protein energy malnutrition. However, sarcopenia (determined by measurement of the MAC) and dynapenia (determined by measurement of hand grip strength) seen in malnutrition has a higher prevalence in older than in young patients with CKD [1, 13].

In the current study, there were conflicting findings regarding the relations of EFS and FFS scores with sex and age. Here, EFS and FFS scores showed no significant relationship with sex (P=0.639 and P=0.109), but were significantly related to age

Table 3. Laboratory results and anthropometric measurements of patients with chronic kidney disease based on Fried Frailty Scale subgroups

Parameters	F1	F2	F3	P value
Age (year)	62.5±5.0	61.8±9.0	67.2±9.3	0.028
Gender (M/F) (n)	5/1	21/9	33/31	0.109
Urea (mg/dL)	66.4±43.4	73.1±35.2	99.9±38.6	<0.0001
Creatinine (mg/dL)	1.4 (1.2-6.7)	1.9 (1.1-11.8)	3.1 (1.2-13.6)	0.032
Albumin (g/dL)	4.3±0.3	3.8±0.6	3.7±0.4	0.034
Total cholesterol (mg/dL)	173±49.8	197.5±57.5	182.7±34.9	0.504
LDL cholesterol (mg/dL)	110.6±46.3	122.4±50.9	112.8±28.8	0.818
HDL cholesterol (mg/dL)	32±7	40.6±12.8	37.5±11.8	0.323
Iron (uq/dL)	72.5 (33-300)	60 (21-124)	54 (13-212)	0.426
Ferritin (ng/mL)	48.7 (11-490)	158.5 (23-2000)	254 (8.5-2000)	0.142
Vitamin D (ng/mL)	17.2±11.7	19.8±10.2	13.6±8.1	0.018
GFR (mL/dk/1.73 m ²)	38 (7-51)	35 (3-65)	16.5 (4-58)	0.012
Middle arm circumference (cm)	27.3±2.5	25.4±4.2	23.4±3.5	0.009
Calf circumference (cm)	33±2.8	34±5.8	31.8±4	0.163
Hip circumference (cm)	104.6±8.9	105±14.3	102.7±10.9	0.798
Waist circumference (cm)	97.1±10.2	97.8±13.7	94.6±12.4	0.306
Biceps skin fold thickness (mm)	2.1 (1.5-2.7)	1.6 (0.7-5.4)	1.2 (0.7-9.3)	0.006
Triceps skin fold thickness (mm)	2.5 (2-5.4)	2.2 (1-6.2)	1.8 (1.1-14.2)	0.011

Data are shown as mean±standard deviation or median (minimum-maximum or number. Patients fulfilling none of these criteria were classified as not frail (subgroup F1), those fulfilling 1-2 criteria as pre-frail (subgroup F2), and those fulfilling ≥3 criteria as frail (subgroup F3). LDL=Low-Density Lipoprotein, HDL=High-Density Lipoprotein, GFR=Glomerular Filtration Rate

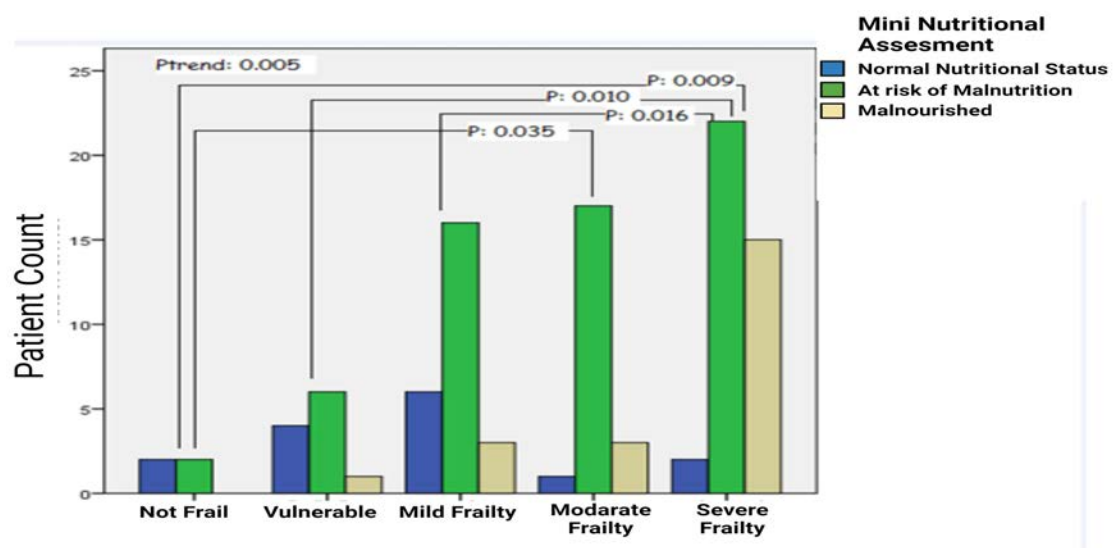


Fig. 1. Comparison of mini-nutritional assessment results of Edmonton Frailty Scale subgroup.

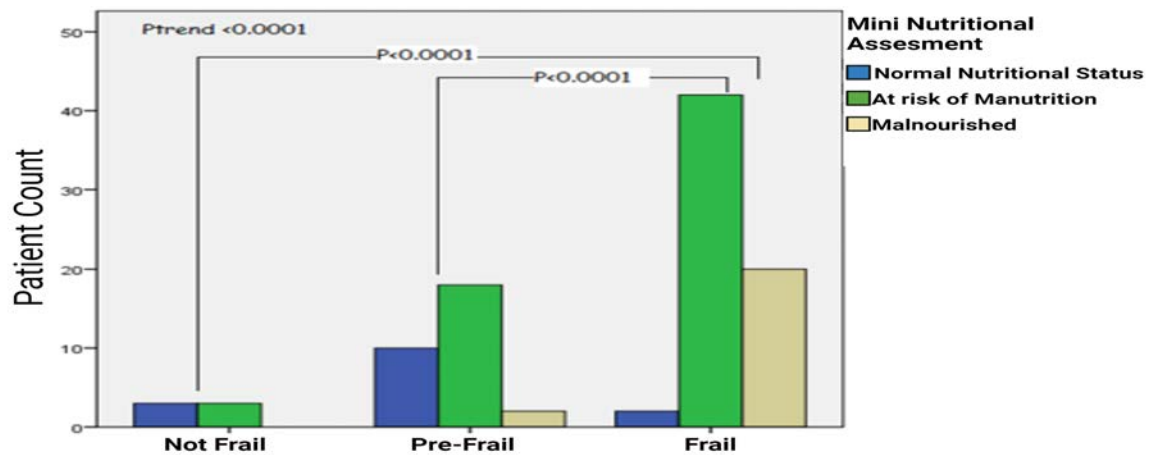


Fig. 2. Comparison of mini-nutritional assessment results of Fried's Frailty Scale subgroup.

($P=0.008$ and $P=0.028$, respectively). Subgroup analyses showed that these differences were mainly between patients with severe frailty and those without frailty.

The actual incidence of frailty was shown to be higher than that detected using clinical assessment indexes, which is thought to be due to differences in the definitions of frailty [14]. In systematic review, Colvard *et al.* [15] reported significant relationships between both increasing age and female sex with frailty in community-residing adults aged 65 and above. The same study showed that the prevalence of frailty differs among countries due to the different scales used for evaluation.

A strong relationship was found between CKD and frailty. The incidence of frailty was reported to increase according to increasing CKD stage [1, 16, 17]. Consistent with the literature, GFR was found to be associated with both EFS and FFS independently of other factors in the present study. In patients with CKD receiving hemodialysis, malnutrition is seen at high rates of up to 22.2%, and malnutrition is strongly related to both morbidity and mortality [18]. Malnutrition is seen in 23%–76% of patients on hemodialysis and 15%–50% of those on peritoneal dialysis [19]. In the present study, MNA scores showed significant differences according to EFS and FFS in patients with CKD ($P_{trend}=0.005$, $P_{trend}=0.001$); the rate of malnutrition increased with increasing frailty.

Low serum albumin levels are a good indicator of malnutrition in HD patient groups [20]. Research in-

dicates a reverse correlation between serum albumin levels and mortality and morbidity, both in the community and in patients admitted to the hospital [21]. Chia-ter Chao *et al.* [22] identified a negative correlation between frailty and serum albumin levels in HD patients. Similarly, in our study, serum albumin levels were notably reduced in CKD patients with frailty compared to those without frailty, as evaluated through EFS and FFS ($P=0.003$ and $P=0.034$).

Reduced vitamin D levels are correlated with fractures, sarcopenia, disability, and frailty. In the InCHIANTI study, low vitamin D level was accepted as a predictor of frailty [23]. Similarly, Puts *et al.* [24] reported a highly significant relationship between low 25-hydroxyvitamin D levels and the presence of frailty. In the present study, vitamin D levels were similar between the groups with and without frailty as assessed by EFS ($P=0.240$). However, a significant difference was observed between the groups regarding frailty when assessed using FFS ($P=0.018$). This difference may have been due to implementation of different physical performance criteria in these scales. Matos *et al.* [25] examined the correlation between the MNA and hand grip test, and reported that hand grip strength could be used as a significant predictor of malnutrition. In the current investigation, it was also observed that hand grip strength decreased as the severity of frailty, as assessed by EFS, increased ($P<0.0001$). In the present study, MAC measurement was similar within EFS groups ($P=0.114$), while MAC was significantly different between different FFS

groups ($P=0.009$). These observations indicated that MAC measurement alone could not be used as an indicator of frailty.

Skinfold thickness measurements offer dependable data for estimating body fat. About 50% of body fat is subcutaneous, making skinfold thickness a directly measurable indicator using a well-calibrated caliper [26]. Triceps skinfold thickness is frequently employed due to its straightforward application. Triceps skinfold thickness was found to be the most accurate parameter for calculating total body fat percentage in a study using dual-energy X-ray scanning as a reference, in a population of hemodialysis patients [27]. In our study, biceps skinfold thickness and triceps skinfold thickness measurements showed a statistically significant difference in the whole study group for both EFS and FFS. Thus, both biceps and triceps skinfold thicknesses can be implemented to assess malnutrition in frail patients with CKD.

Malnutrition is a prevalent condition among individuals with CKD. Malnutrition increases frailty and adversely affects rates of morbidity and mortality if not diagnosed and treated. Although both frailty and malnutrition are common in patients with CKD, the associations of frailty with nutritional parameters are not fully understood. A few studies are available on the relationship between frailty and nutritional parameters in CKD patients. In the present study, frailty was shown to be correlated with a number of nutritional parameters (albumin, LDL, vitamin D, hemoglobin, biceps skin fold thickness, triceps skin fold thickness, muscle strength, MAC) in patients with CKD over 50 years old. In this study, we showed that malnutrition was a strong indicator of frailty in patients with CKD. Similarly, age and GFR were independently linked to frailty in our population of patients with CKD.

CONCLUSION

Malnutrition is independently related to frailty among individuals with CKD. Screening for malnutrition and appropriate treatment beginning from the early stages of CKD is warranted for prevention of the development of frailty.

Authors' Contribution

Study Conception: RE, REA; Study Design: RE,

REA; Supervision: REA; Funding: REA, MZK; Materials: RE; Data Collection and/or Processing: RE; Statistical Analysis and/or Data Interpretation: REA, MZK; Literature Review: RE, MZK; Manuscript Preparation: RE, MZK and Critical Review: REA.

Conflict of interest

The authors disclosed no conflict of interest during the preparation or publication of this manuscript.

Financing

The authors disclosed that they did not receive any grant during conduction or writing of this study.

REFERENCES

1. Kennard A, Glasgow N, Rainsford S, Talaulikar G. Frailty in chronic kidney disease: challenges in nephrology practice. A review of current literature. *Intern Med J.* 2023;53(4):465-472. doi: 10.1111/imj.15759.
2. Weiss CO. Frailty and chronic diseases in older adults. *Clin Geriatr Med.* 2011;27(1):39-52. doi: 10.1016/j.cger.2010.08.003.
3. Lorenzo-López L, Maseda A, de Labra C, Regueiro-Folgueira L, Rodríguez-Villamil JL, Millán-Calenti JC. Nutritional determinants of frailty in older adults: A systematic review. *BMC Geriatr.* 2017;17(1):108. doi: 10.1186/s12877-017-0496-2.
4. Shastri S, Katz R, Rifkin DE, et al. Kidney function and mortality in octogenarians: Cardiovascular Health Study All Stars. *J Am Geriatr Soc.* 2012;60(7):1201-1207. doi: 10.1111/j.1532-5415.2012.04046.x.
5. Rifkin DE, Shlipak MG, Katz R, et al. Rapid kidney function decline and mortality risk in older adults. *Arch Intern Med.* 2008;168(20):2212-2218. doi: 10.1001/archinte.168.20.2212.
6. Buford TW, Anton SD, Judge AR, et al. Models of accelerated sarcopenia: critical pieces for solving the puzzle of age-related muscle atrophy. *Ageing Res Rev.* 2010;9(4):369-833. doi: 10.1016/j.arr.2010.04.004.
7. Roshanravan B, Khatri M, Robinson-Cohen C, et al. A prospective study of frailty in nephrology-referred patients with CKD. *Am J Kidney Dis.* 2012;60(6):912-921. doi: 10.1053/j.ajkd.2012.05.017.
8. Andrassy KM. Comments on 'KDIGO 2012 Clinical Practice Guideline for the Evaluation and Management of Chronic Kidney Disease'. *Kidney Int.* 2013;84(3):622-623. doi: 10.1038/ki.2013.243.
9. Cereda E. Mini nutritional assessment. *Curr Opin Clin Nutr Metab Care.* 2012;15(1):29-41. doi: 10.1097/MCO.0b013e32834d7647.
10. Fabricio-Wehbe SC, Schiaveto FV, Vendrusculo TR, Haas VJ, Dantas RA, Rodrigues RA. Cross-cultural adaptation and validity of the 'Edmonton Frail Scale - EFS' in a Brazilian elderly sample. *Rev Lat Am Enfermagem.* 2009;17(6):1043-1049. doi: 10.1590/s0104-11692009000600018.
11. Rolfson DB, Majumdar SR, Tsuyuki RT, Tahir A, Rockwood K. Validity and reliability of the Edmonton Frail Scale. *Age Age-*

- ing. 2006;35(5):526-529. doi: 10.1093/ageing/afl041.
12. Chang CI, Chan DC, Kuo KN, Hsiung CA, Chen CY. Prevalence and correlates of geriatric frailty in a northern Taiwan community. *J Formos Med Assoc.* 2011;110(4):247-257. doi: 10.1016/S0929-6646(11)60037-5.
13. Grupp C. Frailty bei chronischer Nierenerkrankung [Frailty in chronic kidney disease]. *Z Gerontol Geriatr.* 2021;54(3):217-222. [Article in German]. doi: 10.1007/s00391-021-01860-4.
14. Joosten E, Demuynck M, Detroyer E, Milisen K. Prevalence of frailty and its ability to predict in hospital delirium, falls, and 6-month mortality in hospitalized older patients. *BMC Geriatr.* 2014;14:1. doi: 10.1186/1471-2318-14-1.
15. Collard RM, Boter H, Schoevers RA, Oude Voshaar RC. Prevalence of frailty in community-dwelling older persons: a systematic review. *J Am Geriatr Soc.* 2012;60(8):1487-1492. doi: 10.1111/j.1532-5415.2012.04054.x.
16. Dalrymple LS, Katz R, Rifkin DE, et al. Kidney function and prevalent and incident frailty. *Clin J Am Soc Nephrol.* 2013;8(12):2091-2099. doi: 10.2215/CJN.02870313.
17. Wilhelm-Leen ER, Hall YN, Horwitz RI, Chertow GM. Phase angle, frailty and mortality in older adults. *J Gen Intern Med.* 2014;29(1):147-154. doi: 10.1007/s11606-013-2585-z.
18. Leavey SF, Strawderman RL, Jones CA, Port FK, Held PJ. Simple nutritional indicators as independent predictors of mortality in hemodialysis patients. *Am J Kidney Dis.* 1998;31(6):997-1006. doi: 10.1053/ajkd.1998.v31.pm9631845.
19. Stenvinkel P, Heimbürger O, Lindholm B, Kaysen GA, Bergström J. Are there two types of malnutrition in chronic renal failure? Evidence for relationships between malnutrition, inflammation and atherosclerosis (MIA syndrome). *Nephrol Dial Transplant.* 2000;15(7):953-960. doi: 10.1093/ndt/15.7.953.
20. Bergström J. Nutrition and mortality in hemodialysis. *J Am Soc Nephrol.* 1995;6(5):1329-41. doi: 10.1681/ASN.V651329.
21. Gibbs J, Cull W, Henderson W, Daley J, Hur K, Khuri SF. Preoperative serum albumin level as a predictor of operative mortality and morbidity: results from the National VA Surgical Risk Study. *Arch Surg.* 1999;134(1):36-42. doi: 10.1001/archsurg.134.1.36.
22. Chao CT, Hsu YH, Chang PY, et al. Simple self-report FRAIL scale might be more closely associated with dialysis complications than other frailty screening instruments in rural chronic dialysis patients. *Nephrology (Carlton).* 2015;20(5):321-328. doi: 10.1111/nep.12401.
23. Shardell M, Hicks GE, Miller RR, et al. Association of low vitamin D levels with the frailty syndrome in men and women. *J Gerontol A Biol Sci Med Sci.* 2009;64(1):69-75. doi: 10.1093/gerona/gln007.
24. Puts MT, Visser M, Twisk JW, Deeg DJ, Lips P. Endocrine and inflammatory markers as predictors of frailty. *Clin Endocrinol (Oxf).* 2005;63(4):403-411. doi: 10.1111/j.1365-2265.2005.02355.x.
25. Matos LC, Tavares MM, Amaral TF. Handgrip strength as a hospital admission nutritional risk screening method. *Eur J Clin Nutr.* 2007;61(9):1128-1135. doi: 10.1038/sj.ejcn.1602627.
26. Wang J, Thornton JC, Kolesnik S, Pierson RN Jr. Anthropometry in body composition. An overview. *Ann N Y Acad Sci.* 2000;904:317-326. doi: 10.1111/j.1749-6632.2000.tb06474.x.
27. Bross R, Chandramohan G, Kovesdy CP, et al. Comparing body composition assessment tests in long-term hemodialysis patients. *Am J Kidney Dis.* 2010;55(5):885-896. doi: 10.1053/j.ajkd.2009.12.031.

Practical method in the diagnosis of diabetic ketoacidosis: end-tidal carbon dioxide

Ahmet Kayalı¹, Ejder Saylav Bora²

Department of Emergency Medicine, İzmir Katip Çelebi University, Faculty of Medicine, İzmir, Türkiye

ABSTRACT

Objectives: Diabetic ketoacidosis (DKA) poses a life-threatening risk in uncontrolled diabetes. Current diagnostic criteria rely on invasive measures, leading to potential delays in treatment initiation. This study aimed to assess the diagnostic utility of noninvasive end-tidal carbon dioxide (EtCO₂) measurements in DKA patients.

Methods: A prospective, cross-sectional study was conducted in a tertiary-level Emergency Medicine Clinic from January 2021 to January 2023. Participants included adults with DKA symptoms and those with stable vital signs as controls. EtCO₂ levels were measured using a capnograph device. Diagnostic criteria for DKA were blood glucose ≥ 250 mg/dL, ketonuria, ketonemia, and metabolic acidosis (pH < 7.3 or bicarbonate < 15 mEq/dL). Statistical analysis was performed using SPSS Statistics.

Results: Of 730 participants, 120 had DKA, 410 did not, and 200 served as controls. EtCO₂ levels significantly differed between DKA, non-DKA, and control groups (P < 0.05). EtCO₂ correlated with pH, lactate, base deficit, and bicarbonate (P < 0.05). ROC analysis showed an AUC of 0.86 for EtCO₂ in diagnosing DKA (P < 0.01), with 91.67% sensitivity and 74.39% specificity at a cut-off value 23.7.

Conclusion: This study suggests that EtCO₂ measurement is a valuable noninvasive tool for diagnosing and assessing the severity of DKA in the emergency department. An EtCO₂ threshold of < 23.7 could prompt consideration of DKA in patients with elevated blood glucose levels. More extensive multicenter studies are warranted to validate these findings further. EtCO₂ measurement could facilitate early DKA diagnosis and improve patient outcomes.

Keywords: Diabetic ketoacidosis, end tidal CO₂, fast diagnosis, emergency medicine

Diabetic ketoacidosis (DKA) is a life-threatening metabolic complication that can result from poorly managed diabetes mellitus. DKA occurs due to decreased insulin effectiveness and an increase in counter-regulatory hormones. Diabetic ketoacidosis was consistently fatal before the identification of insulin in the 1920s. However, the mortality rate associated with DKA has decreased sig-

nificantly over time [1, 2].

Diabetic ketoacidosis sometimes occurs in newly diagnosed diabetic patients but more commonly in uncontrolled diabetic patients presenting to the emergency department with hyperglycemia, ketonemia, ketonuria, metabolic acidosis, and dehydration [3]. Rapid diagnosis and treatment are of great importance in this disease, which is a mortal picture affecting the

Corresponding author: Ejder Saylav Bora, Assoc. Prof., MD., PhD.,
Phone: +90 232 329 35 35, E-mail: ejdersaylav@gmail.com

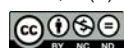
Received: February 1, 2024

Accepted: February 25, 2024

Published Online: April 22, 2024

How to cite this article: Kayalı A, Bora ES. Practical method in the diagnosis of diabetic ketoacidosis: end-tidal carbon dioxide. Eur Res J. 2024;10(3):303-310. doi: 10.18621/eurj.1430099

Copyright © 2024 by Prusa Medical Publishing
Available at <https://dergipark.org.tr/en/pub/eurj>



This is an open access article distributed under the terms of [Creative Commons Attribution-NonCommercial-NoDerivatives 4.0 International License](https://creativecommons.org/licenses/by-nc-nd/4.0/)



state of consciousness. Apart from physical examination, there is still no noninvasive method that will lead the physician to a rapid diagnosis except for blood glucose level ≥ 250 mg/dL, ketonuria, ketonemia, metabolic acidosis (pH <7.3 , bicarbonate level <18 mEq/dL), anion gap > 10 mEq/L (biochemistry, blood gas, and urinalysis) [4]. This may lead to prolonged treatment initiation and undesirable results in DKA patients who cannot be predicted by physical examination [4].

End-tidal carbon dioxide (EtCO₂) measured with a capnograph device indicates end-expiratory carbon dioxide pressure [5]. While it was first used in operations in patients undergoing anesthesia, it has started to be used in non-intubated patients over time [6]. Studies have shown that it can provide information about the patient's metabolic status, and it has been observed to be correlated with pH, bicarbonate, and PCO₂. EtCO₂, a noninvasive, rapid, easy-to-apply method, is increasing daily, especially in cardiopulmonary arrest management [7].

This study aimed to investigate the diagnostic feature of end-tidal carbon dioxide measurement with a capnograph device, which is a noninvasive, practical, and rapid application suitable for use in prehospital and hospital triage in diabetic ketoacidosis patients in a prospective, cross-sectional, controlled plan.

METHODS

Study Design

Our study was conducted as a prospective, cross-sectional, controlled, and single-center study between 01.01.2021 and 01.01.2023 in the Emergency Medicine Clinic of a tertiary-level Izmir Atatürk Training and Research Hospital in Izmir province. Consent was obtained from all volunteers participating in the study by face-to-face interview. The Declaration of Helsinki was complied with at all stages of the study.

Study Population

Patients over 18 who presented to the emergency department were included in the study. Patients presenting to the emergency department with symptoms and signs of diabetic ketoacidosis, nausea, vomiting, altered consciousness, polyuria/polydipsia, weakness, and abdominal pain were included in the study. The study did not include patients with respiratory pathology or diseases such as pneumonia, asthma, or COPD that may affect end-tidal carbon dioxide value. Unconscious patients, patients in whom end-tidal carbon dioxide measurement could not be adequately performed, and intubated patients were excluded from the study. The study did not include patients whose treatment was started before the measurement.

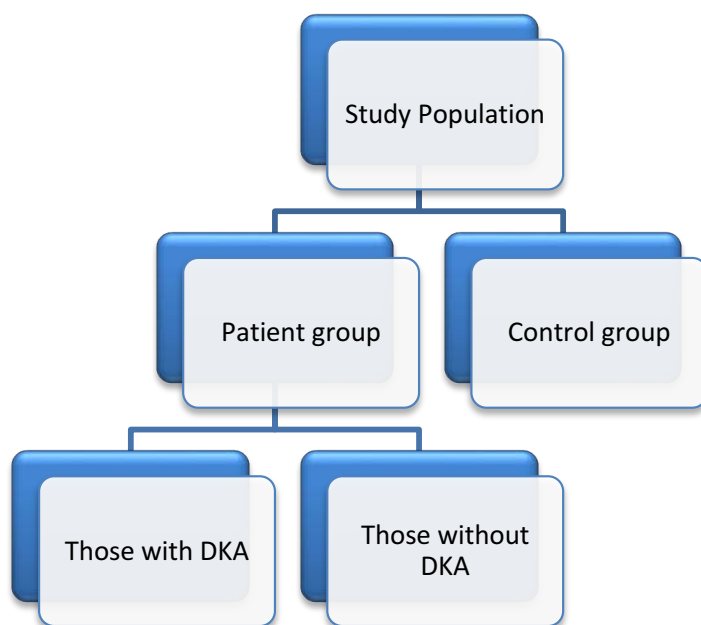


Fig. 1. Graphical explanation of the study population. DKA=Diabetic ketoacidosis.

Study Protocol and Data Collection

Patients presenting to the emergency department with symptoms and signs of diabetic ketoacidosis, such as nausea, vomiting, altered consciousness, polyuria/polydipsia, weakness, and abdominal pain, were evaluated. In the triage area, the SD Gluconavii Pro blood glucose meter is used to measure fingertip stick blood glucose and other vital signs in patients presenting to the emergency department. Those with a blood glucose value of 250 mg/dL and above were included in the study and named as the patient group. Those who met the diagnostic criteria for diabetic ketoacidosis (blood glucose level ≥ 250 mg/dL, ketonuria, ketonemia, metabolic acidosis (pH <7.3 or blood bicarbonate level <15 mEq/dL)) were divided into two groups as patient group-DKA patients and those who did not meet the diagnostic criteria as patient group-non-DKA patients.

Patients who presented to the emergency department for different reasons, whose stick blood glucose level was below 250 mg/dL, who had no respiratory disease or pathology that could affect the end-tidal CO₂ value, and whose vital signs were stable were included in the study as the control group (Fig. 1).

End-tidal CO₂ measurement was performed simultaneously with blood gas collection from the patients included in the study before any treatment was administered. End-tidal CO₂ measurement was performed with the VS2000 Vital Sign Monitor (UTECH CO., LTD. (UTMI) device, which measures with the side-stream technique using a side flow measurement mask.

The patient's vital signs, end-tidal CO₂ values, complaints, blood and urine tests, and outcomes were recorded on the case form. These data were used for statistical analysis.

Outcome Measurements

The primary outcome planned to be achieved in this study is to evaluate the effectiveness of end-tidal CO₂ measured with a mask in diagnosing diabetic ketoacidosis. For this purpose, end-tidal CO₂ levels were measured before treatment in patients grouped as control group, DKA, and non-DKA patients. The secondary outcome was to determine the efficacy of end-tidal CO₂ levels in determining the severity of diabetic ketoacidosis.

Statistical Analysis

Data were analyzed using the IBM SPSS Statistics Standard Concurrent User V 26 (IBM Corp., Armonk, New York, USA) statistical package program. Descriptive statistics were given as number of units (n), percentage (%), and mean \pm standard deviation ($\bar{x}\pm ss$) values. The Shapiro-Wilk normality test evaluated the normal distribution of the data of numerical variables. One-way Analysis of Variance (ANOVA) and Tukey HSD test, one of the multiple comparison tests, was used when the data were normally distributed; Kruskal Wallis and Bonferroni-Dunn test, one of the multiple comparison tests, were used when the data were not normally distributed. The Spearman correlation coefficient was used to analyze the relationships between the data. P <0.05 was considered statistically significant.

RESULTS

Seven hundred thirty people were included in the study. Among the participants, 56.16% were women. The mean age of the women was 59.45 ± 17.04 years, and the mean age of the men was 58.95 ± 14.88 years. In the study groups, there were 120 participants with DKA, 410 participants without DKA, and 200 participants in the control group. There was no statistically significant difference between these groups regarding mean age (P=0.41). Other demographic data about the patient groups are given in Table 1.

Systolic blood pressure, pH, base deficit, HCO₃, and end-tidal CO₂ parameters showed a statistically significant difference between the patient group with DKA and the other two study groups, the patient group without DKA and the control group (P <0.05). Pulse rate glucose parameters showed a statistically significant difference between the patient and control groups (P <0.05). The lactate parameter showed a statistically significant difference in all study groups (P <0.05). PO₂ and PCO₂ parameters showed no statistically significant difference between the study groups. Age, vital signs, blood gas, and end-tidal CO₂ values and p values of the patient groups are shown in Table 2.

The relationship between end-tidal and blood gas parameters, which were statistically significantly different between the study groups, was evaluated. End-

Table 1. Demographic characteristics of patients

			Patient group-Those with DKA	Patient group-Those without DKA	Control group	Total
Gender	Woman	n	13	51	18	82
		%	15.9%	62.2%	22.0%	100.0%
	Male	n	11	31	22	64
		%	17.2%	48.4%	34.4%	100.0%
Arrival complaint	Weakness	n	4	15	12	31
		%	12.9%	48.4%	38.7%	100.0%
	Abdominal pain	n	1	5	11	17
		%	5.9%	29.4%	64.7%	100.0%
	Nausea/vomiting	n	6	7	6	19
		%	31.6%	36.8%	31.6%	100.0%
	Chills/shivering	n	0	3	2	5
		%	0.0%	60.0%	40.0%	100.0%
	Shortness of breath	n	0	5	7	12
		%	0.0%	41.7%	58.3%	100.0%
	Dizziness	n	4	7	2	13
		%	30.8%	53.8%	15.4%	100.0%
	Polyuria/polydipsia	n	1	4	0	5
		%	20.0%	80.0%	0.0%	100.0%
Hypertension	None	n	17	30	18	65
		%	26.2%	46.2%	27.7%	100.0%
	There is	n	7	52	22	81
		%	8.6%	64.2%	27.2%	100.0%
Coronary artery disease	None	n	21	65	27	113
		%	18.6%	57.5%	23.9%	100.0%
	There is	n	3	17	13	33
		%	9.1%	51.5%	39.4%	100.0%
Congestive heart failure	None	n	24	76	33	133
		%	18.0%	57.1%	24.8%	100.0%
	There is	n	0	6	7	13
		%	0.0%	46.2%	53.8%	100.0%
Outcome	Discharge	n	6	61	24	91
		%	6.6%	67.0%	26.4%	100.0%
	Service hospitalization	n	11	18	15	44
		%	25.0%	40.9%	34.1%	100.0%
	Intensive care hospitalization	n	7	3	1	11
		%	63.6%	27.3%	9.1%	100.0%

Table 2. Vital signs, blood gas, and end-tidal CO₂ values of the patient groups

	DKA Patients	Non-DKA patients	Control group	P value
Age (years)	50.75±18.53	59.84±14.55	63.08±16.1	¥ 0.41
SBP (mmHg)	122.46±25.42 ^a	138.3± 25.16 ^b	127.43±19.89 ^b	¥ 0.01
DBP (mmHg)	70.88±13.38 ^a	77.51±13.83 ^b	71.68±11.92 ^a	£ 0.02
Saturation (%)	96.88±1.75	96.21±2.14	96.6±2.27	£ 0.34
Pulse (bpm)	99.08±17.53 ^a	89.91±13.84 ^a	86.8±14.23 ^b	¥ 0.01
Temperature (°)	50.02±66.45	40.53±36.07	36.43±0.3	£ 0.38
pH	7.23±0.1 ^a	7.39±0.05 ^b	7.41±0.07 ^b	¥ 0.001
PCO ₂ (mmHg)	37.7±30.09	48.35±47.11	38.15±7.88	£ 0.26
PO ₂ (mmHg)	63.46±34.22	51.55±38	54.83±29.69	£ 0.35
Glucose (mg/dL)	488.08±181.33 ^a	411.72±104.46 ^a	125.43±31.32 ^b	¥ 0.001
Lactate (mmol/L)	2.27±1.89 ^a	2.25±1.12 ^b	1.53±1.01 ^c	£ 0.01
Base excess (mEq/L)	12.82±7.84 ^a	3.3±2.66 ^b	3.4±2.9 ^b	¥ 0.001
HCO ₃ (mEq/L)	15.33±5.28 ^a	24.41±3.26 ^b	23.59±3.41 ^b	¥ 0.001
End-tidal CO ₂ (mmHg)	18.88±4.71 ^a	26.28±5.1 ^b	28.08±5.3 ^b	¥ 0.001

¥One-Way Anova- Post Hoc Test Tukey, SBP= Systolic blood pressure, DBP=Diastolic blood pressure

Table 3. Correlation values of end-tidal CO₂ and blood gas values of the patient group - DKA patients

DK groups		End-tidal CO ₂	pH	PO ₂	Lactate	Base minus
Patient group-DK patients	pH	r	0.421 *			
		P value	0.040			
		n	24			
	PO ₂	r	-0.365	-0.174		
		P value	0.080	0.415		
		n	24	24		
	Lactate	r	-0.476*	-0.031	-0.072	
		P value	0.019	0.885	0.739	
		n	24	24	24	
	Base minus	r	-0.437*	-0.857	0.482	0.020
		P value	0.033	0.000	0.017	0.928
		n	24	24	24	24
	HCO ₃	r	0.440*	0.843**	-0.300	-0.095
		P value	0.032	0.000	0.154	0.658
		n	24	24	24	24

*P<0.05, **P<0.01

Table 4. ROC analysis showing the diagnostic accuracy of ETCO₂

Criterion	Sensitivity	95% CI	Specificity	95% CI	+LR	95% CI	-LR	95% CI
≤23.7	91.67	73.0-99.0	74.39	63.6-83.4	3.58	2.43-5.28	0.11	0.030-0.42

tidal CO₂ was found to be statistically significantly correlated with pH, lactate, base minus, and bicarbonate (P<0.05) (Table 3).

ROC analysis was performed to examine the sensitivity and specificity of end-tidal CO₂ in diagnosing DKA patients with increased blood glucose levels. The surface area under the curve (AUC) was calculated as 0.86 with 91.67% sensitivity and 74.39% selectivity below the end-tidal CO₂ cut-off value of 23.7, and this result was statistically significant (P<0.01). (Table 4, Figs. 2 and 3).

DISCUSSION

More studies must be done on the diagnostic value of End-tidal CO₂ patients presenting to the emergency department. This study is one of the rare studies eval-

uating the use of capnography in prehospital and emergency department triage for the diagnosis of diabetic ketoacidosis.

Assessment of end-tidal CO₂ by capnography is a valuable method used in the emergency department and critical care settings, especially in the context of cardiac arrest and procedural sedation [8]. This study demonstrated that EtCO₂ measured with a capnograph device has diagnostic value in DKA patients.

Capnography has shown a consistent ability to aid in identifying and diagnosing metabolic acidemia. Linearity has been observed between EtCO₂ and serum bicarbonate levels. Many studies have investigated this relationship, particularly in DKA and diarrhea [9-14]. As the severity of acidemia increases, there is a decrease in bicarbonate levels, which leads to respiratory compensation and a subsequent decrease in EtCO₂ levels [9-12]. There is a direct relationship between the severity of acidemia and the decrease in bicarbonate and EtCO₂ levels. Furthermore, these EtCO₂ levels are closely related to venous pH and bicarbonate levels, which may aid the diagnostic process

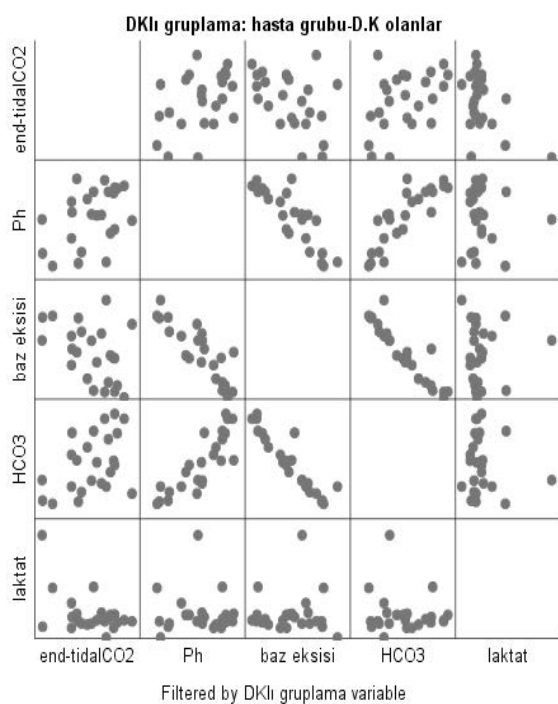


Fig. 2. Graph showing the correlation of end-tidal CO₂ with pH, lactate, base deficit, and bicarbonate.

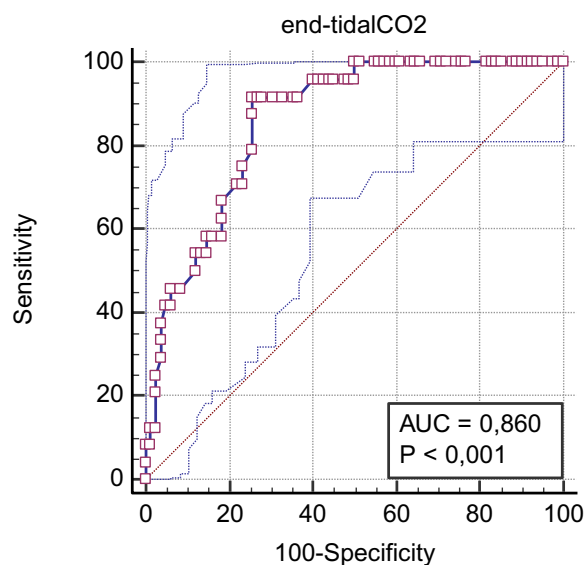


Fig. 3. ROC curve showing the diagnostic accuracy of ETCO₂.

[13-15]. This finding has potential for diabetic individuals in the evaluation of the presence of ketoacidosis [13, 14].

Recent studies investigate the relationship between metabolic acidosis and end-tidal CO₂ measured by capnography. However, the majority of these studies were performed in pediatric patients. In a study by Fearon and Steele [9] investigating the presence and severity of acidosis in children with diabetes mellitus by end-tidal CO₂ measurement, it was reported that end-tidal CO₂ <29 and below suggested a diagnosis of DKA. A recently published study by Bhattaram *et al.* [16] investigated the relationship between end-tidal CO₂ measurement and prognosis in adult DKA patients. They concluded that the diagnosis of DKA should be considered in patients with EtCO₂ values ≤24 measured by capnography [16]. Soleimanpour *et al.* [17] investigated the diagnostic utility of end-tidal CO₂ measurement in patients with suspected DKA presenting to the emergency department. They concluded that capnography could rule out DKA in patients with EtCO₂>24.5 and elevated blood glucose [17]. This study concluded that an end-tidal CO₂ limit value below 23,7 may be significant for diagnosing DKA. This result is similar to other studies.

This supports the idea that end-tidal CO₂ can be used for diagnostic purposes in DKA patients, where mortality and morbidity can be changed with rapid diagnosis in emergency departments.

Among the limited number of studies conducted on adult patients on this subject, in a single-center study conducted by Bou *et al.*, [18] it was reported that EtCO₂ may be helpful in adults in the differential diagnosis of DKA in patients presenting to the emergency department with glucose levels >550 mg/dL [18]. However, Taghizadieh *et al.* [19] compared arterial blood gas (ABG) with EtCO₂ and reported that capnographic EtCO₂ helped detect metabolic acidosis in spontaneously breathing patients. However, it should be remembered that ABG is the gold standard [19]. Similarly, this study showed a significant correlation between blood gas and capnographic EtCO₂ values.

In our study, it was concluded that there was a significant correlation between EtCO₂ and bicarbonate (P<0.05). Similarly, previous studies have reported a significant linear correlation between end-tidal CO₂

and bicarbonate [20-22]. As low bicarbonate level explains the metabolic acidosis present in patients with DKA, the linear significant correlation found between EtCO₂ and bicarbonate is another result supporting that EtCO₂ measurement can be used for diagnostic purposes in these patients.

In this study, we indirectly suggest that including EtCO₂ measurements in the diagnostic process may facilitate rapid triage of patients in the emergency department. By quickly identifying potential cases of DKA using EtCO₂, healthcare providers can prioritize these patients for immediate intervention. This would reduce the burden on the healthcare system while optimizing resource allocation and ensuring that critically ill individuals receive care quickly.

We also see the potential of EtCO₂ as a screening tool. By using EtCO₂ measurements as a first diagnostic step, healthcare providers can avoid unnecessary laboratory tests and imaging procedures in patients with hyperglycemia but not DKA. This would not only save time and resources, but it would also reduce patient discomfort and radiation exposure.

Limitations

The limitations of our study include the fact that it was a single-center study and the number of patients was limited. The study exclusion criteria included conditions that caused significant changes in end-tidal CO₂ value, and it may not have been possible to exclude all other confounding factors that affect EtCO₂ value. In addition, no comparison of end-tidal CO₂ measurement with other diagnostic methods was performed in the study. In addition, since the types of diabetic ketoacidosis were not analyzed separately, the possibility of different results in some types should not be overlooked.

CONCLUSION

This study showed that the EtCO₂ measurement may be an effective diagnostic tool in identifying DKA patients in the emergency department and evaluating their severity. DKA should be among our preliminary diagnoses in patients with elevated blood glucose levels if the end-tidal CO₂ value is <23,7. Larger scale and multicentre studies are needed in this regard.

Ethics Approval

Ethics committee approval was obtained from İzmir Katip Çelebi University non interventional Ethics Committee (No: 01/05.01.2023).

Authors' Contribution

Study Conception: AK, ESB; Study Design: AK, ESB; Supervision: N/A; Funding: N/A; Materials: AK, ESB; Data Collection and/or Processing: N/A; Statistical Analysis and/or Data Interpretation: N/A; Literature Review: AK, ESB; Manuscript Preparation: AK, ESB and Critical Review: N/A.

Conflict of interest

The authors disclosed no conflict of interest during the preparation or publication of this manuscript.

Financing

The authors disclosed that they did not receive any grant during conduction or writing of this study.

REFERENCES

- Kitabchi AE, Nyenwe EA. Hyperglycemic crises in diabetes mellitus: diabetic ketoacidosis and hyperglycemic hyperosmolar state. *Endocrinol Metab Clin North Am.* 2006;35(4):725-751, viii. doi: 10.1016/j.ecl.2006.09.006.
- Dhatariya KK. Defining and characterising diabetic ketoacidosis in adults. *Diabetes Res Clin Pract.* 2019;155:107797. doi: 10.1016/j.diabres.2019.107797.
- Karslioglu French E, Donihi AC, Korytkowski MT. Diabetic ketoacidosis and hyperosmolar hyperglycemic syndrome: review of acute decompensated diabetes in adult patients. *BMJ.* 2019;365:11114. doi: 10.1136/bmj.11114.
- Kitabchi AE, Umpierrez GE, Miles JM, Fisher JN. Hyperglycemic crises in adult patients with diabetes. *Diabetes Care.* 2009;32(7):1335-1343. doi: 10.2337/dc09-9032.
- Garcia E, Abramo TJ, Okada P, Guzman DD, Reisch JS, Wiebe RA. Capnometry for noninvasive continuous monitoring of metabolic status in pediatric diabetic ketoacidosis. *Crit Care Med.* 2003;31(10):2539-2543. doi: 10.1097/01.CCM.0000090008.79790.A7.
- Ward KR, Yealy DM. End-tidal carbon dioxide monitoring in emergency medicine, Part 1: Basic principles. *Acad Emerg Med.* 1998;5(6):628-636. doi: 10.1111/j.1553-2712.1998.tb02473.x.
- Long B, Koyfman A, Vivirito MA. Capnography in the Emergency Department: a review of uses, waveforms, and limitations. *J Emerg Med.* 2017;53(6):829-842. doi: 10.1016/j.jemermed.2017.08.026.
- Karaali R, Çakır A, Bora ES, Akyol PY, Kavalcı C, Acar H. The evaluation of end tidal carbon dioxide values in intubated patients with COVID-19. *Acta Biomed.* 2022;93(1):e2022032. doi: 10.23750/abm.v93i1.11989.
- Fearon DM, Steele DW. End-tidal carbon dioxide predicts the presence and severity of acidosis in children with diabetes. *Acad Emerg Med.* 2002;9(12):1373-1378. doi: 10.1111/j.1553-2712.2002.tb01605.x.
- Whitaker DK. Time for capnography - everywhere. *Anaesthesia.* 2011;66(7):544-549. doi: 10.1111/j.1365-2044.2011.06793.x.
- Kodali BS. Capnography outside the operating rooms. *Anesthesiology.* 2013;118(1):192-201. doi: 10.1097/ALN.0b013e318278c8b6.
- Nassar BS, Schmidt GA. Capnography during critical illness. *Chest.* 2016;149(2):576-585. doi: 10.1378/chest.15-1369.
- Manifold CA, Davids N, Villers LC, Wampler DA. Capnography for the nonintubated patient in the emergency setting. *J Emerg Med.* 2013;45(4):626-632. doi: 10.1016/j.jemermed.2013.05.012.
- Kartal M, Eray O, Rinnert S, Goksu E, Bektas F, Eken C. ETCO₂: a predictive tool for excluding metabolic disturbances in nonintubated patients. *Am J Emerg Med.* 2011;29(1):65-69. doi: 10.1016/j.ajem.2009.08.001.
- Agus MS, Alexander JL, Mantell PA. Continuous non-invasive end-tidal CO₂ monitoring in pediatric inpatients with diabetic ketoacidosis. *Pediatr Diabetes.* 2006;7(4):196-200. doi: 10.1111/j.1399-5448.2006.00186.x.
- Bhattaram S, Shinde VS, Khumujam PP, Anilkumar AP, Reddy DK. Capnography as a tool for triaging and diagnosis of diabetic ketoacidosis in the emergency department: a prospective observational study. *Turk J Emerg Med.* 2023;23(3):169-175. doi: 10.4103/tjem.tjem_15_23.
- Soleimanpour H, Taghizadieh A, Niafar M, Rahmani F, Golzari SE, Esfanjani RM. Predictive value of capnography for suspected diabetic ketoacidosis in the emergency department. *West J Emerg Med.* 2013;14(6):590-594. doi: 10.5811/westjem.2013.4.14296.
- Bou Chebl R, Madden B, Belsky J, Harmouche E, Yessayan L. Diagnostic value of end tidal capnography in patients with hyperglycemia in the emergency department. *BMC Emerg Med.* 2016;16:7. doi: 10.1186/s12873-016-0072-7.
- Taghizadieh A, Pouraghaei M, Moharamzadeh P, et al. Comparison of end-tidal carbon dioxide and arterial blood bicarbonate levels in patients with metabolic acidosis referred to emergency medicine. *J Cardiovasc Thorac Res.* 2016;8(3):98-101. doi: 10.15171/jcvtr.2016.21.
- Gilhotra Y, Porter P. Predicting diabetic ketoacidosis in children by measuring end-tidal CO₂ via non-invasive nasal capnography. *J Paediatr Child Health.* 2007;43(10):677-680. doi: 10.1111/j.1440-1754.2007.01186.x.
- Hunter C, Putman M, Foster J, et al. Utilizing end-tidal carbon dioxide to diagnose diabetic ketoacidosis in prehospital patients with hyperglycemia. *Prehosp Disaster Med.* 2020;35(3):281-284. doi: 10.1017/S1049023X20000485.
- Sezik S, Hakoğlu O, Okuş O, Sorgun O. Trends in Emergency Department visits, and hospital admissions pre- and during Covid 19 pandemic. *Arch Curr Med Res.* 2023;4(1):47-57. doi: 10.47482/acmr.1199056.

The relationship between fibromyalgia syndrome and inflammation parameters in hemodialysis patients

Semahat Karahisar Şirali¹, Refika Büberci²

¹Department of Nephrology, Ufuk University, Dr. Rıdvan Ege Hospital, Ankara, Türkiye; ²Department of Radiology, University of Health Sciences, Ankara Training and Research Hospital, Ankara, Türkiye

ABSTRACT

Objectives: Diagnosing fibromyalgia, a condition characterized by widespread body pain of unknown origin accompanied by various additional symptoms, poses a challenge in hemodialysis patients, who frequently experience musculoskeletal disorders. To investigate the relationship between fibromyalgia syndrome and inflammation parameters in hemodialysis patients.

Methods: The study enrolled 311 hemodialysis patients undergoing treatment for over three months. Demographic characteristics, complete blood count, and biochemical values were documented as part of the study. To assess fibromyalgia, the researchers recorded the patients scores on the Generalized Pain Scale and Symptom Severity Scale based on data provided by the American College of Rheumatology. The patients were then divided into two groups: those with fibromyalgia and those without fibromyalgia, and their laboratory values and rates were compared. Inflammatory parameters such as erythrocyte sedimentation rate, c reactive protein, monocyte-to-lymphocyte ratio, lymphocyte-to-c reactive protein ratio, and c reactive protein to albumin ratio were recorded.

Results: The study included 311 patients on hemodialysis for more than three months. Among the study participants, 48.9% of the patients and 62.9% of those with fibromyalgia were women. The mean age was 54±26 years and was significantly higher in patients with fibromyalgia (P<0.001). Monocyte (P<0.03), C-reactive protein (P<0.01), erythrocyte sedimentation rate (P<0.02), Monocyte to lymphocyte ratio (P=0.028), c reactive protein to albumin ratio (P<0.005) were significantly higher, lymphocyte to c reactive protein ratio (P<0.004) and albumin (P=0.018) were significantly lower in the fibromyalgia group.

Conclusions: Fibromyalgia should be considered in the presence of high inflammation parameters in hemodialysis patients with diffuse musculoskeletal pain.

Keywords: Fibromyalgia, hemodialysis, inflammation parameters, hematological indices

Chronic kidney disease represents a significant public health concern and has a detrimental impact on the quality of life [1]. Hemodialysis is the most commonly employed renal replacement therapy for individuals with chronic kidney disease, a con-

dition frequently associated with musculoskeletal disorders [2]. Fibromyalgia syndrome (FS) is a prevalent pain disorder characterized by tenderness and stiffness in specific anatomical regions. Mood and sleep disturbances, fatigue, and functional impairments often ac-

Corresponding author: Semahat Karahisar Şirali, MD, Assistant Prof.
Phone: 0850 308 83 85, E-mail: drsemahat@hotmail.com

How to cite this article: Karahisar Şirali S, Büberci R. The relationship between fibromyalgia syndrome and inflammation parameters in hemodialysis patients. Eur Res J. 2024;10(3):311-318. doi: 10.18621/eurj.1361155

Received: September 15, 2023

Accepted: January 25, 2024

Published Online: March 16, 2024

Copyright © 2024 by Prusa Medical Publishing
Available at <https://dergipark.org.tr/en/pub/eurj>



This is an open access article distributed under the terms of [Creative Commons Attribution-NonCommercial-NoDerivatives 4.0 International License](https://creativecommons.org/licenses/by-nc-nd/4.0/)

company it. FS is an extra-articular rheumatic disease influenced by non-modifiable risk factors such as age, gender, cultural and ethnic background, genetics, inflammation, and low socioeconomic status. The pain experienced in fibromyalgia tends to worsen with movement, leading to reduced physical activity and limited sun exposure. These factors contribute to an increased risk of osteoporosis and pose challenges in diagnosing and treating both bone mineral disorders and fibromyalgia in hemodialysis patients [3-7].

The 2010 American College of Rheumatology (ACR) criteria for fibromyalgia syndrome, which can affect all ages and genders and for which no clear pathophysiologic cause is known, have facilitated diagnostic evaluation [8]. Since there are no predictable biomarkers for the diagnosis, evaluation requires more active use of questionnaire methods questioning the severity, location, and prevalence of pain. Complete blood counts and laboratory tests are requested from every patient admitted to the hospital. Many diseases are associated with inflammatory processes, and standard parameters such as erythrocyte sedimentation rate (ESR), and C-reactive protein (CRP) have been used in the past. The role of non-routinely used indices in defining inflammation is increasing. Many studies have shown that tests such as neutrophil-lymphocyte ratio (NLR), platelet lymphocyte ratio (PLR), mean platelet volume (MPV), red blood cell distribution volume (RDW), CRP, monocyte lymphocyte ratio (MLR), CRP albumin ratio (CRP/ALB), lymphocyte CRP ratio (LCRPO) are associated with inflammatory processes [9-21].

Hemodialysis patients are known to be in an inflammatory process. It has been stated that half of the patients with the glomerular filtration rate (GFR) level of 15-60 mL/min had a CRP level of >2.1 mg/dL [22]. Uremic environment, decreased clearance and increased proinflammatory cytokines, oxidative stress, acidosis, acute and chronic diseases related to the dialysis process. Factors related to infections, changing adipose tissue metabolism and extracorporeal circulation (purity of dialysis water, microbiological quality, membrane compatibility) also play an additional role in inflammation [23]. The aim of this study was to investigate the guiding value of inflammatory parameters in the diagnosis of fibromyalgia in hemodialysis patients in the inflammatory process.

This study aimed to investigate the guiding value

of inflammatory parameters in diagnosing fibromyalgia in hemodialysis patients with inflammatory processes.

METHODS

The study included 311 patients on hemodialysis for more than three months. Patients with known rheumatologic disease, osteoporosis, malignancy, hemiplegia, hypothyroidism or hyperthyroidism, malnutrition, inflammatory bowel disease, and those on hemodialysis for less than three months were excluded. Demographic data such as age and gender and history of hypertension, diabetes mellitus, coronary artery disease, cerebrovascular diseases, hypothyroidism, anxiety, depression, and dementia were recorded. Monthly income level and home heating type were recorded for socioeconomic status. Complete blood count and neutrophil-lymphocyte ratio (NLO), monocyte lymphocyte ratio (MLO), platelet mean platelet volume ratio (PMPVO), CRP albumin ratio (CRP/ALB), platelet lymphocyte ratio (PLO), lymphocyte CRP ratio (LCRP) and albumin, Laboratory results including calcium, phosphorus, ferritin, parathormone (PTH), uric acid, c-reactive protein (CRP), erythrocyte sedimentation rate (ESR), thyroid stimulating hormone (TSH), bicarbonate, alkaline phosphatase (ALP) were recorded.

The diagnosis of fibromyalgia is based on the examination of tenderness at specific anatomical sites and is made using the widespread pain scale (WPI) and symptom severity scale (SS) in the American College of Rheumatology (ACD) 2010 update. The degree of physical disability is determined with the Fibromyalgia Impact Scale (FES). In our study, FS diagnosis and FES were determined by applying these questionnaires to the patients. The widespread pain scale (WPI) is a scoring scale ranging from 0 to 19 for persistent pain in at least four of the five zones (upper and lower left, upper and lower right abdomen, upper and lower right abdomen, and axial region) in the last seven days. The SS consists of two groups. First group A (all items including fatigue, waking up without rest, cognitive findings, and somatic symptoms in the last week are scored between 0-3) and second group B (headache in the last six months, pain-cramps in the lower abdomen, presence of depression are assessed)

A+B total is a maximum of 12 points. The maximum WPI+SS total is 31 points. Accordingly, scores below a total of 12 points are not suggestive of fibromyalgia. The data obtained from each patient were summed for these scores, and those with fibromyalgia were identified.

The fibromyalgia impact scale (FES) was recorded according to the American College of Rheumatology (ACR) criteria. The FES consists of 4 components, and in the first component, 11 activities of daily living, such as shopping, laundry, cooking, and making the bed, are evaluated on a Likert scale from 0-3. The total score obtained is divided by the number of questions, and the average score is obtained. This score is multiplied by 3.33 for normalization. In the second component, the number of days the participant feels well is scored inversely proportional to the severity of the disease and multiplied by 1.43 for normalization. In the third component, the number of days unable to go to work and do household chores is multiplied by 1.43 for normalization. In the fourth component, the scores of questions 4-10 are taken. A total of 50 points and above means that physical disability has increased.

The study group was divided into two groups as those with fibromyalgia (FS+) and those without (FS-). Inflammation and hematologic parameters, ratios, and biochemistry parameters were compared between the groups.

The study was approved by Health Sciences University Ankara Training and Research Hospital Ethical Committee (Decision no: E-22-1011, Date: 27.07.2022). All procedures were carried out in accordance with the ethical rules and the principles of the Declaration of Helsinki.

Statistical Analysis

Analyses were conducted using UN Statistical Package for the Social Sciences 22.0 version (IBM SPSS Corp.; Armonk, NY, USA). Categorical variables were expressed as frequency (n) and percentage (%). Continuous variables were tested for conformity to a normal distribution by Kolmogorov-Smirnov and expressed as arithmetic mean, standard deviation, median, minimum, and maximum values. The student-t test was used to compare continuous variables with normal distribution, while those without normal distribution were analyzed by the Mann-Whitney U test.

Pearson- χ^2 and Fisher's exact tests were used for categorical variables. Spearman's correlation was used for correlation analysis, and $P < 0.05$ was accepted as the significance level. Receiving operating characteristic (ROC) curve was used to find the sensitivity and specificity threshold values of hematologic ratios.

RESULTS

Among the patients who participated in the study, 48.9% were women, and 62.9% of patients with fibromyalgia were women. The mean age was 54 years (IQR 26). Age was significantly higher in FS+ hemodialysis patients ($P < 0.001$), and female gender was significantly higher ($P < 0.002$). FS+ hemodialysis patients had significantly higher rates of hypertension ($p < 0.027$), anxiety ($P = 0.016$), depression ($P < 0.001$), and dementia ($P = 0.010$). In the FS+ group, the rate of catheter access to hemodialysis was high ($P < 0.002$), and home heating was stove ($P = 0.024$). A comparison of demographic and laboratory data of the groups is presented in Table 1, and co-morbid conditions and socioeconomic status are presented in Table 2.

There was no difference in the duration of dialysis and KT/V ratio between FS+ and FS- groups on hemodialysis. There was no difference between white cell count, lymphocyte, and neutrophil cell counts in both groups. Monocyte cell count was significantly higher in the FS+ group ($P < 0.03$). Hemoglobin, platelet, and mean platelet volume did not differ between the groups.

There was no significant difference between the groups in glucose, calcium, phosphorus, magnesium, total protein, uric acid, alkaline phosphatase, total cholesterol, thyroid stimulating hormone, total iron saturation, vitamin B12, creatinine kinase, and bicarbonate levels. PTH was significantly lower in FS+ patients compared to non-FS+ patients ($P = 0.013$). The folic acid level was significantly lower in the FS+ group. CRP, a marker of inflammation, was significantly higher in the FS+ group ($P < 0.01$), and erythrocyte sedimentation rate was significantly higher ($P < 0.02$). Ferritin, a negative acute phase reactant, was significantly higher in the FS+ group ($P < 0.05$). Albumin level was significantly lower in the FS+ group ($P = 0.018$).

In the ratios of inflammation parameters, CRP/PALBO was significantly higher ($P < 0.005$), MLO was

Table 1. Group demographic and laboratory data

	Total (n=311)	FS (+) (n=89)	FS (-) (n=222)	t, z, x ²	P value
Age (years)	54 (26)	62 (21)	51 (27)	-4.458	<0.001
Gender					
Female	48.9%	62.9%	43.2%		<0.002
Male	51.1%	37.1%	56.8%		
Dialysis time (h)	4 (4.5)	4 (4.5)	4 (4.5)	-0.392	0.695
KT/V	1.6 (0.48)	1.63 (0.49)	1.60 (0.52)	0.973	0.330
WBC ($\times 10^9/L$)	6.98 (3.09)	7 (2.91)	6.93 (3.14)	-0.089	0.929
Neutrophil ($\times 10^9/L$)	4.66 (2.42)	4.62 (2.36)	4.66 (2.46)	-0.347	0.729
Lymphocyte ($\times 10^9/L$)	1.6 (0.86)	1.55 (0.86)	1.61 (0.87)	-1.015	0.310
Monocytes ($\times 10^9/L$)	0.60 (0.28)	0.64 (0.33)	0.57 (0.27)	-2.169	<0.030
Hb (g/dL)	10.97 \pm 1.6	10.79 \pm 1.54	11.05 \pm 1.63	1.291	0.198
PLT ($\times 10^9/L$)	202 (94)	208 (96)	199.5 (89)	-0.869	0.385
MPV (fL)	10.32 \pm 1.11	10.43 \pm 1.09	10.27 \pm 1.11	-1.142	0.254
CRP (mg/dL)	7.4 (13.7)	8.6 (18.8)	6.3 (12.5)	-2.588	<0.010
ESR (mm/h)	27 (33)	33 (37.5)	24.5 (29.2)	-2.331	<0.020
Glucose	105 (63)	106 (78)	104.5 (54)	-0.440	0.660
Calcium	8.63 (0.92)	8.55 (0.93)	8.68 (0.91)	-1.057	0.290
Phosphorus	4.72 \pm 1.5	4.54 \pm 1.55	4.78 \pm 1.47	1.284	0.200
Magnesium	2.04 (0.74)	2.01 (0.60)	2.08 (0.79)	-0.995	0.320
Total protein	6.7 \pm 0.80	6.8 \pm 0.90	6.65 \pm 0.88	-1.712	0.088
Albumin	3.9 (0.5)	3.8 (0.5)	3.9 (0.5)	-2.361	0.018
Uric acid	6.1 (1.80)	5.9 (1.55)	6.2 (1.92)	-1.791	0.073
ALP (IU/L)	121.09 (83)	113.98 (75)	123.2 (84)	-0.621	0.535
PTH (IU/L)	389 (488.7)	346.7 (366.3)	405 (505.9)	-2.497	0.013
Cholesterol (mg/dL)	155 (50)	162 (56)	151 (50)	-1.609	0.109
Ferritin (ng/mL)	575 (479.1)	663.3 (503.4)	560.2 (477.4)	-1.936	0.053
TSH (mIU/L)	1.7 (1.8)	1.82 (2)	1.65 (1.6)	-1.396	0.163
B12 vitamin (pg/mL)	479 (495)	494 (520)	465 (483)	-0.457	0.648
Folate (ng/mL)	10.5 (17.7)	8.65 (14.2)	12.38 (17.8)	-2.132	0.033
CK (U/L)	60 (61)	54 (72)	61 (57)	-0.232	0.817
Bicarbonate (mEq/L)	21.2 (4.5)	21.1 (5.2)	21.3 (4.1)	-0.364	0.716
NLO	2.88 (1.88)	2.73 (1.9)	2.98 (1.88)	-0.079	0.937
MLO	0.354 (0.20)	0.38 (0.18)	0.33 (0.20)	-2.204	0.028
PMPVO	20 (10.08)	20 (12.09)	20 (9.01)	-0.407	0.684
CRPALBO	1.89 (3.49)	2.45 (5.5)	1.57 (3.04)	-2.814	<0.005
PLO	126.7 (71.2)	131 (75.7)	125.9 (69.9)	-1.196	0.232
LCRPO	0.217 (0.41)	0.167 (0.29)	0.243(0.42)	-2.876	<0.004

Data are shown as mean \pm standard deviation^a or mean (IQR)^b. WBC=White blood cell, Hb=Hemoglobin, PLT=Platelets, MPV=Mean platelet volume, CRP=C-reactive protein, ESR=erythrocyte sedimentation rate, ALP=Alkaline phosphatase, PTH=Parathormone, TSH=Thyroid stimulating hormone, CK=Creatinine kinase, NLO=Neutrophil lymphocyte ratio, MLO=Monocyte lymphocyte ratio, PMPVO=Platelet MPV ratio, CRPALBO= CRP albumine ratio, PLO= Platelet lymphocyte ratio, LCRPO=Lymphocyte CRP ratio.

Table 2. Co-morbid diseases and socioeconomic status of groups

		FS (-)	FS (+)	P value
Diabetes mellitus	No	71.6%	61.8%	0.091
	Yes	28.4%	38.2%	
Hypertension	No	37.8%	24.7%	0.027
	Yes	62.2%	75.3%	
Coronary artery disease	No	80.2%	75.3%	0.340
	Yes	19.8%	24.7%	
Cerebrovascular accident	No	96.8%	92.1%	0.070
	Yes	3.2%	7.9%	
Hypothyroidi	No	95%	98.9%	0.113
	Yes	5%	1.1%	
Anxiety	No	92.3%	83.1%	0.016
	Yes	7.7%	16.9%	
Depression	No	92.8%	79.8%	<0.001
	Yes	7.8%	20.2%	
Dementia	No	99.5%	95.5%	0.010
	Yes	0.5%	4.5%	
Vascular Acces	AVF	71.2%	52.8%	<0.002
	Catheter	28.8%	47.2	
Warming	Stove	63.1%	76.4%	0.024
	Radiator	36.9%	23.6%	
Monthly income	<5.000	75.7%	78.7%	.853
	5.000-10.000	21.6%	19.1%	
	>10.000	2.7%	2.2%	

AVF=arteriovenous fistula

significantly higher ($P=0.028$), and LCRPO was significantly lower ($P<0.004$) in the FS+ group. There was no significant difference between NLO, PMPVO, and PLO between the two groups.

There was a negative correlation between the fibromyalgia effect score and LCRPO ($r=-.237$, $P<0.001$), a positive correlation between CRPALBO ($r=.237$, $P<0.001$), a positive correlation with ESR ($r=.166$, $P<0.003$), a positive correlation with MLO ($r=.116$, $P=0.041$) and a strong positive correlation with CRP ($r=.223$, $P<0.001$) between the FS+ group and the FS- group.

When ROC analysis was performed for MLO, CRPALBO, and LCRP, which showed significant dif-

ferences in the FS+ group, the area under the curve was found to be significant at $P=0.028$, $P<0.005$ and $P<0.004$, respectively (Fig. 1).

DISCUSSION

This study showed that inflammation was more prominent in the group with fibromyalgia in hemodialysis patients. In addition to the significant difference in MLO, CRPALBO, and LCRPO ratios between FS+ and FS- groups, these ratios were correlated with fibromyalgia effect score, and ROC analysis supported these data. This study suggests that inflammatory

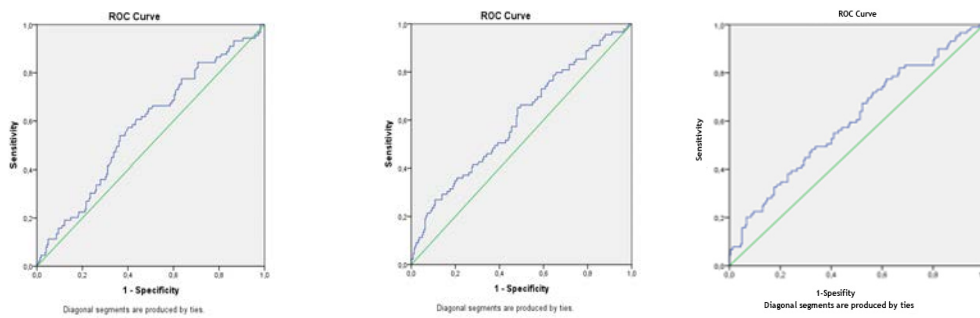


Fig. 1. ROC analysis of MLO, CRPALBO and LCRPO between FS (+) and FS (-) groups.

Ratio	AUC (95%)	Cutt-off	P value	Sensitivity (%)	Spesifity (%)
MLO	.580(.510-.650)	.36	0.028	.419	.581
CRPALBO	.602(.532-.672)	1.97	<0.005	.450	.550
LCRP	.604(.534-.674)	.20	<0.004	.562	.563

MLO=Monocyte lymphocyte ratio, CRPALBO= CRP albümine ratio, LCRPO=Lymphocyte CRP ratio

markers may serve as predictors for the diagnosis of fibromyalgia in hemodialysis patients.

The absence of differences in dialysis duration and KT/V between FS+ and FS- hemodialysis patients indicate the comparability of the two groups and suggests the absence of bias. Furthermore, the significant findings of MLO, CRPALBO, and LCRPO in FS+ hemodialysis patients suggest the involvement of inflammation in the condition. In a previous study by Varim *et al.* [11], it was reported that the lymphocyte-to-monocyte ratio was significantly lower in the fibromyalgia group compared to healthy volunteers, which aligns with the significantly higher Monocyte lymphocyte ratio and monocyte count observed in this study involving hemodialysis patients.

NLO, PLO, and PMPVO, which have started to be used in the diagnosis of systemic inflammation from non-traditional hematologic ratios, were not found significant in this study. This study's findings, which show a lack of clinically significant correlation between pain severity and MPV in patients with fibromyalgia, are consistent with the study conducted by Jayakrishnan *et al.* [15]. This increase in acute exacerbations may be attributed to chronic inflammation in chronic hemodialysis patients. This study was not compatible with the study of Aktürk and Büyükavcı [16], who found NLO and MPV to be significantly higher and PDW to be significantly lower in the comparison of healthy controls and fibromyalgia patient group. Haliloğlu *et al.* [19] found no difference be-

tween ESR, CRP, white blood cell count, and platelet count in the control group and fibromyalgia group; only MPV was found to be significantly higher and interpreted as increased platelet activation and increased risk of cardiovascular disease. Korniluk *et al.* [20] reported that the hematology standardization committee approved MPV as an acceptable parameter for many diseases. The two groups in the present study consisted of hemodialysis patients, and there was no significant difference in MPV.

In a study conducted by Yazıcı *et al.* [24] in rheumatoid arthritis patients compared with a control group, MPV was found to be correlated with disease activity, ESR, and CRP. In this study, ESR and CRP inflammation markers were significantly higher in the fibromyalgia group. It was not associated with MPV. In a large-scale community screening study by Feinberg *et al.* [189], a significant positive association of fibromyalgia with serum CRP was found in hemodialysis patients with fibromyalgia in this study.

Yüçetürk *et al.* [7] found a high fibromyalgia effect score (FES) in hemodialysis patients with fibromyalgia compared to the control group. In this study, FES was found to be high in hemodialysis patients with fibromyalgia and correlated with MLO, CRPALBO, and LCRPO. No difference was found between albumin, calcium, phosphorus, ALP, TSH, and PTH in the study by Yüçetürk *et al.* In this study, only PTH and albumin were significantly lower in hemodialysis patients with fibromyalgia. It was evalu-

ated as a low-cycling bone mineral disorder due to immobilization. The increase in fibromyalgia pain with movement is considered a factor in this situation's development. In a comparison of healthy volunteers and the fibromyalgia group by Al-Nimer *et al.* [17], it was reported that the evaluation of hemotologic ratios with FES could be used in diagnosis and prognosis follow-up. This study showed a significant positive correlation between the FES score and MLO, CRP, ESR, and CRPALBO.

The study by Taylor *et al.* [14], which investigated monocyte subpopulations in healthy controls and fibromyalgia patient groups, reported a positive correlation between stress, pain, and monocyte subpopulations. This finding aligns with the significantly higher monocyte count observed in hemodialysis patients with fibromyalgia in the current study. Both studies suggest a potential relationship between stress, pain, and alterations in monocyte populations in fibromyalgia, supporting the notion of a similar pattern of association.

In a study by Çağlıyan Türk *et al.* [21] with hemodialysis, peritoneal dialysis, and transplant patients, the relationship between the frequency of depressive symptoms and anxiety in patients with fibromyalgia was also found in this study. Laboratory parameters were not significantly different in hemodialysis, peritoneal dialysis, and transplantation patients. In this study, inflammation parameters MLO, CRPALBO, CRP, ESR, and LCRPO were significant in hemodialysis patients with fibromyalgia. It is known that half of the patients with GFR 15-60% ml/min had CRP >2.1mg/dL [22]. The effect of inflammation in fibromyalgia syndrome is also known. Changes in parameters and rates monitored in hemodialysis patients who are exposed to the same inflammation load, which may also be affected by environmental and genetic factors, may be guiding in patients clinically suggestive of fibromyalgia. The frequency of fibromyalgia, which is found at 2-8% in the general population, in patients receiving renal replacement therapy is not fully known [5].

As in many studies, fibromyalgia was found to be more common in the female gender in this study. Since the gender distribution is not normal, the absence of a significant relationship other than age in the FS+ and FS- group comparisons made only in females can be explained by further studies.

Limitations

The limitations of our study include not to study pro-inflammatory cytokines, adhesion molecules, adipokines and related factors, and anti-inflammatory cytokines and the relatively small number of cases.

CONCLUSION

The results of this study show that inflammation parameters and hematologic ratios can be used in the diagnosis of fibromyalgia, the pathophysiology of which has not been fully elucidated. Monocytes, MLO, CRP, CRPALBO, ESR, and LCRPO and their relationship with fibromyalgia effect score suggest that they can be used in prognosis follow-up. Since the items under the curve in ROC analysis are significant, further studies are needed to determine the exact cut-off values.

Authors' Contribution

Study Conception: SKŞ, RB; Study Design: SKŞ; Supervision: RB; Funding: SKŞ; Materials: SKŞ; Data Collection and/or Processing: SKŞ; Statistical Analysis and/or Data Interpretation: SKŞ, RB; Literature Review: SKŞ; Manuscript Preparation: SKŞ and Critical Review: SKŞ, RB.

Conflict of interest

The authors disclosed no conflict of interest during the preparation or publication of this manuscript.

Financing

The authors disclosed that they did not receive any grant during conduction or writing of this study.

REFERENCES

1. Levey AS, Eckardt KU, Dorman NM, et al. Nomenclature for Kidney Function and Disease: Executive Summary and Glossary From a Kidney Disease: Improving Global Outcomes (KDIGO) Consensus Conference. *Kidney Med.* 2020;2(4):373-376. doi: 10.1016/j.xkme.2020.05.003.
2. Liyanage T, Ninomiya T, Jha V, et al. Worldwide access to treatment for end-stage kidney disease: a systematic review. *Lancet.* 2015;385(9981):1975-1982. doi: 10.1016/S0140-6736(14)61601-9.
3. Maffei ME. Fibromyalgia: Recent Advances in Diagnosis, Classification, Pharmacotherapy and Alternative Remedies. *Int J Mol Sci.* 2020;21(21):7877. doi: 10.3390/ijms21217877.

4. Sarzi-Puttini P, Atzeni F, Masala IF, Salaffi F, Chapman J, Choy E. Are the ACR 2010 diagnostic criteria for fibromyalgia better than the 1990 criteria? *Autoimmun Rev.* 2018;17(1):33-35. doi: 10.1016/j.autrev.2017.11.007.
5. Clauw DJ. Fibromyalgia: a clinical review. *JAMA.* 2014;311(15):1547-55. doi: 10.1001/jama.2014.3266.
6. Wang SM, Han C, Lee SJ, Patkar AA, Masand PS, Pae CU. Fibromyalgia diagnosis: a review of the past, present and future. *Expert Rev Neurother.* 2015;15(6):667-679. doi: 10.1586/14737175.2015.1046841.
7. Yuceturk TE, Yucel AE, Yuceturk H, et al. Fibromyalgia: its prevalence in haemodialysis patients and its relationships with clinical and laboratory parameters. *Nephrol Dial Transplant.* 2005;20(11):2485-2488. doi: 10.1093/ndt/gfi028.
8. Cuyul-Vásquez I, Araya-Quintanilla F, Gutiérrez-Espinoza H. Comment on Siracusa et al. Fibromyalgia: Pathogenesis, Mechanisms, Diagnosis and Treatment Options Update. *Int. J. Mol. Sci.* 2021;22, 3891. *Int J Mol Sci.* 2021;22(16):9075. doi: 10.3390/ijms22169075.
9. Germolec DR, Shipkowski KA, Frawley RP, Evans E. Markers of Inflammation. *Methods Mol Biol.* 2018; 1803:57-79. doi: 10.1007/978-1-4939-8549-4_5.
10. Khamisy-Farah R, Fund E, Raibman-Spector S, Adawi M. Inflammatory Markers in the Diagnosis of Fibromyalgia. *Isr Med Assoc J.* 2021;23(12):801-804.
11. Varim C, Çelik F, Sunu C, et al. Inflammatory cell rations in the patients with fibromyalgia. *Georgian Med News* 2021;(315):108-113.
12. Metyas SK, Solyman JS, Arkfeld DG. Inflammatory Fibromyalgia: Is it Real? *Curr Rheumatol Rev.* 2015;11(1):15-17. doi: 10.2174/1573397111666150522095004.
13. Coskun Benlidayi I. Role of inflammation in the pathogenesis and treatment of fibromyalgia. *Rheumatol Int.* 2019;39(5):781-791. doi: 10.1007/s00296-019-04251-6.
14. Taylor AG, Fischer-White TG, Anderson JG, et al. Stress, Inflammation and Pain: A Potential Role for Monocytes in Fibromyalgia-related Symptom Severity. *Stress Health.* 2016;32(5):503-513. doi: 10.1002/smi.2648.
15. Rajaram Jayakrishnan AK, Easwar SV, Thattil J, et al. Studying the Relation Between Fibromyalgia Severity and Neutrophil-to-Lymphocyte Ratio, Platelet-to-Lymphocyte Ratio, and Mean Platelet Volume. *Cureus.* 2022;14(5):e24847. doi: 10.7759/cureus.24847.
16. Aktürk S, Büyükavcı R. Evaluation of blood neutrophil-lymphocyte ratio and platelet distribution width as inflammatory markers in patients with fibromyalgia. *Clin Rheumatol.* 2017;36(8):1885-1889. doi: 10.1007/s10067-017-3647-0.
17. Al-Nimer MSM, Mohammad TAM. Correlation of hematological indices and ratios derived from them with FIQR scores in fibromyalgia. *Pak J Med Sci.* 2018;34(5):1219-1224. doi: 10.12669/pjms.345.15169.
18. Feinberg T, Sambamoorthi U, Lilly C, Innes KK. Potential Mediators between Fibromyalgia and C-Reactive protein: Results from a Large U.S. Community Survey. *BMC Musculoskelet Disord.* 2017;18(1):294. doi: 10.1186/s12891-017-1641-y.
19. Haliloğlu S, Carlioglu A, Sahiner E, Karaaslan Y, Kosar A. Mean platelet volume in patients with fibromyalgia. *Z Rheumatol.* 2014;73(8):742-745. doi: 10.1007/s00393-013-1330-7.
20. Korniluk A, Koper-Lenkiewicz OM, Kamińska J, Kemona H, Dymicka-Piekarska V. Mean Platelet Volume (MPV): New Perspectives for an Old Marker in the Course and Prognosis of Inflammatory Conditions. *Mediators Inflamm.* 2019;2019:9213074. doi: 10.1155/2019/9213074.
21. Çağlıyan Türk A, Özkurt S, Doğan İ, Şahin F. Fibromyalgia syndrome and related factors in hemodialysis, peritoneal dialysis, and renal transplant patients: A cross-sectional study. *Arch Rheumatol.* 2021;37(1):67-76. doi: 10.46497/ArchRheumatol.2022.8227.
22. Öztürk NÜ, Nergis-Ural R. Relationship Between Renal Inflammation and Some Current Dietary Components in Chronic Kidney Disease. *Turkish J Nephrol.* 2018;27(1):14-25. doi: 10.5262/tndt.2018.1001.02.
23. Akchurin OM, Kaskel F. Update on inflammation in chronic kidney disease. *Blood Purif.* 2015;39(1-3):84-92. doi: 10.1159/000368940.
24. Yazici S, Yazici M, Erer B, et al. The platelet indices in patients with rheumatoid arthritis: mean platelet volume reflects disease activity. *Platelets.* 2010;21(2):122-125. doi: 10.3109/09537100903474373.

Ultrasound-guided platelet-rich plasma vs. radiofrequency nerve ablation for refractory plantar fasciitis

Furkan Erdoğan¹, Tolgahan Cengiz², Alparslan Yurtbay³, İsmail Büyükceran⁴

¹Department of Orthopedics and Traumatology, Amasya Sabuncuoğlu Şerefeddin Training and Research Hospital, Amasya, Türkiye;

²Department of Orthopedics and Traumatology, Inebolu State Hospital, Kastamonu, Türkiye; ³Department of Orthopedics and Traumatology, Samsun University Faculty of Medicine, Samsun, Türkiye; ⁴Department of Orthopedics and Traumatology, Ondokuz Mayıs University Faculty of Medicine, Samsun, Türkiye

ABSTRACT

Objectives: Plantar fasciitis (PF), which accounts for approximately 80% of heel pain, is a common condition affecting adults' quality of life. There are many different treatment modalities used in the treatment of PF. In this study, we compared the clinical and functional outcomes of patients diagnosed with chronic PF in our clinic who underwent USG-guided PRP (platelet-rich plasma) injection and patients who underwent RFNA (radiofrequency nerve ablation) treatment.

Methods: Ultrasound-guided PRP injection or RFNA was performed on 95 patients who were diagnosed with chronic PF and met the inclusion criteria. This group of patients was followed for at least one year (October 2021-October 2023), and the clinical and functional results of the patients were compared.

Results: The mean pre-treatment Visual Analog Scale (VAS), Foot Function Index (FFI), and American Orthopaedic Foot and Ankle Society (AOFAS) posterior-ankle scores were similar, and no significant difference was found ($P>0.05$). A significant improvement was observed in the groups' FFI, VAS, and AFOAS scores after treatment ($P<0.05$). However, no significant difference was found in treatment modalities ($P>0.05$).

Conclusions: As a result of the study, it was concluded that PRP injection and RFNA are effective treatment methods in patients diagnosed with chronic plantar fasciitis without response to other conservative treatment methods, but these two methods are not superior to each other.

Keywords: Plantar fasciitis, platelet-rich plasma, radiofrequency nerve ablation

Plantar fasciitis (PF) is the most prevalent cause of heel pain, accounting for about 80% of cases; its occurrence in society is estimated at 7% [1]. This common condition is a health problem that frequently affects the quality of life of adults. Sharp, excruciating pain is the hallmark of plantar

fasciitis, and it typically flares up at the most inconvenient times - first thing in the morning or right before an activity begins. Although this pain tends to improve over time, in some cases, it can become chronic and become a limiting factor in patients' daily lives.

Corresponding author: Tolgahan Cengiz, MD.,
Phone: +90 366 811 31 94, E-mail: tolgahancengiz@hotmail.com

How to cite this article: Erdoğan F, Cengiz T, Yurtbay A, Büyükceran İ. Ultrasound-guided platelet-rich plasma vs. radiofrequency nerve ablation for refractory plantar fasciitis. Eur Res J. 2024;10(3):319-325. doi: 10.18621/eurj.1388703



This is an open access article distributed under the terms of [Creative Commons Attribution-NonCommercial-NoDerivatives 4.0 International License](https://creativecommons.org/licenses/by-nc-nd/4.0/)

Received: November 9, 2023

Accepted: January 6, 2024

Published Online: March 17, 2024

Copyright © 2024 by Prusa Medical Publishing
Available at <https://dergipark.org.tr/en/pub/eurj>



The etiology of plantar fasciitis, one of the insidious causes of heel pain, is still not fully understood. However, it is a disorder that is associated with several risk factors such as age, increased body mass index (BMI), overuse, Achilles strain, calcaneal sprain, pes planus, pes cavus, lack of flexibility of the plantar flexors (reduced ankle dorsiflexion) [2]. Pathophysiologically, in the presence of increased fascial load, it causes changes in the extracellular matrix after being detected by the gap junctions (mechanotransduction) between fibrocytes, causing myxoid degeneration and disintegration of the plantar fascia [3]. Current literature suggests that PF has a degenerative pathology rather than an inflammatory process, and the term plantar fasciitis is recommended instead of PF due to chronic inflammatory changes without histological signs of fibroblastic proliferation [4].

There is a notable range of treatments available for plantar fasciitis. Conservative treatment methods are frequently used and include the use of anti-inflammatory drugs, physical therapy, stretching exercises, foot pads, and orthotic devices. Remarkably, the success rate of these conservative treatments can be as high as 90% [5]. Additionally, surgical treatment can be applied in resistant cases by releasing the fascia, and success rates vary between 70% and 90% [6]. Nonetheless, because the plantar fascia area is subject to pressure, there is a risk of complications, including issues with soft tissue healing, superficial infections, or even arch collapse. To mitigate the potential for these significant complications, minimally invasive treatments have been suggested over the years to manage this condition. These options include injections (e.g., steroids or platelet-rich plasma [PRP]), extracorporeal shock wave therapy (ESWT), and radiofrequency nerve ablation (RFNA) targeting the plantar fascia [7-9].

The purpose of this article is to evaluate and compare the functional and clinical results of patients with persistent plantar fasciitis who were treated at our clinic using RFNA or PRP.

METHODS

Patients with plantar fasciitis in our clinic who received conservative or minimally invasive treatment (ESWLT, steroid injection, etc.) but still had chronic

plantar heel pain for longer than six months were included in this study. Diagnosing plantar fasciitis was established through clinical findings, adhering to the diagnostic criteria outlined in the guidelines presented by McPoil *et al.* [10]. Plantar fasciitis was diagnosed by considering particular clinical observations, such as tenderness when pressing on the inner part of the heel's sole, heightened discomfort during initial steps following extended inactivity, worsened pain after prolonged standing or walking, and frequently experiencing pain due to recent increases in weight-bearing activities. These findings were indicative of the condition. PRP or RFNA was applied to 95 patients who met the inclusion criteria for the study due to persistent heel pain. The patients data who were followed for at least one year (October 2021-October 2023) were analyzed, and their clinical and functional results were compared.

The inclusion and exclusion criteria for patients can be found in Table 1. Our institute's clinical research ethics committee approved the study (approval number 23.10.2023/20230040), and we obtained informed consent from each patient. Patients' age, gender, and BMI were recorded. Information was obtained about the types of treatment previously applied to the patients, previous trauma, or systemic disease status. Three scales assessed the patients' clinical scores before and 12 months after treatment. Initially, pain was evaluated using the Visual Analog Scale (VAS), where a score of 0 represented the absence of pain, and a score of 10 indicated the most severe pain imaginable. The Foot Function Index (FFI) comprises a questionnaire with 23 items categorized into three subgroups: 5 items related to activity limitations, nine items focusing on pain severity, and another nine items addressing disability. Finally, the assessment of foot function involved using the American Orthopedic Foot and Ankle Society (AOFAS) posterior-ankle scale.

Preparation and Application of PRP

It was prepared for our patients according to the method described by Anitua *et al.* [11-12]. Under aseptic precautions, 30 ml of peripheral blood is collected from the antecubital area into tubes containing 3.2% sodium citrate. With the double centrifugation technique, approximately 3 mL of PRP is extracted after centrifugation for 10 minutes at 1300 rpm and 3500 rpm to separate erythrocytes and concentrate

platelets. Under sterile conditions, a 13 MHz linear transducer-enabled ultrasound probe (Clarius L7 HD3, Clarius Health Corp, Canada) is placed on the most sensitive point of the foot by palpation in the medial region of the foot and applied to the area where the plantar fascia is thickest (Figure 1). The procedure was completed by using two PRP injections with a two-week interval in between.

Percutaneous radiofrequency ablation

The region of highest sensitivity on the affected side of the plantar fascia is pinpointed, and specific locations where radio frequency treatment will be applied are marked within the area of pain, ensuring a 5 mm spacing between each marked point. Following standard disinfection using iodine and alcohol and skin preparation with a sterile cover, the calcaneal branch of the posterior tibial nerve is localized and locally anesthetized using 1% lidocaine under the guidance

of ultrasound, approximately 2 centimeters distal to the tip of the medial malleolus. After administering local anesthesia, entry points on the skin for radiofrequency are established using a 1.5 mm Kirschner wire. This is done to facilitate the insertion of the radiofrequency probe beneath the skin. Subsequently, percutaneous radiofrequency ablation is conducted by positioning a radiofrequency probe at the level of the plantar fascia under ultrasound guidance at each of the marked grid's puncture points (CoATherm AK-A304, Gyeonggi-do, South Korea). At the end of the procedure, a sterile dressing is applied locally. Standard Achilles and plantar fascia stretching and strengthening exercises were given during the follow-up of patients in both groups. Patients were advised not to exercise and to rest on the first day after the injection. Non-steroidal anti-inflammatory drugs were not recommended to any patient in the PRP group after the procedure, and paracetamol was given to the patients in the RFNA group; however, no orthosis or splint was recommended.

Statistical Analysis

Data files were processed using IBM SPSS Statistics version 25 (IBM Corp, based in the USA). The Shapiro-Wilk test was employed to assess the distribution of continuous variables. When comparing normally distributed variables among groups, one-way analysis of variance (ANOVA) was the chosen statistical method. In cases where the variables did not exhibit a normal distribution, the Kruskal-Wallis test was utilized for group comparisons. The Friedman Test was selected to compare variables that showed non-normal distribution at various time points. We employed the Pearson Chi-Square and Fisher-Freeman-Halton tests to assess qualitative data. A P-value less than 0.05 indicated a statistically significant difference for all the statistical tests performed.

RESULTS

Demographic data of the patients included in our study are shown in Table 2. Treatment groups were similar in age, gender, and BMI distribution. However, the mean VAS, FFI, and AFOAS scores before the procedure were similar in all treatment groups, and no significant difference was found ($P>0.05$). VAS, FFI, and



Fig. 1. PRP (platelet-rich plasma) application under ultrasound guidance in the treatment of plantar fasciitis.

Table 1. Inclusion and exclusion criteria of the patients

Inclusion Criteria	Exclusion Criteria
Patients with chronic plantar fasciitis after failure of conservative treatment for at least six months	Patients aged < 18 years
Failure of conservative treatment (stretching exercises, nonsteroidal anti-inflammatory drugs, and heel pads) for at least six months	Associated pathology involving the lower limb such as – a history of tarsal tunnel syndrome, ankle fractures, any deformity of foot and ankle, Achilles tendinopathy
Patient should be able to understand the informed consent	Patients with inflammatory diseases (e.g., ankylosing spondylitis, rheumatoid arthritis, Reiter syndrome)
Visual analog scale pain higher than 5 (on a 10-point visual analog scale)	Pregnancy or lactation

AFOAS score changes in PRP and RFNA groups before and after treatment are presented in Table 3. Following the treatment, a notable enhancement was noted in the groups' FFI, VAS, and AFOAS scores ($P < 0.05$). Nevertheless, no significant distinction was found when comparing the various treatment methods ($P > 0.05$). Although the percentage decrease trend in mean VAS and FFI scores after treatment was consistent among the groups, there was a notably more substantial improvement in mean AFOAS (American Foot and Ankle Outcome Score) scores in favor of the PRP group (88.6 ± 12.8 compared to 92.7 ± 11.6). Body mass index, thought to be one of the factors that may

affect the treatment outcome, did not affect the functional outcome of either treatment group ($P > 0.05$). When previously unsuccessful treatment groups were compared with new treatment methods, it was seen that there was no significant effect on the outcome ($P > 0.05$).

DISCUSSION

Most heel pain cases, around 70% to 90%, can be effectively managed through conservative treatment. However, for the remaining 10% to 30% of patients,

Table 2. Distribution of different variables in 2 groups

	PRP	RFNA	P value
Age (years)			
Mean \pm SD	45.3 \pm 10.2	47.4 \pm 8.3	0.647
Range	34-59	37- 62	
Gender, n			
Female	34	21	0.369
Male	23	17	
BMI (kg/m²)			
Mean \pm SD	29.4 \pm 2.2	31.4 \pm 3.6	0.415
Range	25-33	25-34	
Previous treatments, n			
Steroid injection	47		0.745
Steroid injection+ESWL	27		
PRP	21		

BMI= body mass index, SD=standard deviation, ESWL=extracorporeal shock wave lithotripsy, PRP=platelet-rich plasma, RFNA=radiofrequency nerve ablation

Table 3. Distribution of functional outcome variables in 2 groups

	Preinjection	6 Month (First Follow-up)	12 Month (Second Follow-up)	P value
VAS				
PRP	8.1±2.2	4.8±1.7	3.2±0.9	0.016
RFNA	7.8±1.5	5.6±1.3	3.4±1	0.022
P value	0.785	0.689	0.572	
AFOAS				
PRP	68.2±14.4	89.1±16.2	92.7±11.6	0.031
RFNA	70.2±11.3	86.7±11.8	88.6±12.8	0.036
P value	0.943	0.879	0.347	
FFI				
PRP	71.1±13.5	38.7±16.4	34.1±19.0	0.031
RFNA	68.3±14.7	51.2±21.7	32.3±17.2	0.029
P value	0.658	0.753	0.699	

Data are shown as mean±standard deviation. PRP=platelet-rich plasma, RFNA=radiofrequency nerve ablation, VAS=Visual Analog Scale, FFI=Foot Function Index, AOFAS=American Orthopaedic Foot and Ankle Society score

more invasive or surgical interventions may be necessary [6]. The histopathological characteristics of this condition involve elevated vascularity, an abundance of ground substance proteins, localized regions with fibroblast overgrowth, and damaged collagen fibers. Additionally, some studies have shown nonspecific signs of inflammation in plantar fasciitis. Etiologically, chronic plantar heel pain can develop due to many factors, including nerve lesions. However, regarding the calcaneal spur formations that may first come to mind in the etiology of patients with plantar fasciitis, the results are contradictory regarding the relationship between the size of the spurs and pain and symptoms [13, 14]. For this reason, different treatments for many other mechanisms, including spur excision, can be used to treat the disease [15, 16]. In this study, the mean age of the patients was 41, which is consistent with the age range often observed in similar studies. Furthermore, some research has indicated that plantar fasciitis affects individuals within their fourth decade. Additionally, evidence suggests that plantar fasciitis is more prevalent in the obese population. In our study, the average BMI of the patients was found to be 31.4 kg/m², which was similar to the literature. Although there was a slight female predominance in

terms of gender in our study, it could not be shown to be associated with plantar fasciitis.

Substantial enhancements were noted in all assessment scores for both treatment groups. The RFNA group displayed superior outcomes in terms of VAS and AOFAS scores when compared to the PRP group at 6 and 12 months. Nevertheless, by the 12th month, a slight increase in the decrease of all scores was observed in the PRP group compared to the other group (Table 3). While there was no statistically significant distinction in functional scores, it is noteworthy that the clinical outcomes exhibited more significant improvement in the RFNA group compared to the PRP group (Table 3).

A meta-analysis conducted by Ling *et al.* [17] reported that PRP effectively reduces pain and improves physical function in patients with plantar fasciitis. However, they also found that long-term PRP applications can improve pain and physical function over 12 months, whereas short-term PRP treatments, lasting from 1 to 6 months, did not yield the same effect [17]. In the study conducted by Say *et al.* [18], they determined VAS and AFOAS scores at baseline and after a 6-month follow-up as 8.8±1 and 62.9±8.5 at the 0th month, and 1±0.8 and 90.6±2.6 at 6th month, respec-

tively. They thus concluded that PRP injections showed an excellent clinical response in patients with chronic plantar fasciitis [18]. Jain *et al.* [19] found that the mean VAS and AOFAS scores in patients who underwent PRP were 8.3 and 58.6 before the procedure and 3.3 and 88.5 at 12 months, respectively. Our study is similar to the literature (Table 3). However, although there are many application guidelines in clinical practice regarding the procedure of the PRP method, platelet density, and number of sessions, there is no consensus. Generally, PRP injections can be administered in several sessions once a week or more per week.

The superiority of ultrasound-guided injections over palpation-guided injections is still controversial. To treat plantar fasciitis, some prior research has recommended using ultrasound guidance for injection, as this may enable more accurate injection administration [20]. However, the results of trials by Kane [21] suggest that ultrasound-guided injection is less effective than palpation-guided injection in treating idiopathic plantar fasciitis. Specific authors propose that employing ultrasound guidance can help prevent complications, such as the development of flexor hallucis longus tendinosis resulting from excessively deep punctures [22]. The patients in the study were treated with ultrasound guidance, so subgroup analysis could not be performed to investigate whether it was more effective than palpation-guided injection.

Erken *et al.* [7] reported that this method dramatically improved the results in patients in whom they applied RFNA and followed up long-term, with the VAS score before the procedure being 9.2 ± 1.9 , the score after one year being 1.3 ± 1.8 and the AOFAS scores being 66.9 ± 8.1 and 93 ± 7.5 , respectively [7]. In a retrospective study by Liden *et al.* [23], they reported that the VAS was 8.12 ± 1.61 before the procedure and 2.07 ± 2.06 in the 6th month after the injection and that the treatment was successful at a rate of 92%. Yuan *et al.* [24] reported that VAS and AFOAS scores improved significantly in 12 months in patients who underwent RFNA and were followed up for an average of 58.7 months. In the 12th month, it was determined that VAS scores changed from 7.87 ± 1.73 to 0.73 ± 1.28 , and AFOAS scores changed from 42.73 ± 10.75 to 98.40 ± 4.24 . Our clinical results in the study are consistent with the literature; however, in the literature,

we did not come across an isolated survey comparing both treatment methods. Nevertheless, reports compare different methods for treating plantar fasciitis [9, 25].

This study demonstrates that the two methods used for treating plantar fasciitis have similar effectiveness, and no complications were detected in the following patients. Both treatment methods have different technical requirements. PRP injection includes disadvantages such as equipment setup, blood collection, and PRP preparation, but it may be a relatively more cost-effective option. On the other hand, the RFNA procedure can lead to peripheral nerve damage, muscle-tendon injury, and the use of expensive equipment, and it should be applied with caution.

Limitations

The study's shortcomings were a small sample size, a brief follow-up period, and the need for a control group. More studies with a bigger patient population, extended follow-up periods, and a control group might offer a more thorough knowledge of how well both treatment approaches work.

CONCLUSION

These findings suggest that these standard treatment methods can potentially improve chronic plantar fasciitis symptoms that do not respond to other conservative treatment methods, but they do not appear to have a superiority over each other.

Authors' Contribution

Study Conception: FE; Study Design: TC; Supervision: İB; Funding: FE; Materials: FE; Data Collection and/or Processing: FE; Statistical Analysis and/or Data Interpretation: AY; Literature Review: TC; Manuscript Preparation: FE and Critical Review: AY, İB.

Conflict of interest

The authors disclosed no conflict of interest during the preparation or publication of this manuscript.

Financing

The authors disclosed that they did not receive any grant during conduction or writing of this study.

REFERENCES

1. Gollwitzer H, Saxena A, DiDomenico LA, et al. Clinically relevant effectiveness of focused extracorporeal shock wave therapy in the treatment of chronic plantar fasciitis: a randomized, controlled multicenter study. *J Bone Joint Surg Am.* 2015;97(9):701-708. doi: 10.2106/JBJS.M.01331.
2. Hill CL, Gill TK, Menz HB, Taylor AW. Prevalence and correlates of foot pain in a population-based study: the North West Adelaide health study. *J Foot Ankle Res.* 2008;1(1):2. doi: 10.1186/1757-1146-1-2.
3. McMillan AM, Landorf KB, Barrett JT, Menz HB, Bird AR. Diagnostic imaging for chronic plantar heel pain: a systematic review and meta-analysis. *J Foot Ankle Res.* 2009;2:32. doi: 10.1186/1757-1146-2-32.
4. Rhim HC, Kwon J, Park J, Borg-Stein J, Tenforde AS. A Systematic Review of Systematic Reviews on the Epidemiology, Evaluation, and Treatment of Plantar Fasciitis. *Life (Basel).* 2021;11(12):1287. doi: 10.3390/life11121287.
5. Alshami AM, Souvlis T, Coppieters MW. A review of plantar heel pain of neural origin: differential diagnosis and management. *Man Ther.* 2008;13(2):103-111. doi: 10.1016/j.math.2007.01.014.
6. LeMelle DP, Kisilewicz P, Janis LR. Chronic plantar fascial inflammation and fibrosis. *Clin Podiatr Med Surg.* 1990 Apr;7(2):385-9.
7. Erken HY, Ayanoglu S, Akmaz I, Erler K, Kiral A. Prospective study of percutaneous radiofrequency nerve ablation for chronic plantar fasciitis. *Foot Ankle Int.* 2014;35(2):95-103. doi: 10.1177/1071100713509803.
8. Franceschi F, Papalia R, Franceschetti E, Paciotti M, Maffulli N, Denaro V. Platelet-rich plasma injections for chronic plantar fasciopathy: a systematic review. *Br Med Bull.* 2014;112(1):83-95. doi: 10.1093/bmb/ldu025.
9. Uğurlar M, Sönmez MM, Uğurlar ÖY, Adıyeke L, Yıldırım H, Eren OT. Effectiveness of Four Different Treatment Modalities in the Treatment of Chronic Plantar Fasciitis During a 36-Month Follow-Up Period: A Randomized Controlled Trial. *J Foot Ankle Surg.* 2018;57(5):913-918. doi: 10.1053/j.jfas.2018.03.017.
10. McPoil TG, Martin RL, Cornwall MW, Wukich DK, Irrgang JJ, Godges JJ. Heel pain--plantar fasciitis: clinical practice guidelines linked to the international classification of function, disability, and health from the orthopaedic section of the American Physical Therapy Association. *J Orthop Sports Phys Ther.* 2008;38(4):A1-A18. doi: 10.2519/jospt.2008.0302.
11. Anitua E. Plasma rich in growth factors: preliminary results of use in the preparation of future sites for implants. *Int J Oral Maxillofac Implants.* 1999;14(4):529-535.
12. Anitua E, Andia I, Ardanza B, Nurden P, Nurden AT. Autologous platelets as a source of proteins for healing and tissue regeneration. *Thromb Haemost.* 2004;91(1):4-15. doi: 10.1160/TH03-07-0440.
13. Kirkpatrick J, Yassaie O, Mirjalili SA. The plantar calcaneal spur: a review of anatomy, histology, etiology and key associations. *J Anat.* 2017;230(6):743-751. doi: 10.1111/joa.12607.
14. Kuyucu E, Koçyiğit F, Erdil M. The association of calcaneal spur length and clinical and functional parameters in plantar fasciitis. *Int J Surg.* 2015;21:28-31. doi: 10.1016/j.ijso.2015.06.078.
15. Saylik M, Fidan F, Lapçin O. Comparison of Isolated Calcaneal Spur Excision and Plantar Fasciotomy in Addition to Spur Excision in Patients With Plantar Heel Pain Accompanied by Calcaneal Spur. *Cureus.* 2022;14(11):e31768. doi: 10.7759/cureus.31768.
16. Johannsen F, Konradsen L, Herzog R, Krogsgaard MR. Endoscopic fasciotomy for plantar fasciitis provides superior results when compared to a controlled non-operative treatment protocol: a randomized controlled trial. *Knee Surg Sports Traumatol Arthrosc.* 2020;28(10):3301-3308. doi: 10.1007/s00167-020-05855-3.
17. Ling Y, Wang S. Effects of platelet-rich plasma in the treatment of plantar fasciitis: A meta-analysis of randomized controlled trials. *Medicine (Baltimore).* 2018;97(37):e12110. doi: 10.1097/MD.00000000000012110.
18. Say F, Gürler D, İnkaya E, Bülbül M. Comparison of platelet-rich plasma and steroid injection in the treatment of plantar fasciitis. *Acta Orthop Traumatol Turc.* 2014;48(6):667-72. doi: 10.3944/AOTT.2014.13.0142.
19. Jain K, Murphy PN, Clough TM. Platelet rich plasma versus corticosteroid injection for plantar fasciitis: A comparative study. *Foot (Edinb).* 2015;25(4):235-7. doi: 10.1016/j.foot.2015.08.006.
20. Tsai WC, Wang CL, Tang FT, Hsu TC, Hsu KH, Wong MK. Treatment of proximal plantar fasciitis with ultrasound-guided steroid injection. *Arch Phys Med Rehabil.* 2000;81(10):1416-21. doi: 10.1053/apmr.2000.9175.
21. Kane D, Greaney T, Shanahan M, et al. The role of ultrasonography in the diagnosis and management of idiopathic plantar fasciitis. *Rheumatology (Oxford).* 2001;40(9):1002-1008. doi: 10.1093/rheumatology/40.9.1002.
22. Campillo-Recio D, Ibañez M, Martín-Dominguez LA, Comas-Aguilar M, Fernández-Morales M, Alberti-Fito G. Local Percutaneous Radiofrequency for Chronic Plantar Fasciitis. *Arthrosc Tech.* 2021;10(5):e1315-e1320. doi: 10.1016/j.eats.2021.01.031.
23. Liden B, Simmons M, Landsman AS. A retrospective analysis of 22 patients treated with percutaneous radiofrequency nerve ablation for prolonged moderate to severe heel pain associated with plantar fasciitis. *J Foot Ankle Surg.* 2009;48(6):642-647. doi: 10.1053/j.jfas.2009.05.013.
24. Yuan Y, Qian Y, Lu H, Kou Y, Xu Y, Xu H. Comparison of the therapeutic outcomes between open plantar fascia release and percutaneous radiofrequency ablation in the treatment of intractable plantar fasciitis. *J Orthop Surg Res.* 2020;15(1):55. doi: 10.1186/s13018-020-1582-2.
25. Yucel I, Ozturan KE, Demiraran Y, Degirmenci E, Kaynak G. Comparison of high-dose extracorporeal shockwave therapy and intralesional corticosteroid injection in the treatment of plantar fasciitis. *J Am Podiatr Med Assoc.* 2010;100(2):105-110. doi: 10.7547/1000105.

Assessment of hiatus defect size in hiatal hernia patients using computed tomography

Seray Gizem Gür Özcan¹, Nezh Zengin², Burak Bilir², Nurcan Kaçmaz Kat¹, Dođukan Durak²

¹Department of Radiology, University of Health Sciences, Bursa Yüksek İhtisas Training and Research Hospital, Bursa, Türkiye; ²Department of General Surgery, University of Health Sciences, Bursa Yüksek İhtisas Training and Research Hospital, Bursa, Türkiye

ABSTRACT

Objectives: The aim of this study is to investigate the hiatus defect diameter by measuring on multi-detector computed tomography images in hiatal hernia patients.

Methods: The multi-detector computed tomography images of 50 patients and 50 individuals in control group included in this study were investigated. The hiatus surface area (cm²), hiatus antero-posterior and transverse diameters (cm), and the thickness of both diaphragmatic crura (mm) were measured by reformatting contrast-enhanced thoraco-abdomino-pelvic computed tomography images using the region of interest method.

Results: In this study, a significant difference was obtained among groups according to hiatus surface area, hiatus antero-posterior, and transverse diameter measurements, and both left and right diaphragmatic crural thickness measurements (P<0.001). In the patient group, the cut-off values were determined by using ROC analysis, and the values above these cut-off values enabled a hernia diagnosis with high sensitivity and specificity.

Conclusion: Measuring the hiatus surface area on multi-detector computed tomography images could serve as a supplementary criterion for diagnosing of hiatal hernia.

Keywords: Computed tomography, gastroesophageal reflux, hiatal hernia, hiatal surface area

Hiatal hernia (HH) occurs through the herniation of abdominal contents into the mediastinum via an enlarged esophageal hiatus [1]. In the Western hemisphere, it is most associated with Gastroesophageal reflux disease (GERD) [2]. In the study conducted by Shamiyeh *et al.* on cadavers, the mean hiatal surface area (HSA) was measured as 5.84 cm² [3]. In the study by Moten *et al.* [4], patients with HH had a mean HSA of 6.9 cm², while ones without HH had a mean HSA of 2.5 cm². It was observed that the frequency of GERD was higher in patients with HH [4].

HH is classified as 3 subtypes. Type 1 is a sliding type HH, where the gastroesophageal junction (GEJ) moves over the hiatus due to the laxity of the phrenoesophageal ligament [1, 2]. Type 1 is the most associated with GERD. It is also the most frequently observed HH type, with reported rates ranging 10%-80% [2]. Type 2 is characterized by the normal position of the GEJ, but the fundus of the stomach moves upwards through the hiatus. This type is rare and constitutes less than 5% of cases. Type 3 involves both the GEJ and the stomach fundus shifting into the mediastinum. This type is generally observed in elderly

Corresponding author: Seray Gizem Gür Özcan, MD.,
Phone: +90 224 295 50 00, E-mail: seraygizemgur@yahoo.com.tr

How to cite this article: Gür Özcan SG, Zengin N, Bilir B, Kaçmaz Kat N, Durak D. Assessment of hiatus defect size in hiatal hernia patients using computed tomography. Eur Res J. 2024;10(3):326-332. doi: 10.18621/eurj.1392696



This is an open access article distributed under the terms of [Creative Commons Attribution-NonCommercial-NoDerivatives 4.0 International License](https://creativecommons.org/licenses/by-nc-nd/4.0/)

Received: November 18, 2023

Accepted: February 7, 2024

Published Online: March 18, 2024

Copyright © 2024 by Prusa Medical Publishing
Available at <https://dergipark.org.tr/en/pub/eurj>



adults and more commonly in women [1, 2].

HH and GERD are diagnosed through symptom scoring, upper gastrointestinal system endoscopy (GISE), and barium radiographs [5]. However, there is a limited correlation between barium radiographs with intraoperative findings, and the herniated volume of the stomach, and there is no consensus on the use of barium radiographs in the diagnosis [5]. Additionally, possessing the defect diameter is significant in terms of antireflux treatment [6]. The presence of a wide hiatus preoperatively can result in surgical failure and possessing the hiatus diameter can lead to the use of primary surgical repair methods in such cases with large defects [6].

Recently, the widespread use of multi-detector computed tomography (MDCT) and multiplanar reconstruction images for investigation and measuring HSA enable a more precise determination of associated conditions and the normal range of HSA. Furthermore, MDCT permits visualization of the structure, thickness, and variations of the right and left diaphragmatic crura thickness (DCT) [7].

In patients with HH, the main symptom occurs due to GERD, and the initial approach in treatment is commonly antireflux therapy, which aims to manage symptoms [8]. However, definitive treatment is achieved via surgery [8]. Surgical options include Nissen fundoplication (NF), Toupet fundoplication (TF) (in the presence of esophageal dysmotility), Door fundoplication (DF), or NF with primary surgical mesh repair [8].

In this study we aimed to investigate the accuracy of preoperative MDCT images in diagnosing HH by measuring the HSA, hiatus AP and transverse diameters (TD), and both DCT. Furthermore, we aimed to observe the association between these measurements and the accuracy of HH diagnosis, the type of surgery performed, and the relationship between GERD and defect size.

METHODS

This retrospective study was conducted in accordance with the Declaration of Helsinki as well as reviewed and approved by the ethics committee of our hospital (Approval date: 05.07.2023 and no: 2011-KAEK-25 2023/07-26).

Patient Population

A total of 50 patients who presented to the General Surgery department between September 2019 and December 2022 and, were diagnosed with HH based on their symptoms, preoperative gastroscopy results, and MDCT findings, all of which were subsequently confirmed by the surgery outcomes, were randomly included in the patient group. The control group consisted of 50 individuals who presented to the general surgery clinic with complaints of abdominal pain and based on the results of computed tomography, did not show evidence of hiatal hernia. Participants in the control group were randomly selected to match the age and gender distribution of the patient group.

The demographic data (gender, age), blood parameters (hemoglobin, albumin, MCV, chloride), preoperative gastroscopy data (gastroscopic Z-line, gastroscopic hiatus level, gastroscopic hill grade), MDCT images, and esophageal manometry results for reflux were investigated. Measurement results of hiatus AP and TD (cm), HSA (cm²), the right and left DCT (mm), and the type of hernia (type 1, 2, or 3) were surveyed. The presence of GERD was investigated clinically, manometrically, and radiologically respectively.

As inclusion criteria for the study.

1. Age 18 years or older.
2. Confirmed diagnosis of HH via GISE and MDCT.
3. Availability of preoperative CT images, GISE results, and manometry results in the hospital system.

As exclusion criteria.

1. Younger than 18 years old or older than 80 years old.
2. Absence of preoperative CT images and GISE results in the hospital system.
3. Absence of confirmed diagnosis of reflux through manometry

Analysis of CT Images

All abdomen CT scans were performed using a 128-slice multi-detector-row CT scanner (Toshiba Aquillion, Japan). For measurements, preoperative thin-slice MDCT images available in the hospital system were investigated. The images were acquired at deep inspiration with a slice thickness of 1.25 mm in

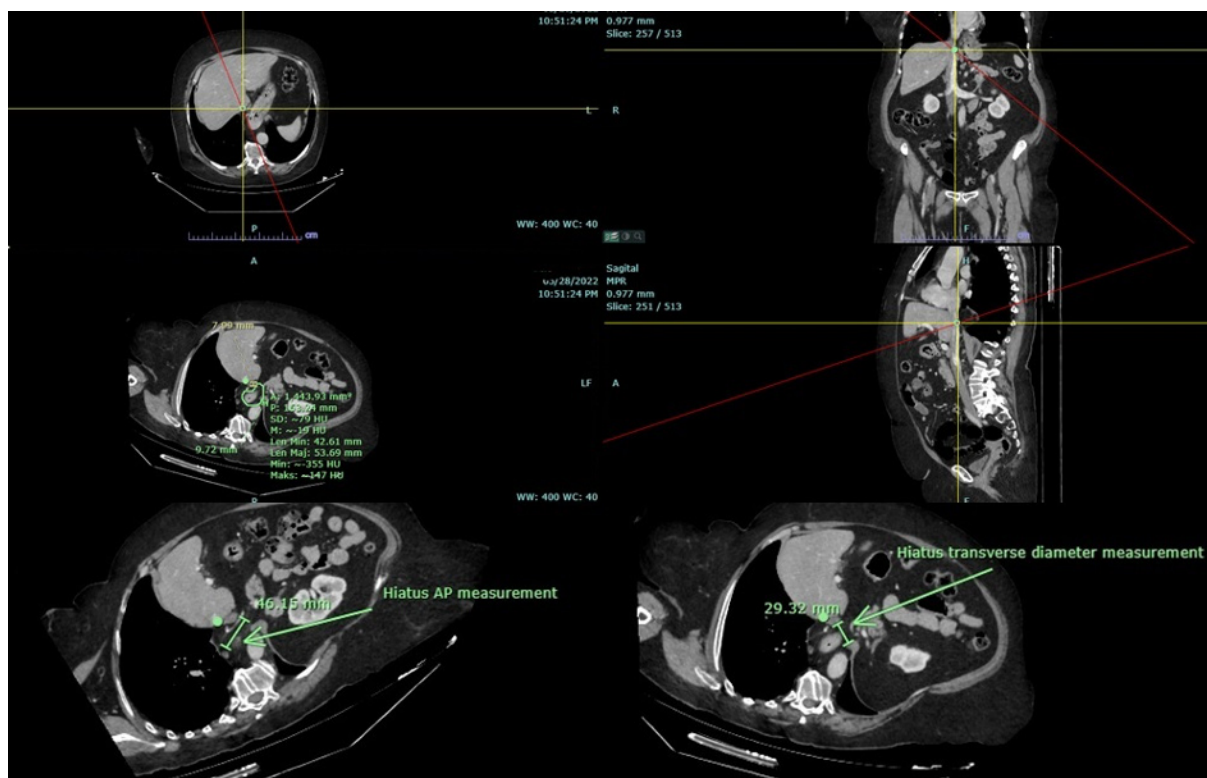


Fig. 1. Measurement of the hiatal surface area on axial, coronal, oblique axial, and sagittal computed tomography images with the corrected angle (Measurements of hiatus antero-posterior and transverse diameter using reformatted oblique axial images are shown).

the form of Intravenous contrast-enhanced thoraco-abdomino-pelvic CT. Multiplanar reformat (MPR) images of each MDCT scan were obtained, and the measurements were performed based on the reconstructed images adjusted to the appropriate angle of the hiatus (Fig. 1). This method is similar to the measurement technique used in a previous study by Moten *et al.* [4]. On a suitable image of the esophageal hiatus obtained, the AP and TD of the hiatus were initially measured, followed by the measurement of HSA in an elliptical shape that fits the esophageal hiatus, using the Region of Interest (ROI) measurement tool in an elliptical manner (Fig. 1). Additionally, the right and left DCT were measured. Radiological evidence of reflux was assessed by examining content retention.

Statistical Analysis

IBM Statistical Package for the Social Sciences (SPSS) version 22 for Windows, Chicago, IL, USA, was used for all statistical analyses. The Kolmogorov-Smirnov test was conducted to test the homogeneity

of distributions among groups. Mean values, standard deviations, and median values of normally distributed and non-normally distributed groups were calculated. T-test was performed to compare age averages and gender distributions between the patient and control groups. The cut-off values for right and left DCT, HSA, hiatus AP, and TD were determined using ROC analysis. Sensitivity, specificity, and the area under the curve (AUC) with a 95% confidence interval (CI) were also calculated. All variables were included in the univariate analysis. Explanatory factors with a $P \leq 0.2$ in this step were entered into the multivariate analysis. Results were given as odds ratio (OR) and 95% CI. The association between the presence of hernia with HSA, Hiatus AP, and TD as well as right and left DCT was assessed using Spearman's correlation test. The association between hernia types and GERD was analyzed using the Pearson-Chi Square test. Differences were considered statistically significant at $P < 0.05$.

RESULTS

Fifty patients (24 females and 26 males) with mean age of 55.27±11.93 in patient group and 50 individuals (35 females and 15 males) with mean age of 50.74±13.71 in the control group were included in the study (Table 1).

ROC analysis was conducted to determine the cut-off values for HSA, hiatus AP diameter, and TD, as well as the right and left DCT. The cut-off for HSA was acquired as 2.8 cm² in ROC analysis and the hernia can be diagnosed with 87.7% sensitivity and 100% specificity for ones with HAS >2.8 cm² (AUC: 0.961, P<0.001) (Fig. 2). The cut-off of hiatus AP diameter was found to be 1.4 cm and hernia diagnosis can be carried out with 91.8% sensitivity and 92% specificity for ones with AP diameter >1.4 cm (AUC: 0.964, P<0.001) (Fig. 2). The cut-off for Hiatus TD was obtained as 1.7cm and individuals with hiatus TD >1.4 cm can be diagnosed with hernia with 83.6% sensitivity and 98% specificity (AUC: 0.960, P<0.001) (Fig. 2). The cut-off for right DCT was acquired as 4.4mm and HH can be diagnosed with 75.5% sensitivity and 66% specificity for individuals with right DCT >4.4 mm (AUC: 0.756, P<0.001) (Fig. 2). Finally, the cut-off of left DCT was determined as 4.5 mm and HH can be diagnosed with 63.3% sensitivity and 86% specificity in individuals with left DCT >4.5 mm (AUC: 0.786, P<0.001) (Fig. 2).

As per consideration of all variables together in multivariate analysis, the most significant association was between the hiatus AP diameter, and TD with the diagnosis of hernia (Fig. 2).

Subsequently, univariate and multivariate analyses were conducted for HAS, hiatus AP and TD as well as right and left DCT. In both analyses, significant differences were observed in both individual and the de-

pendent variables (Table 2).

A significant correlation between reflux with HSA, hiatus AP, right and left DCT, TD, and esophagoscopic hill grade was determined. It was observed that as HSA, hiatus AP, TD, and esophagoscopic hill grade increased, the risk of reflux formation also increased (P<0.001).

In consideration of the distribution of hernia among patients, type 1 HH was observed in 27 individuals, type 2 HH in 6 individuals, and type 3 HH in 17 individuals respectively. As per the association between HH types and GERD, GERD was noticed in 24 individuals with type 1. There was a statistically significant increase in the frequency of GERD compared to the other group (P<0.001).

In terms of the surgical procedures, NF was performed in 44 individuals, TF in 2 individuals, NF with mesh repair in 3 individuals, and DF in 1 individual. Among the patients who underwent NF, the mean defect diameter of HSA was 10.93±11.49 mm, while the mean value for 3 patients who underwent NF with mesh repair was 46.33±13.6 5mm, indicating a larger defect size in individuals who underwent mesh repair. However, statistical analysis for surgeries apart from NF was not significant due to the restricted quantity of patients.

DISCUSSION

HH occurs as a result of the widening of the esophageal hiatus, leading to the herniation of the GEJ and various layers of the stomach into the mediastinum [6]. HH, which is quite common in the population, can be easily detected with increased screening frequency and more frequently used MDCT. This study proposes that the diagnosis of HH can be carried

Table 1. Demographic characteristics of patients and control groups

Characteristics	Total	Patients Group	Control Group
Gender			
Male	41	26	15
Female	59	24	35
Age (years)			
Mean ± standard deviation	53.47±13.10	55.27±11.93	50.74±13.71

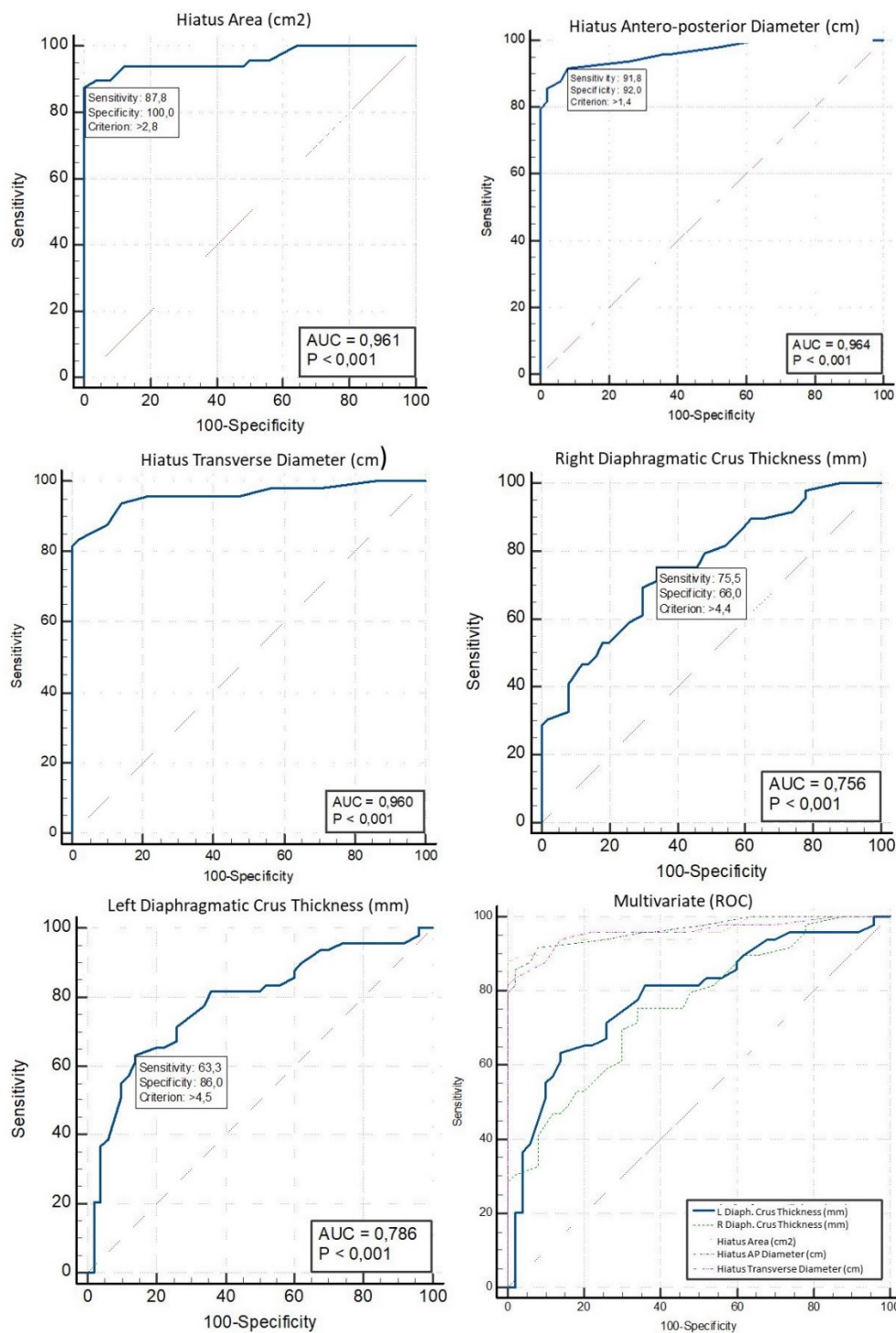


Fig. 2. ROC analyses.

out precisely by measuring HSA, Hiatus AP diameter, and TD using the MDCT in individuals underwent HH surgery.

In this study, the median value of HSA measurement in 50 individuals of patient group was 12.83 ± 3.26 cm², and a cut-off value of 2.8 cm² was

acquired. HH could be diagnosed with high sensitivity and specificity in ones with HSA >2.8 cm². In the control group, the median value of HSA was measured as 1.65 ± 0.26 cm². There was a statistically significant difference between the two groups (P<0.01). In a study conducted by Quayang *et al.* [6], the mean value of

Tablo 2. Measurement results on MDCT in patients with hiatal hernia

	Univariate analysis		Multivariate analysis	
	OR (95% CI)	P Value	OR (95% CI)	P Value
Hiatus area (cm ²)	6.41 (2.39-17.15)	<0.001	25.04 (0.87-715.62)	0.06
Hiatus AP diameter (cm)	371.20 (13.36-103.11)	<0.001	3.47 (0.00-1.63)	0.22
Hiatus transverse diameter (cm)	427.55 (23.71-770.83)	<0.001	10.48(1.22-89.57)	0.03
Right diaphragmatic thickness (mm)	2.42 (1.59-3.69)	<0.001	10.01 (0.80-124.64))	0.07
Left diaphragmatic thickness (mm)	2.68 (1.69-4.23)	<0.001	6.34(0.46-87.39)	0.06
OR=odds ratio, CI=confidence interval, AP=Antero-posterior				

HSA in patients with HH was 6.9cm², whereas in patients without HH, it was 2.5cm². Similar to our study, it was anticipated that HSA could be significantly used for diagnosing HH.

In a study by Moten *et al.* [4], the diagnosis of HH could be carried out with 81% sensitivity and 88% specificity in individuals with HSA >3.5 cm². The results acquired in our study are similar to the previous studies. However, the determination of cut-off values additionally for Hiatus AP and TD sets our study apart and makes it stand out. This aspect becomes significant as it provides a more easily measurable parameter in cases where HSA measurement may not be feasible due to time constraints. In the patient group, the mean Hiatus AP diameter was 3.59 cm with a cut-off value of 1.4 cm, and the mean Hiatus TD was 3.55 cm with a cut-off value of 1.7 cm. In the control group, the mean Hiatus AP diameter was 1.12 cm, while the mean TD was 1.22 cm. There was a significant difference observed among groups (P<0.01).

Since the esophageal hiatus is not parallel to the body axis, measurements from axial or coronal images may not yield accurate results. Therefore, measurements were performed using corrected oblique axial images from MDCT. This method is similar to the oblique axial measurement method used by Moten *et al.* [4] and Quyang *et al.* [6].

As the HSA increases in patients with HH of this study, the frequency of reflux also increases. This finding is consistent with the study conducted by Batirel *et al.*, where they emphasized that an increase in HSA size leads to a decrease in the tone of the lower esophageal sphincter, resulting in an increase in acid reflux [9]. Similarly, in our study, as HSA increased, a more frequent occurrence of reflux was observed in

both the MDCT images and manometry. Franzen *et al.* also stated a similar result in their study, associating an increase in HSA value with an increase in reflux frequency based on manometry and pH results [10]. The lower esophageal sphincter (LES) is a structure located in the GEJ, consisting of a 3-4 cm long segment of smooth muscle with tonic contraction function [11]. Composed mainly of the crural part of the diaphragm, it plays a protective role against GERD [11]. The LES pressure ranges from 10-40 mmHg and is considered one of the classical defense mechanisms against GERD [12]. NF, in addition to hernia repair, includes antireflux effects, and the underlying mechanism involves alterations in LES motor functions [12].

HH can be categorized into 3 types. Type 1, representing the sliding type of HH, occurs due to the looseness of the phrenoesophageal ligament, which leads to the displacement of the gastroesophageal junction (GEJ) above the hiatus. Type 2 involves the normal position of the GEJ, but the stomach fundus displaces upward through the hiatus. Type 3 involves the displacement of both the GEJ and the stomach fundus into the mediastinum [1, 2]. There is an association between hernia type and GERD, with the highest reflux frequency appeared in type 1 HH, which is attributed to the looseness of the phrenoesophageal ligament. In this study, 27 individuals were observed with type 1, 6 individuals with type 2, and 17 individuals with type 3 HH. When considering the association between HH types and GERD, 24 out of 27 patients with type 1 were diagnosed with GERD. This group exhibited a statistically significant increase in the frequency of GERD compared to the other groups (P<0.001). However, there was no statistically significant increase in the frequency of GERD in patients

with type 2 HH and type 3 HH.

The presence of information on the opening and anatomy of the esophageal hiatus is essential for making informed decisions regarding the surgical approach and minimizing the risk of recurrence. In this study, NF was performed in 44 patients, TF in 2 patients, NF with mesh repair in 3 patients, and DF in 1 patient. Among the 3 patients who underwent NF with mesh repair, the mean HSA was acquired as $46.33 \pm 13.65 \text{ cm}^2$, indicating a larger defect size compared to other surgical groups.

Limitations

There are some limitations in this study. Apart from inadequate quantity of patients, there is an unequal distribution of surgical procedures. A cut-off of HSA can be determined with a patient group comprising similar and enough patients for each surgical procedure. Additionally, due to the small number of patients in this study, diaphragmatic crura variations were not investigated, and an adequate sample size could not be obtained for classification in this regard. Prospective studies including diaphragmatic crura variations can provide significant preoperative data to surgeons.

CONCLUSION

The measurement of HAS, hiatus AP and TD using the MDCT can serve as a supplementary criterion in diagnosing of HH. Furthermore, it can offer insight into the association between the defect size and reflux, the correlation between defect size and the chosen surgical approach, as well as the associated variations. This information proves highly advantageous for preoperative planning, optimizing the surgical strategy, and achieving better outcomes for the surgery.

Authors' Contribution

Study Conception: SGGÖ, DD; Study Design: SGGÖ, NKK, DD; Supervision: SGGÖ, DD; Funding: N/A; Materials: N/A; Data Collection and/or Processing: NZ, BB; Statistical Analysis and/or Data Interpretation: SGGÖ, NKK; Literature Review: NZ, BB; Manuscript Preparation: SGGÖ, DD and Critical Review: SGGÖ, DD.

Conflict of interest

The authors disclosed no conflict of interest during the preparation or publication of this manuscript.

Financing

The authors disclosed that they did not receive any grant during conduction or writing of this study.

REFERENCES

- Zheng Z, Liu X, Xin C, et al. A new technique for treating hiatal hernia with gastroesophageal reflux disease: the laparoscopic total left-side surgical approach. *BMC Surg.* 2021;21(1):361. doi: 10.1186/s12893-021-01356-3.
- Watson TJ, Ziegler KM. The Pathogenesis of Hiatal Hernia. *Foregut.* 2022;2(1):36-43. doi: 10.1177/26345161221083020.
- Shamiyeh A, Szabo K, Grandrath FA, Syré G, Wayand W, Zehetner J. The esophageal hiatus: what is the normal size? *Surg Endosc.* 2010;24(5):988-991. doi: 10.1007/s00464-009-0711-0.
- Moten AS, Ouyang W, Hava S, et al. In vivo measurement of esophageal hiatus surface area using MDCT: description of the methodology and clinical validation. *Abdom Radiol (NY).* 2020;45(9):2656-2662. doi: 10.1007/s00261-019-02279-7.
- Boru CE, Rengo M, Iossa A, et al. Hiatal Surface Area's CT scan measurement is useful in hiatal hernia's treatment of bariatric patients. *Minim Invasive Ther Allied Technol.* 2021;30(2):86-93. doi: 10.1080/13645706.2019.1683033.
- Ouyang W, Dass C, Zhao H, Kim C, Criner G; COPDGene Investigators. Multiplanar MDCT measurement of esophageal hiatus surface area: association with hiatal hernia and GERD. *Surg Endosc.* 2016;30(6):2465-2472. doi: 10.1007/s00464-015-4499-9.
- Kumar D, Zifan A, Ghahremani G, Kunkel DC, Horgan S, Mittal RK. Morphology of the Esophageal Hiatus: Is It Different in 3 Types of Hiatus Hernias? *J Neurogastroenterol Motil.* 2020;26(1):51-60. doi: 10.5056/jnm18208.
- Sfara A, Dumitrascu DL. The management of hiatal hernia: an update on diagnosis and treatment. *Med Pharm Rep.* 2019;92(4):321-325. doi: 10.15386/mpr-1323.
- Batirel HF, Uygur-Bayramicli O, Giral A, et al. The size of the esophageal hiatus in gastroesophageal reflux pathophysiology: outcome of intraoperative measurements. *J Gastrointest Surg.* 2010;14(1):38-44. doi: 10.1007/s11605-009-1047-8.
- Franzén T, Tibbling L. Is the severity of gastroesophageal reflux dependent on hiatus hernia size? *World J Gastroenterol.* 2014;20(6):1582-1584. doi: 10.3748/wjg.v20.i6.1582.
- Kahrilas PJ. GERD pathogenesis, pathophysiology, and clinical manifestations. *Cleve Clin J Med.* 2003;70 Suppl 5:S4-19. doi: 10.3949/ccjm.70.suppl_5.s4.
- Vandenplas Y, Hassall E. Mechanisms of gastroesophageal reflux and gastroesophageal reflux disease. *J Pediatr Gastroenterol Nutr.* 2002;35(2):119-136. doi: 10.1097/00005176-200208000-00005.

Solitary myofibroma in children: a report of two cases

Çağrı Coşkun¹, Kemal Kösemehmetoğlu², Mehmet Ayvaz³, İbrahim Vargel⁴, Üstün Aydingöz⁵, Hatice Nursun Özcan⁵, Ali Varan¹, Bilgehan Yalçın¹

¹Department of Pediatric Oncology, Hacettepe University Faculty of Medicine, Ankara, Turkey; ²Department of Pathology, Hacettepe University Faculty of Medicine, Ankara, Turkey; ³Department of Orthopaedics and Traumatology, Hacettepe University Faculty of Medicine, Ankara, Turkey; ⁴Department of Plastic and Reconstructive Surgery, Hacettepe University Faculty of Medicine, Ankara, Turkey; ⁵Department of Radiology, Hacettepe University Faculty of Medicine, Ankara, Turkey

ABSTRACT

Myofibromas are rare benign tumors of myofibroblasts, seen more commonly in children. These tumors typically involve soft tissues with a predilection for the head and neck. Malignant neoplasia is often suspected for these rapidly growing tumors in early childhood. Clinical and radiological findings are not typical, and histopathological examination makes the definitive diagnosis. This pathology requires the intervention of a multidisciplinary team and regular follow-up. We report our experience with two children with myofibromas, one in the right arm of a 5-year-old girl and the other in the right axilla of a 9-year-old boy. Tumors were totally resected in both children, who are under follow-up with no adjuvant treatment free of disease after surgery. Myofibroma should be considered in the differential diagnosis of pediatric soft tissue tumors. Surgical resection is sufficient for treatment and patients should be followed regularly for possible recurrences.

Keywords: Solitary myofibroma, arm, axilla, immunohistochemistry, surgery

Myofibroma is a benign neoplastic proliferation of myofibroblastic cells affecting mainly the early pediatric age group [1]. The tumor may arise in a solitary or multicentric form, with similar histopathological findings, but varied clinical features and prognosis [2]. Myofibromas usually consist of benign nodules in the skin, muscle, or bone. Less often, they can occur in the lungs, heart, gastrointestinal tract, or orbit [3]. The rarity of this lesion may complicate the diagnosis for clinicians and pathologists. Differential diagnosis is important to accurately distinguish neurofibromas and other lesions like benign and locally aggressive vascular tumors and various malignant soft tissue tumors [3]. Here, two cases of solitary myofibroma are presented.

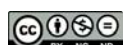
PRESENTATION OF CASES

CASE 1

In November 2020, a five-year-old girl presented with a 10-day history of a painless subcutaneous lump in the upper right arm. She had no history of trauma. Physical examination revealed a firm, slightly tender, immobile palpable mass under the skin proximally in the right arm medial to the humerus measuring approximately 2.5 × 1.5 cm in size with normal color of the overlying skin. Ultrasonography (US) showed a 2.5 × 1.5 × 1.2 cm subcutaneous soft tissue solid lesion with smooth lobulated contours, close to the middle third of the right humerus. Magnetic resonance imaging (MRI) displayed a non-specific fusiform solid

Corresponding author: Çağrı Coşkun, MD.,
Phone: +90 312 305 29 90, E-mail: cagri_730@hotmail.com

How to cite this article: Coşkun Ç, Kösemehmetoğlu K, Ayvaz M, et al. Solitary myofibroma in children: a report of two cases. Eur Res J. 2024;10(3):333-337. doi: 10.18621/eurj.1382704



This is an open access article distributed under the terms of [Creative Commons Attribution-NonCommercial-NoDerivatives 4.0 International License](https://creativecommons.org/licenses/by-nc-nd/4.0/)

Received: November 9, 2023
Accepted: December 19, 2023
Published Online: January 1, 2024

Copyright © 2024 by Prusa Medical Publishing
Available at <http://dergipark.org.tr/eurj>



mass in the middle third of the right arm, abutting the brachial artery, basilic vein, and median nerve; malignancy could not be ruled out (Fig. 1a and b). A trucut biopsy was performed and histopathological examination revealed myofibroma and surgery was planned based on the biopsy result. In the operation, a mass of approximately 3×3 cm was removed totally, preserving the vascular and neural structures. Histological examination revealed the diagnosis of myofibroma showing diffuse positivity with SMA (smooth muscle actin) in the tumor cells, which were negative for caldesmon and desmin (Fig. 2); surgical margins were clear. In the postoperative control examination, no palpable mass or limitation of arm movements was detected. Considering the benign features of the tumor, no adjuvant treatment was indicated. Regular follow-up was planned with physical examination and peri-

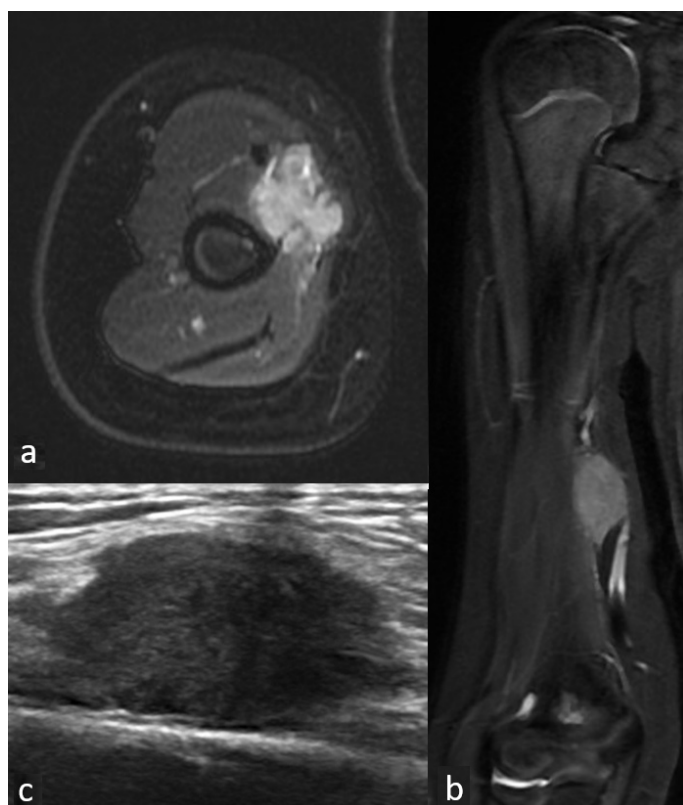


Fig. 1. Magnetic resonance images of case 1. (a) axial fat-saturated T2-weighted image and (b) coronal STIR sequences show an ovoid-shaped hyperintense lesion with lobulated margins in the middle part of the right arm. Ultrasonography of case 2 (c): a well-delineated hypoechoic nodule appeared in the subcutaneous tissue.

odical MR imaging. At a follow-up of 14 months, there was no evidence of disease locally or elsewhere.

CASE 2

In June 2021, a 9-year-old boy presented to our hospital with the complaint of a painless nodule in the right axillary region which was noticed by her parents a few days earlier. He had café-au-lait spots spread over his body. The family history was positive for neurofibromatosis type 1 (NF-1). His brother, uncle, and grandmother had documented NF-1, with multiple neurofibromas and café-au-lait spots. The local US revealed a subcutaneous 0.6×0.8 cm, slightly echogenic, hypoechoic solid nodular lesion in the right axilla (Fig. 1c); myofibroma and neurofibroma were considered in the differential diagnosis. The patient was consulted by the plastic and reconstructive surgery department, whereupon the lesion was excised totally over the right posterior axillary line. The lesional cells were immunoreactive for SMA and desmin, but negative for S-100 protein, CD34 (Fig. 3). Thus, the pathologic diagnosis of myofibroma was rendered. During a 6-month follow-up, no recurrence was identified either locally or systemically. Parents

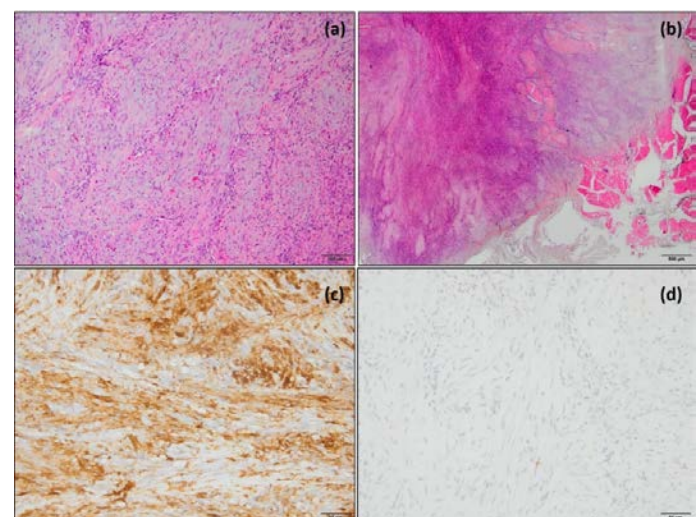


Fig. 2. Histopathological images of case 1. (a and b) well-circumscribed but unencapsulated mesenchymal tumor with intermingled hypocellular and hypercellular areas forming a vague plexiform pattern, benign spindle cell proliferation with hemangiopericytic pattern; (c) SMA showed strong positivity while (d) desmin was negative.

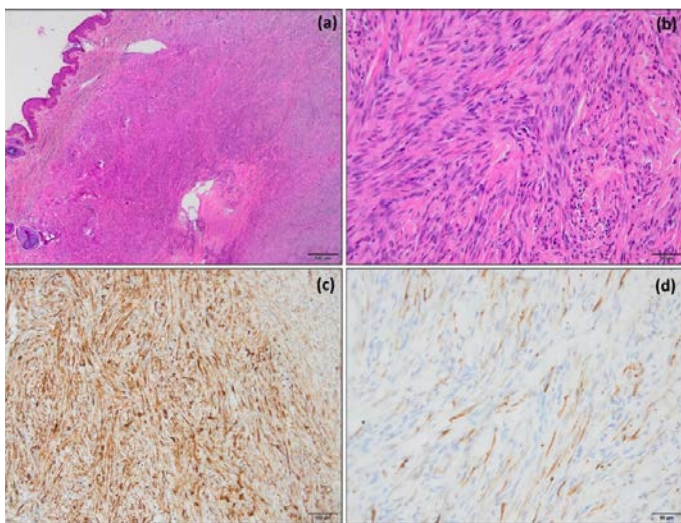


Fig. 3. Histopathological images of case 2. (a) dermal nodule with central degeneration, (b) neoplasm composed of intersecting fascicles of benign spindle mesenchymal cells; (c) SMA was positive in tram-tract (myofibroblastic) pattern, and (d) desmin showed focal positivity.

and patients were informed about the purpose of the case report, and informed consent was obtained from both families for this publication.

DISCUSSION

Myofibroma is a fibrous tumor of childhood and infancy that is characterized by the development of nodular lesions involving the skin, subcutaneous tissue, visceral organs, or bones. It was first described as myofibroblastic proliferation in a newborn in 1951 by Williams and Schrum [3] and was classified according to clinical signs and clinicopathological features by Chung and Enzinger in 1981 [3]. In the WHO 2020 classification of soft tissue tumors, myofibromatosis is classified under the category of pericytic (perivascular) tumors [4].

Myofibroma is classified into three clinical subgroups such as solitary, multiple without or with visceral involvement [5]. In our cases that did not show any evidence of internal organ involvement, the diagnosis was solitary myofibroma. Dhupar *et al.* [6] reported that solitary myofibroma accounts for approximately 70% of cases and Mahajan *et al.* [1] found that 38 (90%) of 42 patients had solitary lesions.

The age of patients ranges from the first few

weeks of life to the end of adolescence. In the study by Mahajan *et al.* [1], the median age at diagnosis of 42 patients was 37 months (range; birth-17 years). A series of 114 cases including adults reported by Qudijk *et al.* [7] in 2012 found that two-thirds presented in the first 2 years of life and 91% before the age of 18. Our cases were 5 and 9 years old, respectively, both within the age range reported in the literature.

The etiology of myofibroma is not well known. Some investigators reported that patients with familial inheritance and inherited genes with autosomal or genetic heterogeneity chromosomes are more susceptible to myofibroma formation [6]. Trauma, injury, and the effects of estrogen are other proposed hypotheses [6]. In our cases, there was no family history of myofibroma or history of trauma.

Both benign and malignant tumors can develop in patients with NF-1, neurofibromas being the most common. Malignant peripheral nerve sheath tumors (MPNSTs) can develop within an associated plexiform neurofibroma and have an extremely poor prognosis with widespread recurrence and distant metastases [8]. The brother of our second case was diagnosed with NF-1 and MPNST had developed based on NF1. The myofibromas described in our cases were benign, and no association of myofibroma with NF1 was found in the literature.

Myofibroma typically develops in the soft tissues of the head, neck, and trunk. However, extremities or the skeleton may also be affected. In our cases, myofibroma localizations were upper extremity and axilla, both of which are rare localizations. In the literature, Qudijk *et al.* [7] reported that myofibromas were located in the arm in four patients and the axilla in a single patient. In the study of Weiliang Wu *et al.* [2], bone myofibromas in the upper extremities were reported in two cases. In addition, Mahajan *et al.* [1] identified 10 of 38 patients had solitary lesions in their extremities.

The presenting symptoms usually reflect the location of the tumor and mainly include swelling or an enlarging mass or nodule; lesions are typically painless. Hemangioma-like discoloration, skin atrophy, and ulceration have also been described [3]. Similar to the literature, our cases presented to the clinic with painless masses. The imaging features of myofibromas are not specific and in the US masses may show a hypoechoic or anechoic center. In our cases, well-con-

toured, solid nodular lesions, hypoechoic in the US, were revealed [2].

Myofibroma shows a characteristic histopathological bi-phasic pattern composed of elongated spindle cells at the periphery and polygonal cells with hyperchromatic nuclei at the center⁶. Tumor cells have characteristic eosinophilic cytoplasm when stained with hematoxylin-eosin, with no atypical pleomorphic or malignant features [2]. Immunohistochemical staining may be helpful in diagnosis. Myofibromas are benign tumors with a characteristic histological and immunohistochemical pattern, displaying SMA- and, to a lesser extent, SMA-positivity, with a low rate of desmin expression⁷. SMA and desmin were positive at immunohistological staining in our cases (Figs. 2 and 3).

The differential diagnosis of myofibroma is extensive, including nodular fasciitis, neurofibroma, fibrous histiocytoma, desmoid tumor, lipofibromatosis, infantile myofibroelastic tumor, and congenital infantile fibrosarcoma. The histology of myofibroma is typical in most cases and immunohistochemistry along with clinical findings may help in diagnosis. Nodular fasciitis is rare in children and is an important differential diagnosis in the adult age group. The histology of nodular fasciitis shows a more prominent myxoid matrix, a tissue culture-like growth pattern, often scattered chronic inflammatory cells, and some erythrocytes. The hemangiopericytoma-like vascular pattern typical of myofibroma is not seen in nodular fasciitis. The peripheral areas of myofibroma may resemble neurofibroma, but the myofibroblastic cells lack S-100 protein and do not have the typical buckled nuclei of neuronal cells. A fibrous histiocytoma consists of cells arranged in a stratiform arrangement and may be SMA positive, such as myofibroma. Generally, fibrous histiocytoma cells express factor XIIIa and CD68. Inflammatory myofibroblastic tumors are characterized by a proliferation of myofibroblastic spindle cells and an inflammatory, predominantly lymphoplasmacytic infiltrate. Inflammatory myofibroblastic tumors can often show rearrangements involving the ALK gene in the 2p23 chromosomal region. Congenital infantile fibrosarcoma is included in the differential diagnosis and can be differentiated from myofibroma by defining the t(12,15) translocation. In general, the identification of myoid cells in the

periphery of the lesion is a useful feature for myofibroma [7].

The recommended treatment for myofibroma is total surgical excision⁹, which was performed in our cases with negative margins resulting in local control. In cases with difficulty in total excision, conservative debulking and then close observation can be planned. In the study consisting of 38 cases with solitary lesions, 12 patients underwent complete and 26 had incomplete resections [1]. In myofibroma with visceral involvement, cytotoxic chemotherapy agents or radiotherapy can be used. However, there is no evidence in the literature of the overall success of these treatments [10]. Recurrences have also been reported, the recurrence rate being 7%-10% in the literature [3]. In a study published in 2017, the median follow-up was 50.5 months, and only 1 in 42 patients developed tumor progression¹. In our cases, although follow-up is short, recurrence did not occur 6- and 15-months after surgery, respectively.

The most common site of involvement of myofibroma is the head and neck, followed by the trunk. On the other hand, myofibromas located in the upper extremity and axilla in our cases were unusual in terms of their localizations. Radiological imaging can define lesion boundaries. Histological analysis is required for a definitive diagnosis. The primary management modality is usually excision of the lesion. This pathological condition requires the intervention and regular follow-up of a multidisciplinary team.

CONCLUSION

In conclusion, although myofibroma is rare, it should be considered in the differential diagnosis of pediatric soft tissue tumors. Surgical resection is sufficient for the more common solitary type, no additional treatment is indicated in most cases. The overall prognosis is favorable even in tumors resected with positive margins. Patients should be followed regularly for possible recurrences.

Patients' Consent

Parents and patients were informed about the purpose of the case report, and informed consent was obtained from both families for this publication.

Authors' Contribution

Study Conception: ÇÇ, KK, MA, IV, ÜA, HNÖ, AV, BY; Study Design: ÇÇ, KK, MA, IV, ÜA, HNÖ, AV, BY; Supervision: KK, MA, IV, ÜA, HNÖ, AV, BY; Funding: N/A; Materials: N/A; Data Collection and/or Processing: ÇÇ, KK, MA, IV, ÜA, HNÖ, AV, BY; Statistical Analysis and/or Data Interpretation: ÇÇ, KK, MA, IV, ÜA, HNÖ, AV, BY; Literature Review: ÇÇ, KK, MA, IV, ÜA, HNÖ, AV, BY; Manuscript Preparation: ÇÇ, KK, MA, IV, ÜA, HNÖ, AV, BY and Critical Review: ÇÇ, KK, MA, IV, ÜA, HNÖ, AV, BY.

Conflict of interest

The authors disclosed no conflict of interest during the preparation or publication of this manuscript.

Financing

The authors disclosed that they did not receive any grant during conduction or writing of this study.

REFERENCES

1. Mahajan P, Hicks J, Chintagumpala M, Venkatramani R. Myofibroma in infancy and childhood. *J Pediatr Hematol Oncol.* 2017;39(3):e136-e139. doi: 10.1097/MPH.0000000000000732.
2. Wu W, Chen J, Cao X, Yang M, Zhu J, Zhao G. Solitary infantile myofibromatosis in the bones of the upper extremities: Two rare cases and a review of the literature. *Oncol Lett.* 2013;6(5):1406-1408. doi: 10.3892/ol.2013.1584.
3. Abujarir R, Salama H, Alsulaiti G, et al. Congenital scalp myofibroma: a case report. *J Neonatal Perinat Med* 2011;4(1):75-78.
4. Choi JH, Ro JY. The 2020 WHO classification of tumors of soft tissue: selected changes and new entities. *Adv Anat Pathol.* 2021;28(1):44-58. doi: 10.1097/PAP.0000000000000284.
5. Ogita A, Ansai SI. Infantile myofibroma: case report and review of the literature. *J Nippon Med Sch.* 2021;87(6):355-358. doi: 10.1272/jnms.JNMS.2020_87-609.
6. Dhupar A, Carvalho K, Sawant P, Spadigam A, Syed S. Solitary intra-osseous myofibroma of the jaw: a case report and review of literature. *Children (Basel).* 2017;4(10):91. doi: 10.3390/children4100091.
7. Oudijk L, den Bakker MA, Hop WC, et al. Solitary, multifocal and generalized myofibromas: clinicopathological and immunohistochemical features of 114 cases. *Histopathology.* 2012;60(6B):E1-11. doi: 10.1111/j.1365-2559.2012.04221.x.
8. Oztürk O, Tutkun A. A case report of a malignant peripheral nerve sheath tumor of the oral cavity in neurofibromatosis type 1. *Case Rep Otolaryngol.* 2012;2012:936735. doi: 10.1155/2012/936735.
9. Davies BM, du Plessis D, Gnanalingham KK. Myofibroma of the cervical spine presenting as brachialgia. *J Neurosurg Spine.* 2014;21(6):916-918. doi: 10.3171/2014.8.SPINE131194.
10. Madhuri BK, Tripathy D, Mittal R. Solitary orbital myofibroma in a child: A rare case report with literature review. *Indian J Ophthalmol.* 2019;67(7):1240-1245. doi: 10.4103/ijo.IJO_1553_18.